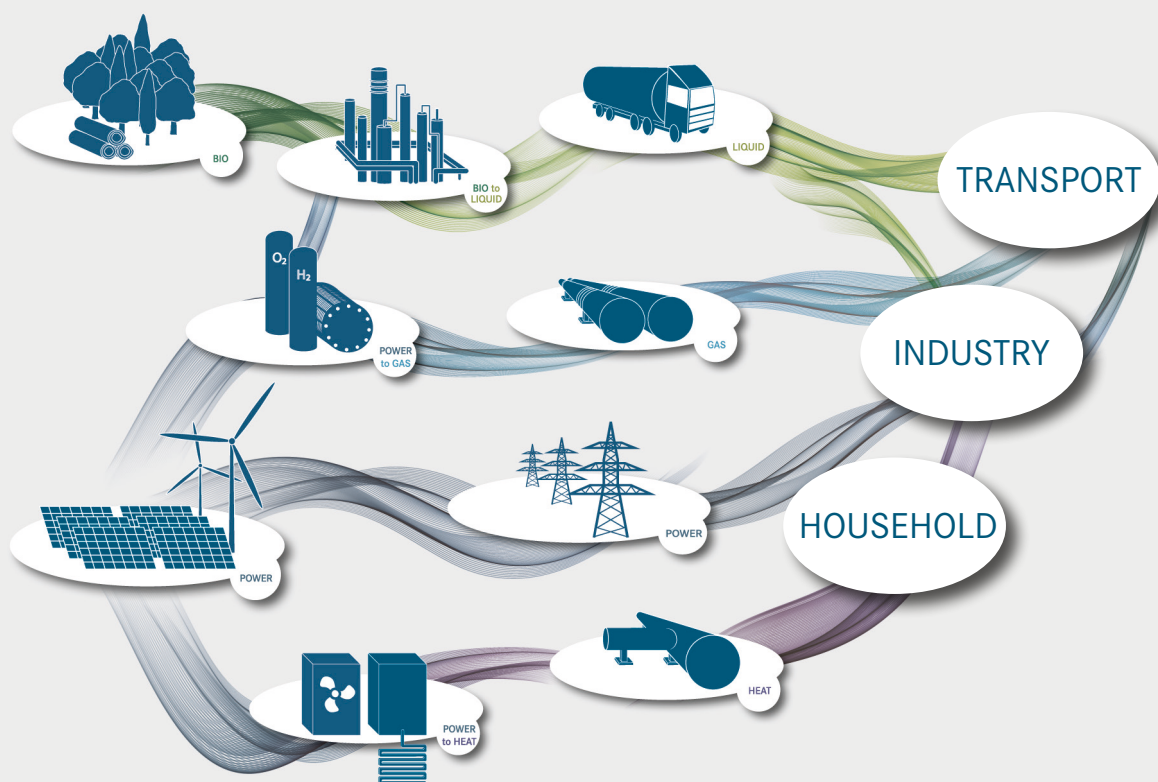


IEK-3 Report 2017

Sector Coupling –
Research for an Integrated Energy System



Energie & Umwelt /
Energy & Environment
Band / Volume 386
ISBN 978-3-95806-258-0

Forschungszentrum Jülich GmbH
Institute of Energy and Climate Research
Electrochemical Process Engineering (IEK-3)

IEK-3 Report 2017

Sector Coupling –
Research for an Integrated Energy System

Bibliographic information published by the Deutsche Nationalbibliothek.
The Deutsche Nationalbibliothek lists this publication in the Deutsche
Nationalbibliografie; detailed bibliographic data are available in the
Internet at <http://dnb.d-nb.de>.

Publisher and
Distributor: Forschungszentrum Jülich GmbH
Zentralbibliothek
52425 Jülich
Tel: +49 2461 61-5368
Fax: +49 2461 61-6103
Email: zb-publikation@fz-juelich.de
www.fz-juelich.de/zb

Cover Design: Grafische Medien, Forschungszentrum Jülich GmbH

Printer: Grafische Medien, Forschungszentrum Jülich GmbH

Copyright: Forschungszentrum Jülich 2017

Schriften des Forschungszentrums Jülich
Reihe Energie & Umwelt / Energy & Environment, Band / Volume 386

ISSN 1866-1793
ISBN 978-3-95806-258-0

The complete volume is freely available on the Internet on the Jülicher Open Access Server (JuSER)
at www.fz-juelich.de/zb/openaccess.



This is an Open Access publication distributed under the terms of the [Creative Commons Attribution License 4.0](https://creativecommons.org/licenses/by/4.0/),
which permits unrestricted use, distribution, and reproduction in any medium, provided the original work is properly cited.

Forward	2
1 Contributions to International Conferences	5
1.1 Preparation, organization and result of TRENDS 2015	6
1.2 Soft matter and neutrons GO energy workshop	9
2 Education and Training	13
2.1 University education	14
2.2 Contributions to information provision, further education, and training	20
3 Scientific and Technical Reports	25
3.1 Solid oxide fuel cells.....	26
3.2 Fuel processing systems.....	43
3.3 High-temperature polymer electrolyte fuel cells	54
3.4 Direct methanol fuel cells	67
3.5 Water electrolysis.....	74
3.6 Process and systems analysis	85
3.7 Physicochemical principles / electrochemistry.....	94
4 Selected Results	103
4.1 Lithium batteries for stationary and mobile applications	104
4.2 Evaluation of carbon dioxide as a raw material in the chemical industry..	107
4.3 Fuel cell / battery hybrid systems for auxiliary power units	112
4.4 Electrodes with reduced Ir content for PEM electrolysis	117
4.5 Solid oxide fuel cell system with integrated shielding-gas production	120
4.6 PRECORS: Spin-off for corrosion-resistant coating technologies.....	125
5 Outlook for New R&D Projects	131
5.1 Solid oxide cells for reversible plant operation.....	132
5.2 The multiscale modeling of fuel cells	136
5.3 Photolysis – photoelectric hydrogen production	138
5.4 Supply systems for alternative fuels	140
5.5 New topics in energy systems analysis and integration.....	146
6 Data, Facts and Figures	149
6.1 The Institute of Electrochemical Process Engineering IEK-3.....	150
6.2 Overview of department expertise	153
6.3 Publications, technology transfer, and resources	157
6.4 Committee work	160
6.5 Contributions to trade fairs and exhibitions.....	166
6.6 How to reach us	169
6.7 List of abbreviations	172

Forward

Dear Readers,

One of the central challenges in the transformation of the energy sector is the reliable integration of all energy sources into the existing system. This requires the use of new and efficient technologies for the conversion, storage, and distribution of renewable power. For years, IEK-3 has been at the forefront of these efforts. Making use of a new funding option from the Helmholtz Association, we have driven and intensified our research in this field in 2015 and 2016.

This funding – from the newly created Helmholtz Energy System 2050 initiative – permits our researchers to work on systems analysis, oriented closely according to the technological institutes. It is set to produce and evaluate innovative technological ideas for the future of the energy system, in line with the objectives set by the Paris climate agreement of December 2015. The additional funding has permitted the team to be expanded to 15 researchers – almost doubling their number. Our systems analysts create and analyze energy scenarios for Germany, Europe, and selected, strategically important regions all over the world. For example, a new calculation method for gas grids was developed, as well as an electricity grid model which allows demand and feed-in of renewables to be considered at spatial and temporal resolution. These developments guarantee technology-neutral systems analysis: although the technologies investigated at IEK-3 are also taken into consideration, they are by no means favored.

The focus of our research – and the area with the most capacities – however, is the hardware development of electrochemical components. Electrolysis – alkaline and acidic low-temperature electrolysis and high-temperature electrolysis – and fuel cells are the priorities in this field. We concentrate particularly on ceramic high-temperature fuel cells, high-temperature polymer fuel cells, and the development of liquid-fuel-based APU systems with fuel cells.

Research into ceramic high-temperature fuel cells succeeded in achieving a special goal: the development and experimental verification of a shielding-gas system with corresponding start-up and power-down cycles. This makes the previously needed external supply mechanism for shielding gas using gas tanks obsolete – and removes one barrier impeding the successful commercialization of fuel cells. Simultaneously, this development increased the electric efficiency to 60 %.

The f-cell Award for innovative fuel cell technology went to Jülich this year. Three scientists from IEK-3 impressed the panel of judges in the research & development category with their method of spray coating metallic bipolar plates, which permits graphene-oxide layers to be manufactured in an extremely cost-efficient manner. The researchers had already won several other awards for their method and are now launching their own start-up company.

I hope these selected examples will encourage you to read more about our research in this report. Please do not hesitate to contact us so we can intensify our work or take up further interesting topics.



Jülich, September 2017

A handwritten signature in blue ink, which appears to read "Detlef Poelmann". The signature is written in a cursive, flowing style.





1

Conferences

Contributions to International Conferences

- Preparation, organization and result of TRENDS 2015
- Soft matter and neutrons GO energy workshop

1.1 Preparation, organization and result of TRENDS 2015

On 3–4 December 2015, IEK-3 hosted a roundtable of experts in Aachen entitled TRENDS – Transition to Renewable Energy Devices and Systems. A group of around 20 scientists discussed relevant topics which may contribute to the transformation of today's energy system to an energy supply system based on sustainable primary energy sources. The concept of the roundtable was to identify high-impact core topics and missing components which will be decisive for reducing CO₂ emissions by 80 % by 2050. Thematically, the conference targeted fuels for transport and essential drive concepts. The transport sector will see a rise in electrification in future, so that auxiliary power units will assume an increasingly significant role. With regard to fuels, the potential of alternative fuels, their production pathways (see Fig. 1), and cost aspects were discussed on the basis of individual introductory talks. The major discussion topics are documented in the following sections:

CO₂ emissions have barely been reduced in the transport sector in the past few years. Sectors such as the energy economy and industrial processes have reduced their CO₂ equivalent emissions by 11.0 - 12.5% between 2007 and 2014. Achieving climate goals will also require new transport concepts, making specific solutions for passenger and goods transport necessary. In the long term, fuel-cell power trains can be operated with hydrogen and battery-electric cars can be used in passenger transport. In goods transport, diesel–electricity hybrid drives with overhead wires and LNG-based combustion engines will be included in the consideration. Any change in the transport sector will be technology-driven and lead to massive changes in production lines. Such technologies require niche applications for their individual development stages as well as attractive funding options and, later, suitable business models. Currently, the available fossil carbon is too cheap and the CO₂ certificates in emissions trading not sufficiently expensive in order to force changes on an economic basis.

An increasing proportion of battery-electric vehicles require an extensive charging infrastructure. Charging stations for a fleet of e-vehicles have been installed and tested in the Ostallgäu region. In order to cover the sum of all charging processes with a corresponding amount of renewable electricity, intelligent charge management is needed since the peaks of electricity demand for charging (6:00 - 7:30) do not coincide with the peak of renewable electricity generation (9:00 - 15:00). Vehicle users will have to notify the system of their planned departure times. Thus, the power demand for a small fleet can be covered by renewable electricity.

In order to drive electromobility forward, industry and research must collaborate. On the one hand, the necessary infrastructure must be developed, and, on the other hand, battery vehicles must be accepted by the customers. This, however, requires new vehicle concepts. Positive developments in this area include the BMW i3 and the adoption of "Streetscooters" in the fleet of the German postal service Deutsche Post. On the part of the electronics, research and development tasks include: integrating power electronics in the drive, modular drive concepts, higher speeds of battery vehicles, new materials for high-temperature semiconductors, permanent magnets, and developing high-voltage batteries (> 5 V).

Especially in the low power range, fuel-cell-based systems for auxiliary power supplies feature several advantages such as a higher system efficiency, fewer emissions, and quiet operation when compared to combustion engines or turbines. Truck applications, however, require compact systems with power densities of 40 W_e/l, which can reliably convert

commercial fuels such as diesel into hydrogen-rich gas. In maritime applications and for aviation purposes, power outputs of 100 - 500 kW_e are required – considerably higher values than the systems currently being tested can achieve, which can only reach about 3 - 10 kW_e. For this performance class in particular, stacks will have to be developed. The overall costs for such systems must also be reduced.

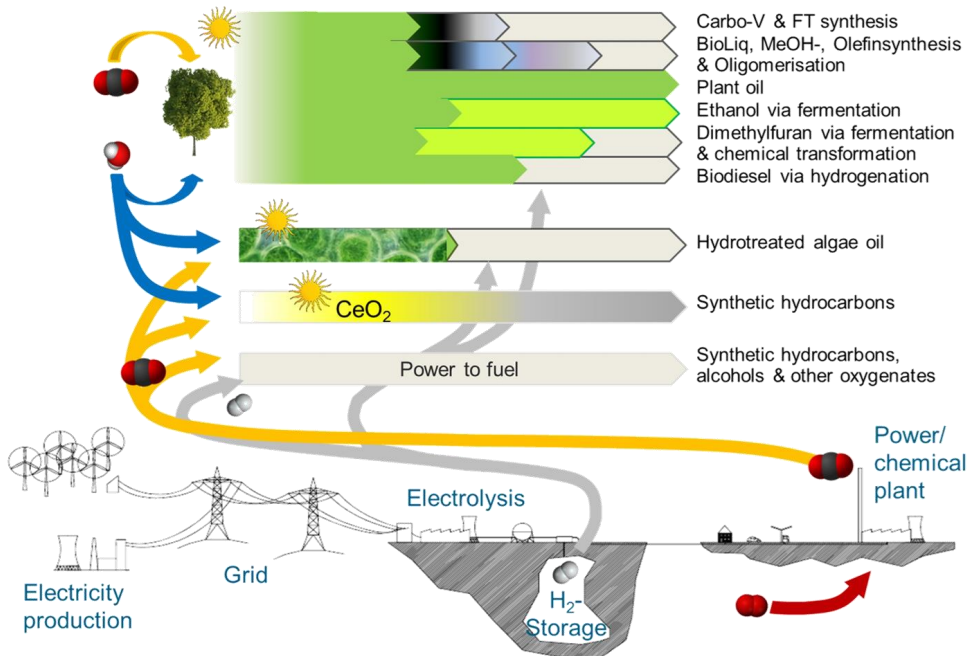


Fig. 1: Various synthesis routes for BtL and PtL fuels

International fuel strategies permitting a reduction of CO₂ emissions by 30 - 40% by 2030 and by 60 - 80% by 2050 are still lacking. Finland and Sweden are viewed as pioneers in introducing renewable fuels to the transport sector. Both countries are focusing on the use of biofuels. Natural gas and biofuels are viewed as alternative fuels globally. In Europe, the use of biofuels has been stagnating at 5% since 2010. Alternative technologies – be it new biofuels and biogases or alternative drive technologies such as electric drives with batteries or fuel cells – tend to develop slowly. A global analysis of biomass potentials according to regions has yet to be conducted but is essential in order to evaluate alternative potentials.

Hydrogen as an energy carrier for the transport sector must be produced from renewable primary energy sources in the medium to long term. Due to the fluctuating nature of wind and solar energy, it is necessary to excessively develop renewables in order to implement an energy supply which – in combination with suitable storage techniques – can lead to a CO₂ reduction of 80% by 2050. The energy concept presented by IEK-3 envisages that Germany will install 170 GW onshore and 59 GW offshore wind energy by 2050. At nominal load, the model predicts annual operating hours of 2,000 h for onshore and 4,000 h for offshore plants. After subtracting the annually needed electrical energy of 528 TWh, an excess of 293 TWh remains – provided grid capacity is taken into account. At an efficiency of 70%, a maximum of 6.2 million tons of hydrogen could thus be produced via electrolysis. If ¾ of Germany's

vehicle fleet – which comprises 44 million cars – were retrofitted with fuel-cell drives by 2050, then 2.9 million tons of hydrogen would be needed annually. A cost analysis estimates the price of hydrogen to be 16.5 ct/kWh with an installed electrolysis output of 28 GW.

Hydrogenation of vegetable oils is one option to convert biomass into various fuels, preferably diesel. All double bonds present in vegetable oils are saturated by hydrogen and the oxygen contained in the acid groups is removed during the formation of carbon dioxide and water. The Finnish company Neste is producing 2.5 million tons of fuel annually using this process. The oil base consists of vegetable oils and animal waste fats (62%), vegetable oils of the first generation such as rapeseed, palm, and soy oils as well as camelina and jatropha oils which, due to their cultivation areas, do not compete with food crops. The chemical and thermodynamic properties are nearly identical to those of synthetic fuels from the Fischer-Tropsch process.

In addition to gasification, biooils can be directly liquefied. Processes already applied include flash pyrolysis as well as hydrothermal and organic solvolysis. The products of these are gases, biochar, and two liquid phases, an aqueous and an organic one. After flash pyrolysis, the oxygen content amounts to 40% at a low heating value of 15 MJ/kg, while organic solvolysis results in an oxygen content of 20% and a considerably better heating value of 30 MJ/kg. The biooils are then processed via hydration to produce fuel. Compared to gasification and subsequent Fischer-Tropsch synthesis, selective biochemical synthesis from biopolymers represents a considerably more elegant method for the production of fuel. RWTH Aachen University's excellence cluster "Tailor-Made Fuels from Biomass" produces fuels such as methyltetrahydrofuran from cellulose and hemicellulose via the intermediates levulinic acid, itaconic acid, and hydroxymethylfurfural.

The task faced by biorefineries which focus on such processes is to recycle all water and solvent flows. Drying waste flows and depositing solid residues, in return, leads to increased energy expenditure, but also improves the water balance of fuel production.

Power-to-fuel processes represent another way of producing fuel: regeneratively produced hydrogen is combined with carbon dioxide separated in industrial processes to form fuels. Ethers, alcohols, and alkanes are all considered. Particularly ethers such as dimethyl ether and polyoxydimethyl ether offer advantages concerning the emission of nitrogen oxides and particles during combustion in engines. Approximately 3 million tons of hydrogen from electrolysis could be used to produce approximately 7.5 million tons of fuel in the form of alkane cuts. The efficiencies of fuel production amount to 30 - 50%, depending on the process and the chemical target substance.

1.2 Soft matter and neutrons GO energy workshop

The first Jülich Workshop “Soft Matter and Neutrons GO Energy” took place in Feldafing from 08 - 09 October. Twenty-five scientists exchanged ideas in an interdisciplinary environment on topics related to soft matter and neutron research for sustainable energy supplies. The event, organized by Dr. Olaf Holderer and Dr. Rainer Bruchhaus, Jülich Centre for Neutron Science (JCNS) and Professor Werner Lehnert, Institute of Energy and Climate Research - Electrochemical Process Engineering (IEK-3), was held in the GIZ Conference Centre (Deutsche Gesellschaft für Internationale Zusammenarbeit).

The quest for a sustainable supply of sufficient energy is one of the grand challenges that societies are facing around the globe. Major research projects focus therefore on tackling “green” energy production as well as efficient energy storage using advanced technologies and materials. Recently, soft matter materials have become very attractive for use in advanced batteries, solar cells and efficient fuel cells. Here, neutrons are a key tool, providing deep insight into the structure and dynamics and thus the function of technologies based on soft matter materials. In addition, neutron scattering methods have significantly contributed to address the open questions surrounding Li-ion battery research.

The idea behind the workshop “Soft Matter and Neutrons GO Energy” was to bring scientists together to improve communication between the different communities and to fully explore the potential of neutron scattering in this field. Twenty-five scientists used the workshop (see Fig. 2) to discuss the most recent developments in the field and explore future possibilities for collaboration and scientific exchange.



Fig. 2: Attendees of the workshop “Soft Matter and Neutrons GO Energy”

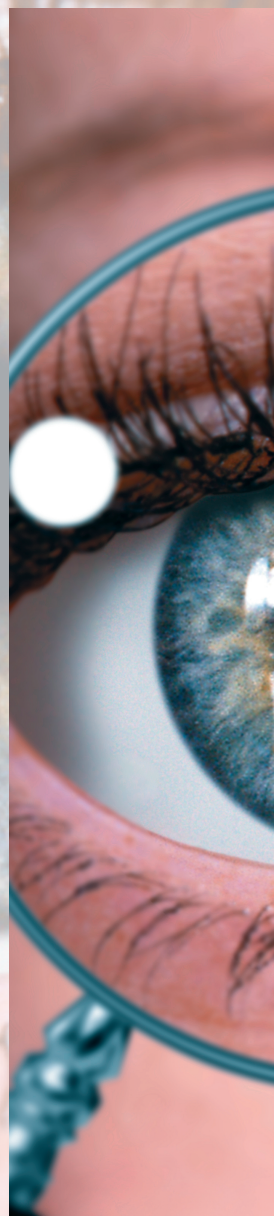
The workshop hosted sessions on batteries, on materials relevant for diverse energy-related applications from solar cells to new types of rubber for tyres, as well as on fuel cells. Lively discussions resulted from the different sessions, showing that energy-related topics and neutron scattering form a very attractive combination. Some of the findings presented during the workshop included neutron radiography and tomography used to bring new insights to the operation of batteries and fuel cells, and quasi elastic neutron scattering was shown to be an excellent tool for studying proton diffusion in complex multicomponent systems.

Furthermore, the grazing incidence SANS was shown to be an extraordinary tool for studying buried interfaces in layered structures.

Referent/in	Vortragstitel
Fr. Dr. W. Lücke	In-situ neutron radiography to characterize MEAs of dynamically operated HT-PEFCs
Dr. M. Höh	Investigation of Two-Phase Flow in Polymer Electrolyte Membrane Water Electrolysis using Neutron Radiography

Table 1: Lectures of IEK-3 speakers

Mrs. Dr. Wiebke Lücke and Dr. Michael Höh, both from the IEK-3, presented their latest neutron radiography results in fuel cells and electrolyzers during the workshop (see Table 1). The first talk was related to the dynamics of phosphoric acid inside a running high-temperature polymer electrolyte fuel cell. The second talk treated the operando observation of gas bubbles in a polymer electrolyte electrolyzer.



A close-up photograph of a human eye with a blue iris and a contact lens. The eye is looking slightly to the left. The contact lens is visible on the lower part of the eye. The background is a soft, out-of-focus light blue.

2

Education

Education and Training

- University education
- Contributions to information provision, further education, and training

In addition to propagating knowledge on pioneering energy conversion technologies, a number of scientists at IEK-3 are involved in education and training for specific target groups. They give lectures and seminars at universities and also support and supervise doctoral researchers' projects. Students enrolled in dual study programs for laboratory technicians and mathematical-technical software developers are guided and trained at the institute. School children in grade 10 and above also benefit from lessons on energy technology given by IEK-3 employees.

2.1 University education

Teaching at universities is a fundamental responsibility of selected research scientists at IEK-3 in addition to their research and development work. Within the framework of the Jülich model, IEK-3 has one full professorship (grade W3) at RWTH Aachen University, which is currently held by Prof. Dr.-Ing. Detlef Stolten. Dr. Martin Müller supports Prof. Stolten, teaching seminars that accompany the lectures and conducting oral examinations at undergraduate level. Prof. Dr. rer. nat. Werner Lehnert is a grade-W2 professor at RWTH Aachen University in the Scientific Faculty. Privatdozent Dr. rer. nat. Carsten Korte lectured at Justus Liebig University Gießen until the summer semester of 2016. Dr. Korte has now obtained authorization to lecture at RWTH Aachen University instead and has been doing so since WS 2016. Two other grade-W2 professorships are held at Aachen University of Applied Sciences Campus Jülich by Prof. Dr.-Ing. Ralf Peters and Prof. Dipl.-Ing. Ludger Blum. Dr.-Ing. Dipl.-Wirt.Ing. Thomas Grube supports Prof. Peters, teaching seminars that accompany the lectures and conducting written examinations at undergraduate level. Since winter semester 2012/2013, Dr.-Ing. Murat Peksen has been lecturing at Aachen University of Applied Sciences Campus Jülich. Furthermore, Dr.-Ing. Martin Robinus has been lecturing on the topic of technical energy systems analysis at RWTH Aachen University since summer semester 2016.



<http://www.rwth-aachen.de/cms/~a/root/?lidx=1>



<http://www.uni-giessen.de/welcome>



FH AACHEN
UNIVERSITY OF APPLIED SCIENCES

<http://www.fh-aachen.de/en/>

Fig. 3: Universities where IEK-3 scientists lecture

Fig. 3 shows the Internet addresses of the three universities at which IEK-3 scientists teach the up-and-coming scientists.

The spectrum of topics taught ranges from the fundamentals of science and theoretical modeling and simulation methods to detailed technical knowledge and the characterization of technical applications. Each semester, one block seminar, five lecture courses and three seminar courses are taught. An additional half-day practical course is offered every summer

semester. Up to eighty students participate in the individual courses each semester. IEK-3 scientists also play an important role in supervising semester papers, bachelor's and master's dissertations, and doctoral theses. In 2015, 9 bachelor's dissertations, 15 master's dissertations, and 9 doctoral theses were successfully completed. In 2016, 4 bachelor's dissertations, 22 master's dissertations, and 8 doctoral theses were successfully completed.

2.1.1 Courses taught by professors

Table 2 provides an overview of the courses taught at universities by IEK-3 professors.

Name	Subject area	Type/hours Semesters		University
Prof. Dr. D. Stolten	Grundlagen und Technik der Brennstoffzellen (<i>Principles and Technology of Fuel Cells</i>)	V/2 Ü/2	WS	RWTH Aachen University
Prof. Dr. W. Lehnert	Modellierung in der Elektrochemischen Verfahrenstechnik (<i>Modeling in Electrochemical Process Engineering</i>)	V/2 Ü/2	WS	RWTH Aachen University
Prof. Dr. R. Peters	Basics and Applications of Chemical Reaction Theory – Simulation of Dynamic Processes in Energy Systems with Matlab/Simulink	V/2 Ü/2	WS	Aachen Univ. of Applied Sciences Jülich site
Prof. L. Blum	Brennstoffzellen – Die Zukunft der dezentralen Energieversorgung!? (<i>Fuel Cells – The Future for Dispersed Power Supply!?</i>)	V/2	WS	Aachen Univ. of Applied Sciences Jülich site
	Fuel Cells – The Future for Dispersed Power Supply!?	V/2	WS	

Table 2: Courses taught by professors

2.1.1.1 Grundlagen und Technik der Brennstoffzellen (Principles and Technology of Fuel Cells)

Prof. Dr.-Ing. Detlef Stolten holds the Chair for Fuel Cells at RWTH Aachen University. The courses offered deal with the conversion of renewable and fossil energy carriers for use in fuel cells in portable, stationary and mobile applications. The process engineering and systems technology aspects include high-temperature and low-temperature fuel cells, as well as the processing of fuels specifically for fuel cells. These aspects are accompanied by an examination of the basic physical and chemical principles involved. Systems analyses of energy process engineering, which include cost estimates, serve as a comprehensive examination with a view to future market launch. As part of the existing cooperation with

Forschungszentrum Jülich, students have the opportunity to write semester papers and undergraduate dissertations at Jülich and to work on projects as research assistants.

2.1.1.2 Modellierung in der Elektrochemischen Verfahrenstechnik (*Modeling in Electrochemical Process Engineering*)

Prof. Werner Lehnert teaches modeling in electrochemical process engineering at RWTH Aachen University. His lecture course focuses on the mathematical description of electrochemical converter systems. In addition to the basic approach to modeling, different modeling techniques are also outlined. Using low- and high-temperature fuel cells as examples, 1D, 2D, and 3D models with varying degrees of complexity are developed and their validity is then discussed. These examples of application form the basis for mathematical descriptions of the interactions of mass and heat transport with the electrochemical processes. Particular attention is paid to the description of processes in the porous components of fuel cells.

2.1.1.3 Basics and applications of chemical reaction theory – simulation of dynamic processes in energy systems with MATLAB/Simulink

Prof. Ralf Peters teaches energy process engineering at Aachen University of Applied Sciences Campus Jülich. The course “Basics and applications of chemical reaction theory – Simulation of dynamic processes in energy systems with Matlab/Simulink” links the basic principles of chemical process engineering with dynamic simulations of reactors. The lectures and seminars look at the examples of fuel cell systems for hydrogen-powered vehicles and systems combined with fuel processing for auxiliary power supply based on diesel. The course is compulsory for the students enrolled in the Master of Science in Energy Systems.

2.1.1.4 Brennstoffzellen – Die Zukunft der dezentralen Energieversorgung!? (The Future for Dispersed Power Supply!?)

Prof. Ludger Blum teaches fuel cell technology at Aachen University of Applied Sciences, Campus Jülich. The optional subject “Fuel cells for dispersed power supply” in the bachelor’s course on energy and environmental technology and the Master of Science in Energy Systems covers the function, construction, behavior, advantages, and disadvantages of different types of fuel cells. It also lays the groundwork for the process engineering design of fuel cell systems. The topics include: basic principles of fuel cells; fuel supply; efficiency, function, and construction of different types of fuel cells; fuel cell system requirements; process engineering of various fuel cell systems for different applications; energy balance of a fuel cell system; and modern plant engineering. An average of 20–30 students in the master’s program and an average of 10 in the bachelor’s program took these courses.

2.1.2 Courses taught by university lectures

Table 3 provides an overview of the courses taught at universities by IEK-3 lecturers.

Name	Subject area	Type/hours Semesters		Uni- versity
PD Dr. C. Korte	Physikalisch-Chemische Methoden zur Präparation und Charakterisierung von dünnen Schichten (Physical and Chemical Methods for the Preparation and Characterization of Thin Films)	S/2 Block	SS until SS16	Giessen University
	Physical Chemistry I for chemistry (teacher training) (V), quantum mechanics	V/2 (Ü/1)	WS from WS16/17	RWTH Aachen University
Dr. M. Robinus	Technical energy systems analysis	V/2 Block	SS from SS16	RWTH Aachen University
	Seminar: technical energy systems analysis	S CP/5	WS from WS16/17	RWTH Aachen University
Dr. Martin Müller	Grundlagen und Technik der Brennstoffzellen (<i>Principles and Technology of Fuel Cells</i>)	Ü/2	WS	RWTH Aachen University
Dr. M. Peksen	Multiphysikalische Modellierung funktionaler Materialien und Komponenten (<i>Multiphysical Modeling of Functional Materials and Components</i>)	V/2	WS	Aachen Univ. of Applied Sciences Jülich site
Dr. T. Grube	Basics and Applications of Chemical Reaction Theory – Simulation of Dynamic Processes in Energy Systems with Matlab/Simulink	Ü/2	WS	Aachen Univ. of Applied Sciences Jülich site
CP: Credit Points				

Table 3: Courses taught by university lecturers

2.1.2.1 Physikalisch-Chemische Methoden zur Präparation und Charakterisierung von dünnen Schichten (Physical and Chemical Methods for the Preparation and Characterization of Thin Films)

PD Dr. Carsten Korte teaches a seminar course at Justus Liebig University Gießen in the Faculty of Biology and Chemistry. The seminar provides a comprehensive introduction to the preparation and analysis of thin oxide-ceramic films and their use in technical applications. It is aimed at all interested students taking master's courses in chemistry, physics, and materials science, as well as at doctoral researchers in the same fields. The course looks at the most important vacuum evaporation processes, including thermal evaporation, sputtering methods, chemical vapor deposition (CVD), molecular beam epitaxy (MBE), and pulsed laser deposition (PLD). Particular emphasis is placed on pulsed laser deposition (PLD). Other topics from the field of preparation are the growth modes for large and small layer thicknesses, which determine layer morphology, and the dependence of these modes on surface energy and surface diffusion. The analytical methods covered are X-ray diffraction (XRD, pole figures, reflectometry), electron microscopy (SEM, TEM) and the associated electron diffraction techniques (EBSD, SAED). A concluding seminar looks at examples from the literature and discusses them. Four students took the block seminars offered in summer semester 2015 and 2016.

2.1.2.2 Physical chemistry I, quantum mechanics

Privatdozent Dr. Carsten Korte lectures on chemistry for students planning to become teachers at the Department of Chemistry in the Faculty of Mathematics, Computer Science and Natural Sciences at RWTH Aachen University. His lecture Physical Chemistry I from the lecture module Physical Chemistry B is attended by students in their third semester. The fields of structure of matter and spectroscopy are taught in the lecture (2 SWS) and the corresponding tutorial (1 SWS, held by Junior-Prof. F. Hausen, IEK-9). For this purpose, the students first learn the basics of quantum mechanics and, based on this, the spectroscopic methods used in chemistry as well as atomic structures and the various forms of chemical bonds. A total of 29 students are registered for the lecture and tutorial in winter semester 2016/17.

2.1.2.3 Technical energy systems analysis

Dr. Martin Robinius and Prof. Dr. Aaron Praktiknjo (Junior-Prof. for energy resources and innovation economy) hold a lecture and corresponding tutorial on technical energy systems analysis. Their collaboration is part of the Jülich Aachen Research Alliance (JARA), the cooperation between Forschungszentrum Jülich and RWTH Aachen University. Extensive technical expertise was pooled in the ENERGY section of JARA concerning the fields of process engineering, mechanical engineering, electrical engineering, geoscience, biotechnology, and chemistry, and the corresponding research institutes have agreed to take part in the interdisciplinary collaboration. Triggered by the increasing demands made on systems analysis with respect to the extensive evaluation of technological innovations to be expected for economic competition with conventional technologies already on the market, the interlinkage of engineering and scientific competence with economic and sociological expertise is crucial. The lectures aim to teach the students this importance in an appropriate manner.

2.1.2.4 Multiphysikalische Modellierung funktionaler Materialien und Komponenten (Multiphysical Modeling of Functional Materials and Components)

Computational modeling has become an important tool for predicting and simulating the multiphysical behavior of complex engineering systems. Dr. Peksen's lecture course therefore aims to familiarize students with theoretical and practical approaches to multiphysical modeling. The necessary skills for analyzing technical problems using numerical simulation products are taught. The lecture course covers the methodology for modeling coupled physical interactions as well as the simulation and analysis of materials and components. The fundamentals of computational modeling are detailed. Thermofluid-structural coupling is discussed using advanced techniques. The linear and non-linear behavior of materials and components under thermofluid, static and dynamic load is elucidated. Advanced modeling topics are taught. The lecture course is held during winter semester for students enrolled in the Master of Science in Energy Systems. Students are expected to successfully complete a written exam and an additional computational project. In winter semester 2015/2016, four students took the course.

2.2 Contributions to information provision, further education, and training

Based on the multidisciplinary expertise and the experience from previous years, IEK-3 organized a variety of different events, was involved in external events on various levels and worked with other institutions preparing, coordinating and offering support. The expansion and consolidation of these activities is the aim of existing and planned partnerships focusing on providing interested target groups with information and further education.

2.2.1 Organization of tours, seminars, practical courses, information events, and visits to the institute

The topics dealt with at the events depend on the requirements and requests of each target group. In other words, the events range from information events and training courses for secondary-school students, university students, teachers, tradesmen, technicians, engineers, and scientists to practical courses on career choice and work experience for secondary-school students, as well as vocational training and study-related placements for undergraduates and postgraduates. The length of each of the events ranges from half a day to several weeks depending on the situation. The tasks assigned to secondary-school students and university students during a placement include shadowing technical and scientific personnel at the institute as well as supervised independent work on selected practical projects.

- Information events and visits to the institute for individuals interested in Jülich's contribution to research and development for fuel cell and hydrogen technology. Every year, around 60 tours are organized at IEK-3 with an average of 20 people per tour. The tours are guided by two doctoral researchers.
- Work experience and placements for secondary-school students from local schools focusing on specialist careers in the area of fuel cell and hydrogen technology (2015: 1 student on placement; 2016: 5 students on placement). A broad interdisciplinary range of laboratory-oriented topics are covered. Placements for secondary-school students are generally for one or two weeks depending on requirements.
- Several single days of experiments dealing with fuel cells as part of the JuLab Schools Laboratory research week "Energy – Researching for the Future" – for 12 school students aged between 14 and 17 from 30 March to 2 April 2015 and for 10 school students aged between 14 and 18 from 21 March to 24 March 2016.
- Several single days of supervised project work on a fuel cell R&D topic as part of JuLab's vocational orientation program on the world of fuel cells – for 11 school students aged between 14 and 17 from 29 June to 3 July 2015. The student placement concerning the topic of mobility, which was hosted one year later, was attended by 10 school students aged 14 to 17.

2.2.2 Involvement in external events

A number of scientists from IEK-3 gave introductory presentations and specialist presentations as invited speakers on fuel cells and hydrogen at diverse external events including training courses, workshops, and continuing professional development courses.

- Courses for developers and users on fuel cells and hydrogen technology as part of the WBZU events in Ulm: These courses were held in March 2015. One IEK-3 scientist gave two presentations on each of the specialist topics of “Lifetime Aspects of PEFC” and “Hydrogen Supply”.
- Summer school on renewable energy at the University of Bonn: two IEK-3 scientists performed laboratory experiments on low-temperature fuel cells in July 2015 with students from the USA, Canada, and China. In July 2016, students from the USA, Canada, Japan, Korea, and Singapore conducted similar experiments.
- Joint European Summer School on Fuel Cell, Battery, and Hydrogen Technology: at the events in September 2015 and 2016 in Athens, Greece, an IEK-3 scientist gave four presentations each on new trends in electrolyte, cathode, and anode material, on cell and stack design, and on cell manufacture for low-temperature fuel cells and electrolyzers.

2.2.3 Collaboration with other organizations

In creating and implementing further education and training and continuing professional development in the field of fuel cell and hydrogen technology, a new topic has been integrated: how applications with fuel cells and hydrogen infrastructures can be launched on the market. This development is proceeding at a rapid pace in response to growing interest in expertise in the areas of fuel cells and hydrogen on the part of the manufacturing industry and the relevant educational establishments. In order to cater for this demand, special initiatives have been launched. The combination of specialist knowledge and existing opportunities provides an excellent basis for collaboration.

- Involvement in the Fuel Cells Qualification Initiative (IQ-BZ), which aims to implement information and training measures for fuel cell and hydrogen technologies.
- Promotion and sale of a “Fuel Cells” CD-ROM through the Federal Technology Centre for Electrical Engineering and Information Technology (Oldenburg) and Vogel Industrie Medien GmbH (Würzburg) which is designed to provide information, increase the acceptance of fuel cells, and promote further training and education.



Fig. 4: Group photos of the winning teams of the 2015 (left) and 2016 (right) competitions

- Involvement in the school student competition “Fuel Cell Box”, organized annually by the EnergyAgency.NRW: assessment of the theoretical and practical results of 20 teams of

students in the final round of the competition. In Fig. 4, the winning teams in 2015 and 2016 are pictured holding their certificates together with the organizers.

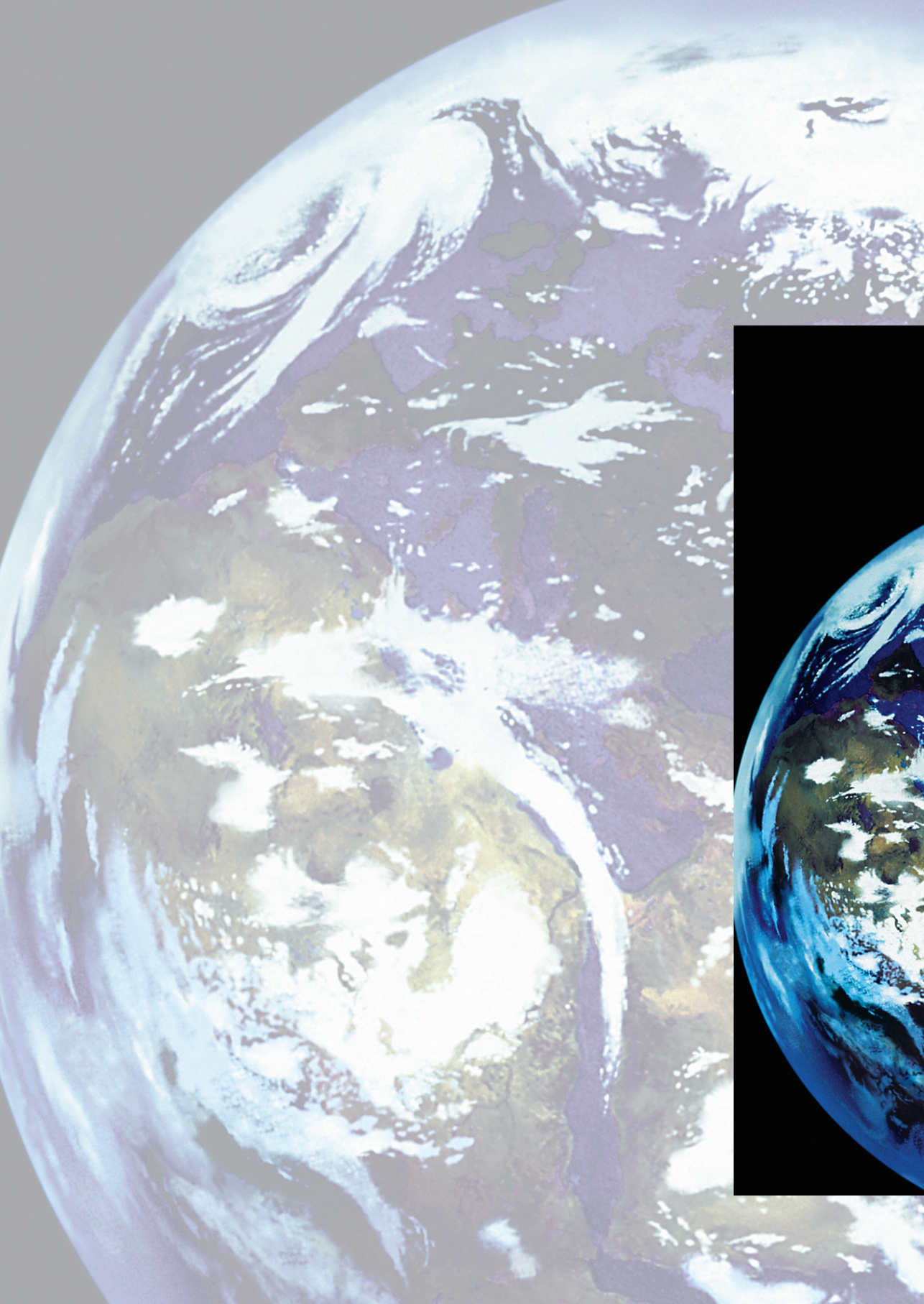
- Assessment of the theoretical and practical results of work in the disciplines of technology, the working world, and geo- and space science in the regional heat of the young scientists' competition "Jugend forscht, Schüler experimentieren", which takes place once a year at Forschungszentrum Jülich.

In 2015, Constantin Zborowska from the Willy-Brandt-Gesamtschule school in Kerpen (left in Fig. 5) achieved first place in the subject area of geo- and space science of the "Jugend forscht" competition. He impressed the panel of judges with his astronomic expertise and his work for reproducing the HR diagram by means of spectral investigation of stars of the MKK classification

In 2016, Marius Ziemke from the Städtisches Gymnasium school in Herzogenrath (right in Fig. 5) achieved first place in the subject area of the working world by combining the data glasses Google Glass with existing storage systems, enabling warehouse workers to use both hands while at the same time receiving requests via the glasses.



Fig. 5: First places in the 2015 and 2016 regional competitions of "Jugend forscht", Constantin Zborowska (left) and Marius Ziemke (right)



Reports

Scientific and Technical Reports

- Solid oxide fuel cells
- Fuel processing systems
- High-temperature polymer electrolyte fuel cells
- Direct methanol fuel cells
- Water electrolysis
- Process and systems analysis
- Physicochemical principles / electrochemistry

3.1 Solid oxide fuel cells

3.1.1 Objectives and fields of activity

Cells, components, stacks, and systems are being developed within the fuel cells program topic for high-temperature fuel cells with solid electrolytes (SOFCs) as well as for high-temperature electrolysis with solid electrolytes (SOE). Strategically, this topic aims to provide electric energy in a highly efficient manner for mobile and stationary applications, both distributed and centralized, on a scale ranging from a few kilowatts to several hundred kilowatts. Work focuses on increasing power density, long lifetimes, the identification of degradation mechanisms in the stack and preventing them, advanced design and highly integrated system engineering. The results of this development work include materials for cells, thermomechanically improved stacks, and highly integrated system components, as well as demonstration plants. Important supporting activities include the modeling of mechanical and thermal component loads as well as the development and characterization of components for fuel cell systems and their evaluation using process engineering analyses.

3.1.2 Important results

3.1.2.1 Tests with cassette stacks

One of the newer areas of research is cassette or lightweight stacks, which are being developed for use in vehicle auxiliary power units (APUs) using a “CS” design.

The new CS^V design was tested with stack CS^V05-04. While the cover plate (level 5) was MnOx coated on the cathode side via WPS at Jülich, the MCF (APS) protective coating was applied for the first time by the project partner Turbo Coating (Italy). Cells manufactured by SolidPower (Italy) were used. Levels 1–4 exhibit much better performance compared to the previous CS^V05-02 stack, which can be clearly attributed to the MCF (APS) protective coating. This previous stack, which only had a MnOx (WPS) protective coating, displayed a performance similar to level 5, which was also MnOx-coated. After one thermal cycle, the performance of levels 1–4 did not decrease, while that of level 5 decreased by approximately 5 %. Due to a sudden drop in cell voltage on level 5, load operation was terminated at 0.5 A/cm² and 750 °C after 1,428 h. The average aging amounts to approximately 1 %kh⁻¹ (not including level 5). At room temperature, a short circuit was detected between level 5 and the cover plate. The entire operating phase is shown in Fig. 6 and the characteristic curves at the beginning and at the end in Fig. 7.

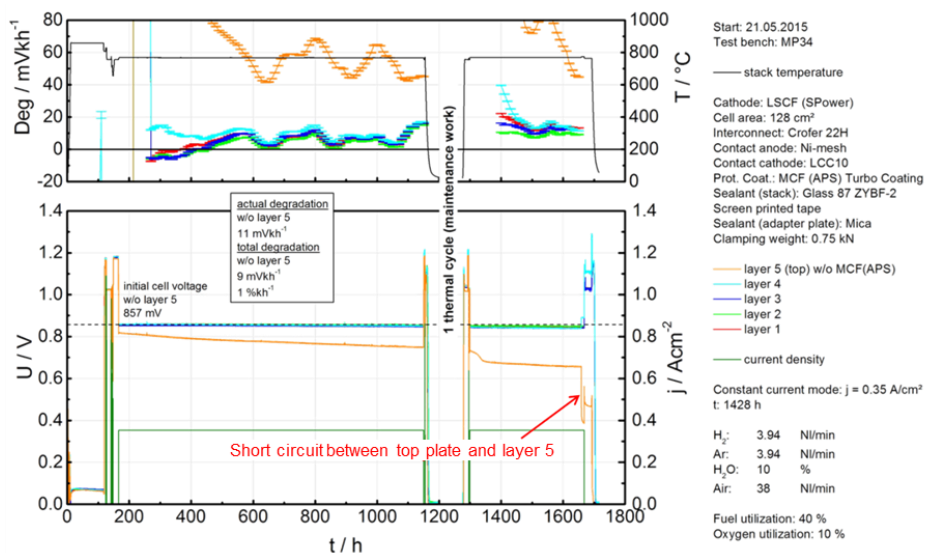


Fig. 6: SOFC stack CS^V05-04, test no. SK 570: load operation

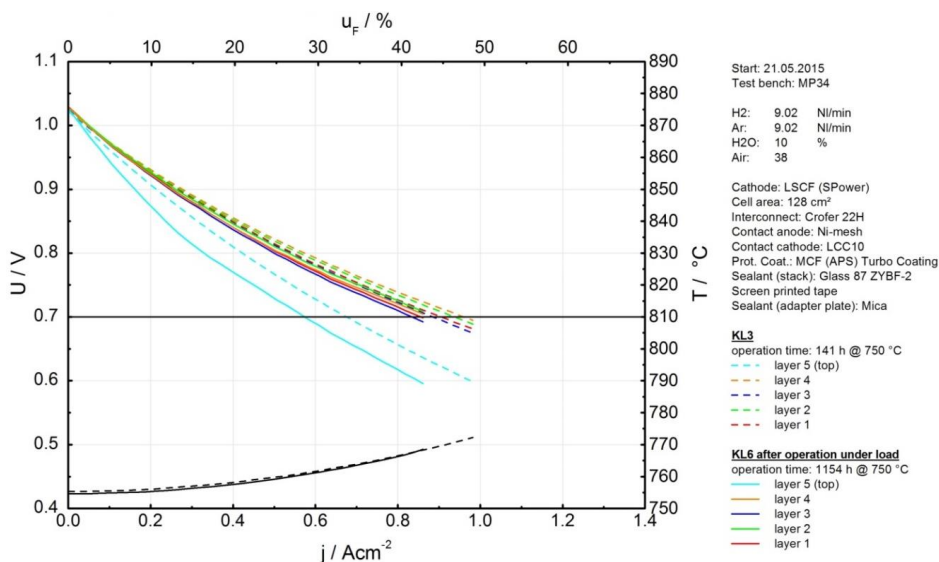


Fig. 7: SOFC stack CS^V05-04, test no. SK 570: characterization before and after load operation

During the subsequent post-examination, a metal particle at the edge of the cassette was identified as the cause of the short circuit (see Fig. 8). The particle originated from the laser welding process during the manufacture of the cassette.

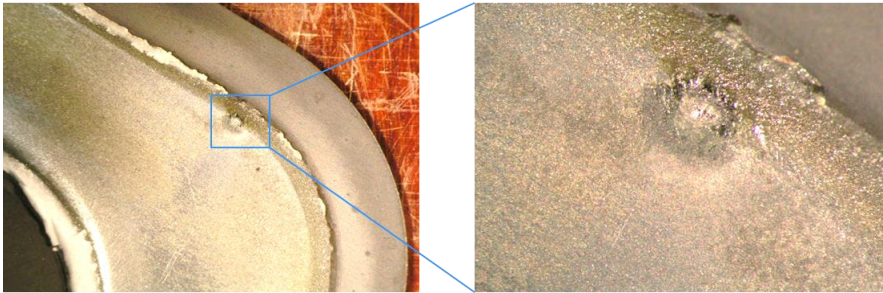


Fig. 8: Stack: CS^V05-04, bottom side of cover plate: location of short circuit between the bottom side of the cover plate and the cathode side of the cassette

The first 10-level stack test (stack test CS^V10-01) yielded good performance, but one of the levels (level 6) also suffered a short circuit, which in the post-examination was similarly attributed to a metal particle at the edge of the cassette. Improved control of the manufacturing processes will avoid this in future. Due to a broken heating element in furnace MP36 the stack had to be moved to a different furnace (MP34). In spite of the short circuit, it was successfully operated for several hundred hours (see Fig. 9). Thermal cycling was not possible, however. This experiment will be repeated.

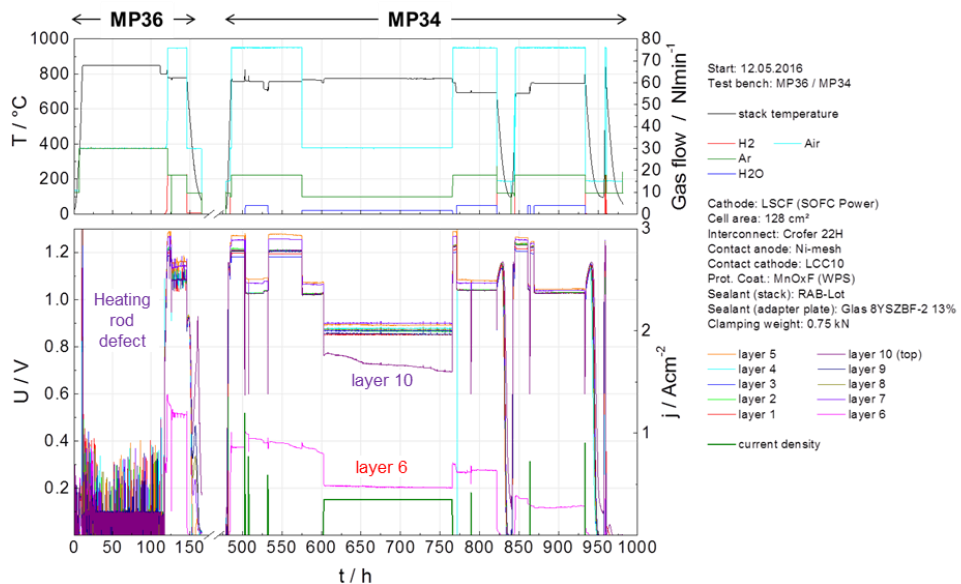


Fig. 9: Stack test CS^V10-01: long-term behaviour

A known weakness of the cassette design is the insufficient stability of the silver solder used in joining the cells. Thanks to the constructive changes implemented in the CS^V design, it was possible to solder the cells into the frame using glass sealant and subsequently weld together the metal parts without damaging the joining. This was successfully demonstrated in a 3-level dummy stack (CS^V03-01). For this first experiment, cells without cathodes were used so that no electrochemical tests were conducted. The stack was subjected to a total of 53 thermal cycles at different heating rates, including several leak tests for which it had to be

removed from the test stand (see Fig. 10). During the entire operating time, no noteworthy decrease in tightness was detected. A 5-level stack is currently being prepared which can also be electrochemically characterized.

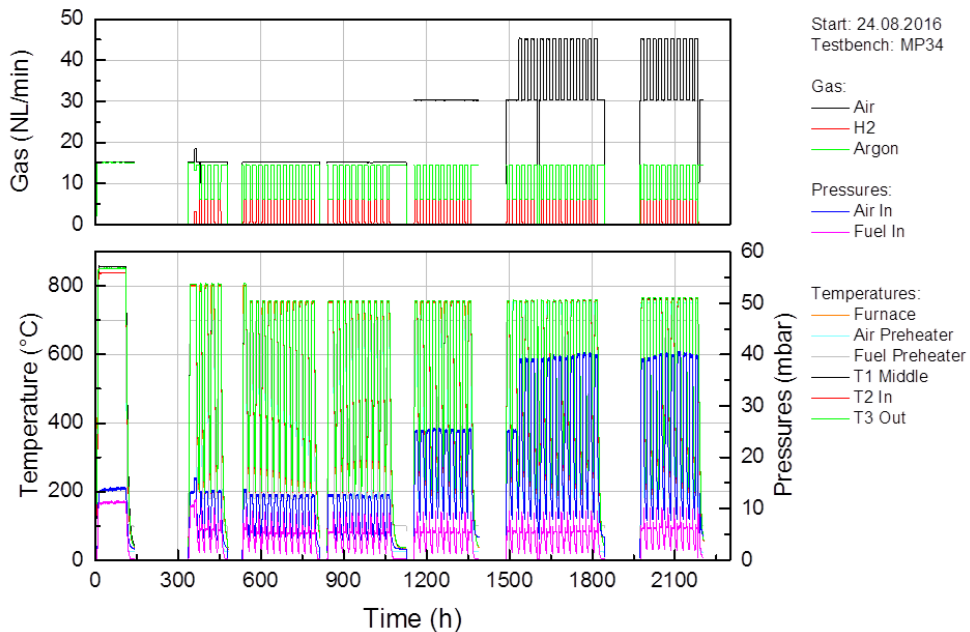


Fig. 10: CS^V03-01: Experimental data over 53 thermal cycles

3.1.2.2 Modellierung von Kassettenstacks

The aim of this work was the development of a multiphysical overall model to predict the structure-mechanic behavior of an SOFC cassette stack under thermal load. A three-dimensional overall model was developed for the numerical fluid-dynamics and thermomechanical analysis of an SOFC stack. It consists of two discrete individual models, a fluid-dynamical finite-volume model and a structure-mechanical finite-element model, which are numerically coupled. Using the overall model, which describes a two-cell stack, the deformation behavior of the structure under thermomechanical load conditions can be described. Fig. 11 shows the structure of a stack.

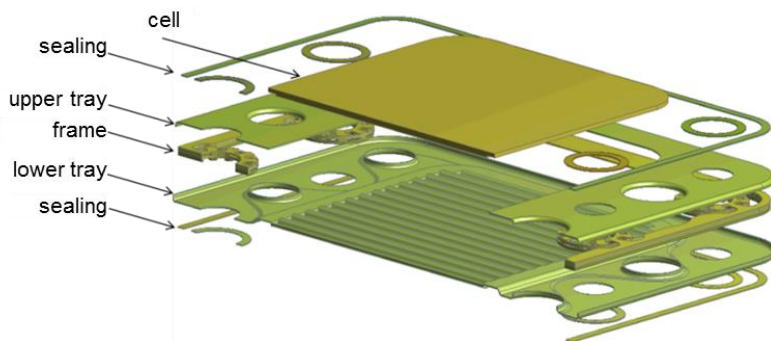


Fig. 11: Exploded view of the cassette

The spatial temperature fields and temperature gradients occurring in the stack were calculated by means of coupled fluid-dynamic analysis, as shown by the example in Fig. 12.

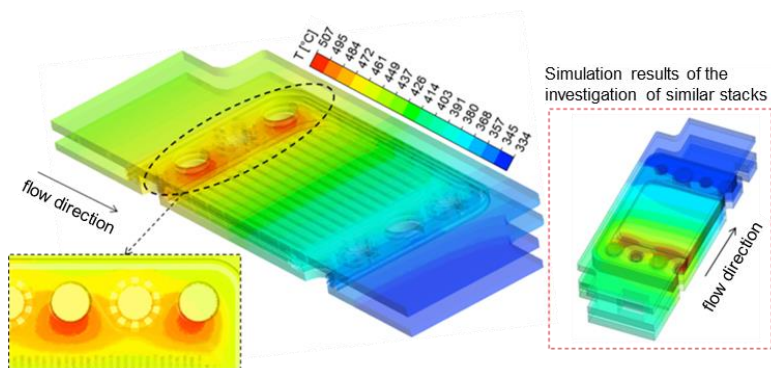


Fig. 12: Temperature distribution in the stack

In order to conduct the quasi-static calculation, the temperature was transferred to the structure-mechanical FE model as thermal load. The coupled fluid-dynamical simulation calculation shows that the model is well suited for the examination of time-dependent thermal stack behavior. The fluid-dynamical model can be used to determine the spatial temperature distribution in the stack in the various stationary and transient process phases. The temperature profiles thus obtained serve as thermal load and define some of the boundary conditions required for conducting the thermomechanical analysis based on the FEM. The results of the fluid-dynamic calculations show that – due to the large temperature gradient – the inlet region of the hot gases is an endangered zone in which high stresses can be expected. The model validation based on experimental data confirms these simulation results.

Based on these models, the following process phases were examined: preheating, operation, cooling. An increase of 7 K/min from 50 °C to 750 °C results in a preheating period of 6000 s (1.67 h). As shown in Fig. 13, the calculation results reveal that the highest stresses occur during preheating.

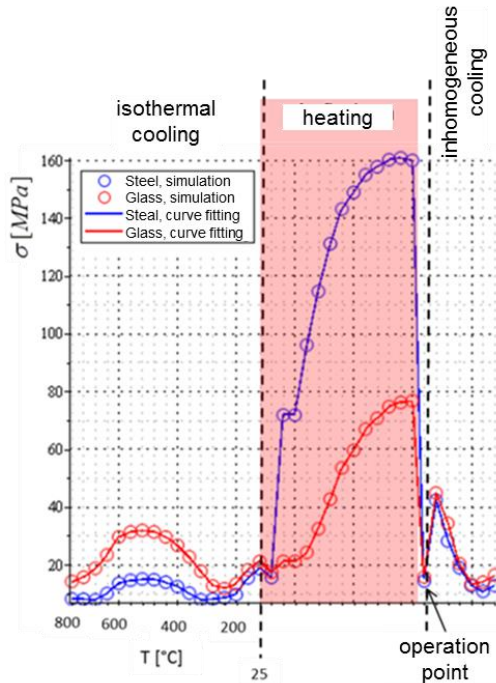


Fig. 13: Stress curve relative to thermal load during a process cycle

3.1.2.3 Long-term tests in F10 design

In October 2015, short stack F1002-97 – which consisted of two cells – achieved an operating time of 70,000 h at a current density of 0.5 Acm^{-2} using hydrogen. The stack from 2007 thus replaced the previous record holder, a tubular cell manufactured by Siemens Westinghouse Power Corporation (SWPC), which had been in operation for approximately 69,000 h.

Over the entire operating time the degradation of the stack was only roughly 0.6 % per 1000 operating hours, which manifested itself in a decrease in voltage and the associated performance loss (see Fig. 14). The stack has now been in operation for more than 83,000 h.

The further developed 4-level short stack F1004-21 from 2010, which featured an improved protective layer on the cathode side, was successfully operated for 34,500 h (see Fig. 14). During this time, it degraded by 0.3 %/kh on average. However, from approximately 28,000 h onwards, the aging process accelerated primarily in one level, so that the experiment had to be terminated. The post-examination revealed that manganese from the contact layer had diffused through the electrolyte to the anode side and mechanically destroyed the electrolyte in that process. These results provide important information about the choice of materials and the structure of future stacks. The 4-level short stack F1004-67, in which the manganese-rich contact layer was replaced with LSCF, has now been in operation for approximately 15,000 h at an aging rate of 0.25 % per 1000 operating hours (see Fig. 14).

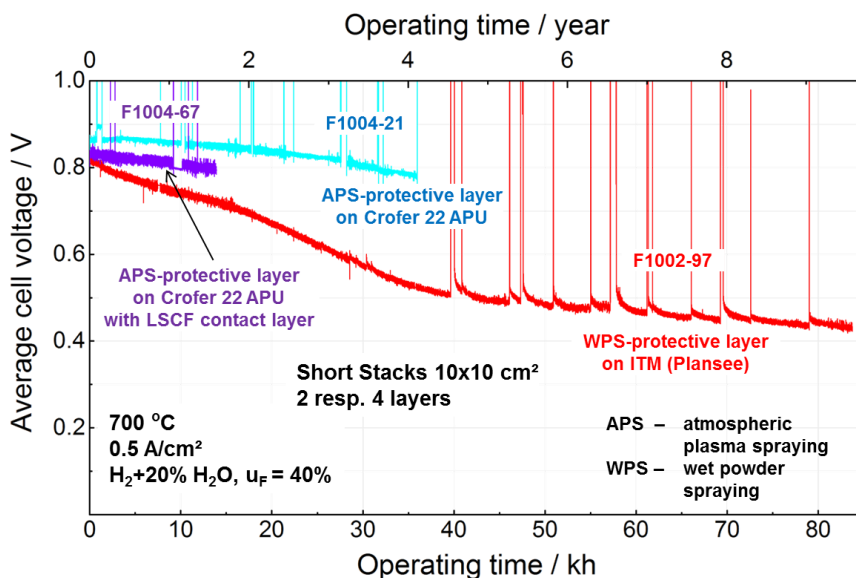


Fig. 14: Long-term behavior of stacks F1002-97, F1004-21, and F1004-67

3.1.2.4 SOE – high-temperature electrolysis

A solid-oxide-electrolysis (SOE) stack consisting of fuel-electrode-supported cells (ASCs in fuel cell mode) was developed according to the F10 design (F1002-165). ASCs are based on Ni/8YSZ (8 mol% yttria-stabilized zirconia) with an LSCF air electrode ($\text{La}_{0.58}\text{Sr}_{0.4}\text{Co}_{0.2}\text{Fe}_{0.8}\text{O}_{3-\delta}$), and 8YSZ electrolyte. A gadolinium-doped cerium oxide (GDC) ($\text{Ce}_{0.8}\text{Gd}_{0.2}\text{O}_{1.9}$) barrier layer was applied between 8YSZ and LSCF using physical vapor deposition (PVD).

The stack was characterized in a furnace environment, both in fuel-cell and in electrolysis mode at between 700 °C and 800 °C with 50 % humidified hydrogen (see Fig. 15). The electrolysis operation was initially conducted at three different temperatures (700 °C, 750 °C, and 800 °C) at a current density of -0.5 Acm^{-2} and a vapor-utilization rate of 50 %. The operating time for each period was more than 500 h. The long-term electrolysis operation was then conducted at 800 °C at the same current density and vapor-utilization rate. The potential influence of reversed operation on aging in SOE mode was investigated by temporarily operating the stack in fuel-cell mode for more than 1000 h. The voltage curve in the subsequent electrolysis operation does not exhibit any change in long-term behavior, however. Electrochemical impedance spectroscopy (EIS) with a subsequent analysis of the distribution function of the relaxation times (DRT) was used for the degradation analysis. After more than 13,000 h of operation, the stack exhibited an average voltage degradation of 0.7 %/kh (see Fig. 16).

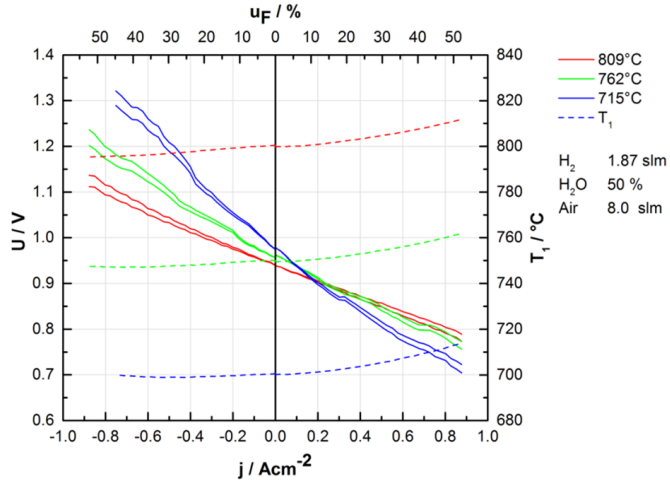


Fig. 15: Stack characteristics (SOFC and SOEC) with 50 % humidified H_2 at furnace temperatures of 715 °C, 762 °C, and 809 °C

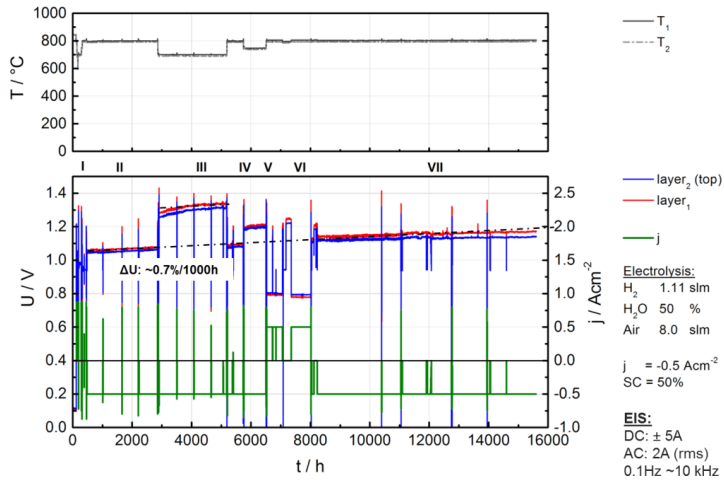


Fig. 16: Stack F1002-165: Long-term behavior in electrolysis mode (phases I, II, III, IV, VII) and fuel-cell mode (phases V, VI) ($H_2O:H_2 = 1:1$, electrolysis: -0.5 Acm^{-2} , 50 % vapor utilization; fuel cell mode: $+0.5 \text{ Acm}^{-2}$, 50 % fuel utilization)

Based on the results from single-cell measurements as well as on previously conducted DRT studies with F-design short stacks (0.1–10 kHz), three processes observed via DRT (shown in Fig. 17) were identified. They are listed in Table 4. A further process not listed in the table was observed during the experiments between 0.1 Hz and 1 Hz with the oxygen partial pressure below 5 %. This process corresponds to the gas diffusion in the air electrode.

The analysis showed that the degradation is primarily due to the rising ohmic resistance. A slight increase in air-electrode polarization was also observed.

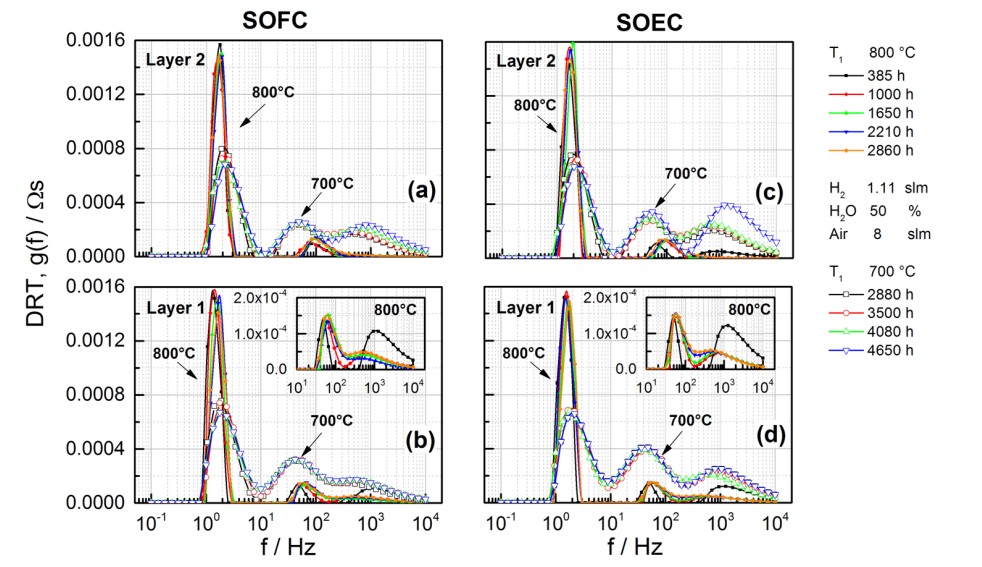


Fig. 17: Calculated distribution curves for both electrode layers at 800 °C and 700 °C in SOFC and SOE mode, using the real part of the impedance spectra; (a) level 2 in SOFC mode; (b) level 1 in SOFC mode; (c) level 2 in SOEC mode; and (d) level 1 in SOEC mode.

Process	Frequency range	Physical process
I	1-10 Hz	Gas diffusion in the substrate (fuel electrode) Overlap with gas-utilization impedance
II	10-300 Hz	Chemical surface exchange of O ₂ and O ²⁻ diffusion in the structure of the air electrode (“bulk diffusion”)
III	200-1000 Hz	Superimposed processes (including gas diffusion), coupled with charge exchange reactions and ion transport in YSZ of the functional layer of the fuel electrode

Table 4: Processes in stack F1002-165 analyzed via DRT

3.1.2.5 Systems engineering

5 kW system with anode off-gas recirculation

Recirculating anode off-gas within an SOFC system has two major advantages: firstly, unused fuel is recirculated from the stack outlet to the stack inlet, reducing the amount of fresh fuel fed into the system. This increases the fuel utilization of the system and permits an electrical efficiency of more than 60 %. Secondly, the recirculated electrochemically produced vapor can be used for the steam reforming process. External steam generation is thus not necessary during operation. The high anode off-gas temperature of at least 700 °C presents a challenge which precludes the use of commercially available blower units. This is why the use of ejectors is discussed in the literature. There are also approaches involving the development of high-temperature blowers or using commercial blowers combined with heat exchangers.

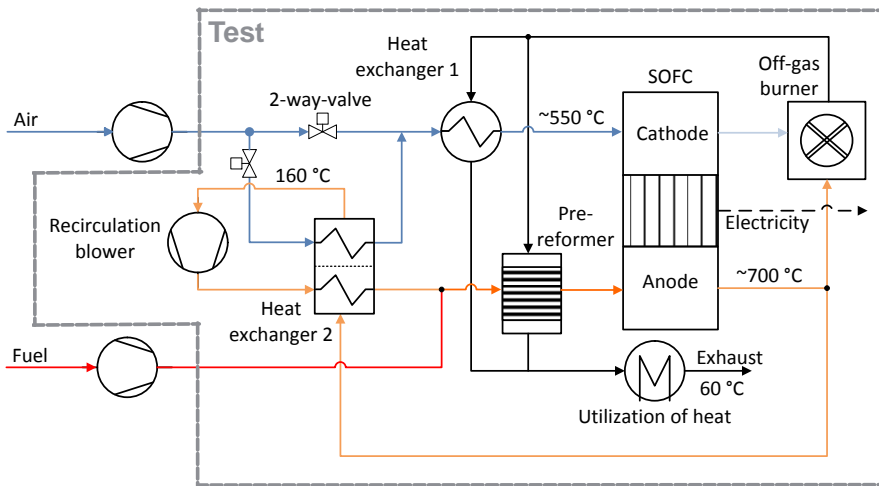


Fig. 18: Flow diagram of the SOFC system

An SOFC system with an anode off-gas recirculation loop was developed. The anode off-gas recirculation loop comprises a heat exchanger and a low-temperature blower, which is functional at temperatures of up to 200 °C. Using this system, experiments were conducted to analyze the influence of the recirculation rate and the fuel utilization on the system operation. During the tests, the fuel utilization of the system was set to 90–93 % while the recirculation rate varied between 73 % and 82 %. The test results show that changes in the recirculation rate influence cell voltages, cathode-side amounts of cooling air, and the electrical efficiency, for example. Basically, high recirculation rates at high current densities reduce cell voltages and the amount of cooling air. The highest electrical efficiency was achieved at a high system fuel utilization, low recirculation rate, and resulting high stack fuel utilization.

The flow diagram of the SOFC system analyzed is shown in Fig. 18. The entire system (excluding the air and fuel blower) was examined within the test bench.

The whole test bench is shown in Fig. 19. The high-temperature components (heat exchanger 1, pre-reformer, SOFC, and off-gas burner) are combined in one module, the “integrated module”. The recirculation unit is located at the front and comprises an electronics box, heat exchanger 2, two two-way valves, a recirculation blower, and a measuring instrument for the recirculation rate.

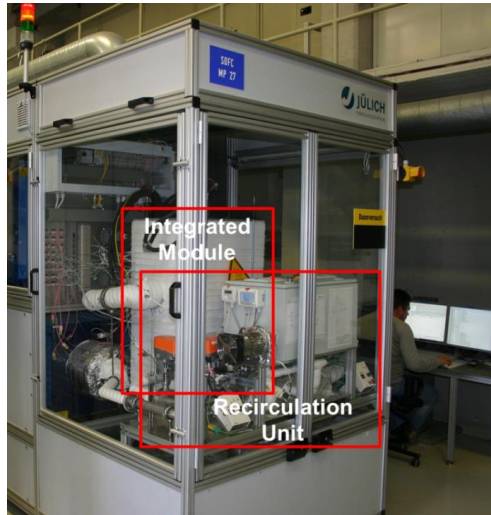


Fig. 19: Recirculation unit with 5 kW integrated module in the system

The effects of anode off-gas recirculation on the electrical efficiency are shown in Fig. 20. The solid lines represent the measured efficiency, which comprises the measured power output of the stack and the measured power requirement of the recirculation blower. The dotted lines show the efficiency of an entire system, including air blower (assumed efficiency: 27 %), additional electrical power requirement of the system (assumed value: 50 W), and inverter (assumed efficiency: 94%). The temperatures show the average stack mass temperature for each test.

At a constant current of 90 A and a constant system fuel utilization of 90 % (diagram on the left-hand side), a reduction of the recirculation rates increases the electrical efficiency to as much as 64 %. At this point, the calculated net system efficiency is approximately 59 %. Fig. 20 also shows the efficiency at a system fuel utilization of 93 %. At the same recirculation rate, the efficiency is higher than with a system fuel utilization of 90 %. This permits the conclusion that the highest efficiencies are achieved at high system fuel utilization and low recirculation rates. Fig. 20 also shows the electrical efficiencies at different DC stack power outputs. By increasing the stack temperature and reducing the recirculation rate, an almost constant electrical efficiency is achievable across a wide power range. The highest DC power output was 4 kW. This measuring point correlated to an average stack temperature of 762 °C and a recirculation rate of 73 % and resulted in a measured efficiency of 60 %.

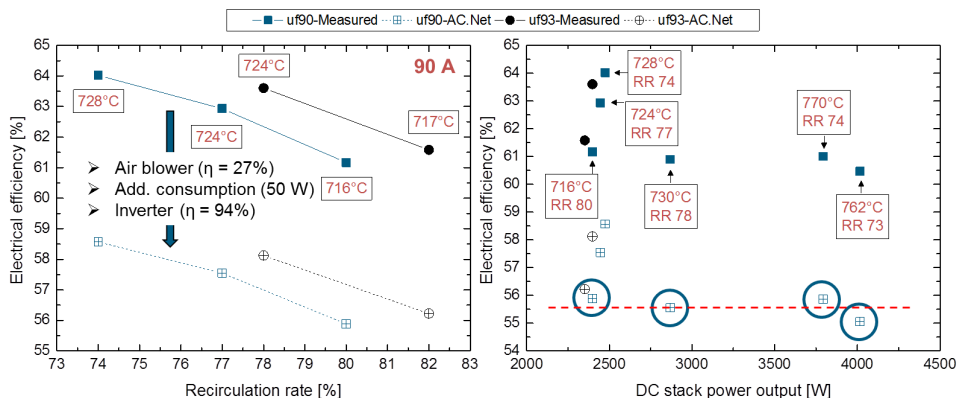


Fig. 20: Electrical efficiency for various recirculation rates and a constant current of 90 A (left-hand side); electrical efficiency for various DC power outputs and various recirculation rates (right-hand side)

The system was tested for more than 2,000 h, revealing the following results:

- Anode off-gas recirculation in combination with the Jülich “integrated module” is feasible
- The recycling and control strategy developed here works well
- High recirculation rates lead to a reduced demand for cooling air by the stack
- The stack tolerates anode off-gas entry temperatures of 500 °C
- The highest electrical efficiencies are achieved at high system fuel utilization in combination with low recirculation rates
- Constant efficiencies are possible over a wide power range (also with temperature increases during operation)
- Net electrical efficiencies exceeding 60 % can be achieved (with a new stack)

5 kW system test with hydrogen and high fuel utilization

In order to investigate the behavior of an SOFC stack in a system environment during operation with hydrogen and at high fuel utilization (which can also be an operating state in rSOC operation), a 5 kW stack (F”2036-08) was installed in the 20 kW system in combination with the integrated module.

This stack comprised two substacks of 18 cell levels each (cell size: 20x20 cm²). This test was also intended as a trial for the substack concept for the next generation of 15 kW stacks.

The individual substacks were first joined separately in a furnace and then characterized. The characteristic curves of both substacks, measured with 20 % humidified hydrogen, are shown in Fig. 21 for a furnace temperature of 700 °C. They display a very similar behavior so that they can be operated as a single stack without problems. In order to verify whether operation is possible at high fuel utilization, both substacks were also operated at fuel utilization rates of 40 %, 70 %, and 80 % for several hours. Fig. 22 shows the performance over time of substack S2. At 80 % fuel utilization and 0.5 Acm⁻², the cell voltages are in the range of 800–830 mV and are very stable.

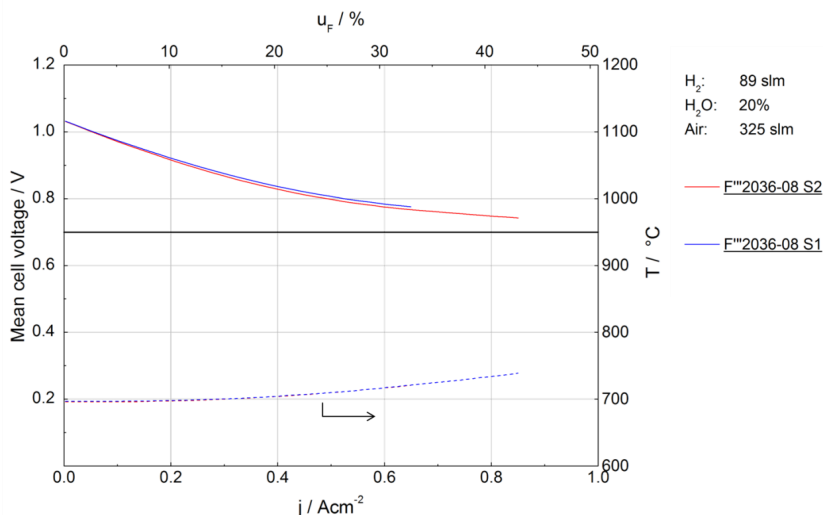


Fig. 21: F'''2036-08: performance of submodule S1 and S2 at 700 °C in the furnace

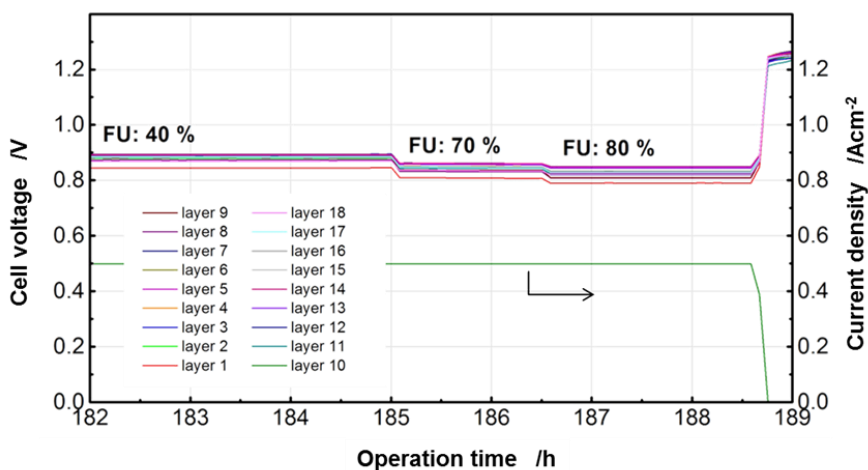


Fig. 22: F'''2036-08 S2: substack behavior as a function of fuel utilization during operation with dry hydrogen at 700 °C in the furnace

Since the 20 kW system and the components of the integrated module developed for it (air preheater, pre-reformer, and afterburner) were to be used, the stack was operated in counterflow mode. The cathode air was preheated to roughly 520 °C. The hydrogen was preheated in the pre-reformer (which functioned solely as a heat exchanger here), heated by the off-gas, to approximately 300 °C. These are the temperatures at which the gases enter the stack. In order to limit the amount of air to an air surplus factor of roughly 5 (which is necessary for efficiency reasons and the admissible overpressure in the stack), the temperature difference between air inlet and air outlet must be at least 200 K. Fig. 23 shows the temperature curve in an interconnector in the center of the stack. The thermocouples are located in drilled holes 10 mm in depth so that the temperature is measured at the edges of

the cells. The results of stack models led to the expectation that the maximum temperature in the center would be approximately 20 K higher. The temperature at the edge of the cell is approximately 630 °C at the air inlet, and approximately 810 °C at the air outlet (= fuel inlet). The stack was operated at 0.5 Acm⁻² and a fuel utilization of 80 %. The power, temperature, and average cell voltage curves are shown in Fig. 24. The power output – initially 4.9 kW at an average cell voltage of 760 mV – is slightly below the values that were expected from the preliminary experiments. This was attributed to the fact that large parts of the stack had a temperature of below 650 °C. The voltage decreased by approximately 1.8%/kh. The reason for this will have to be clarified in the post-test analysis.

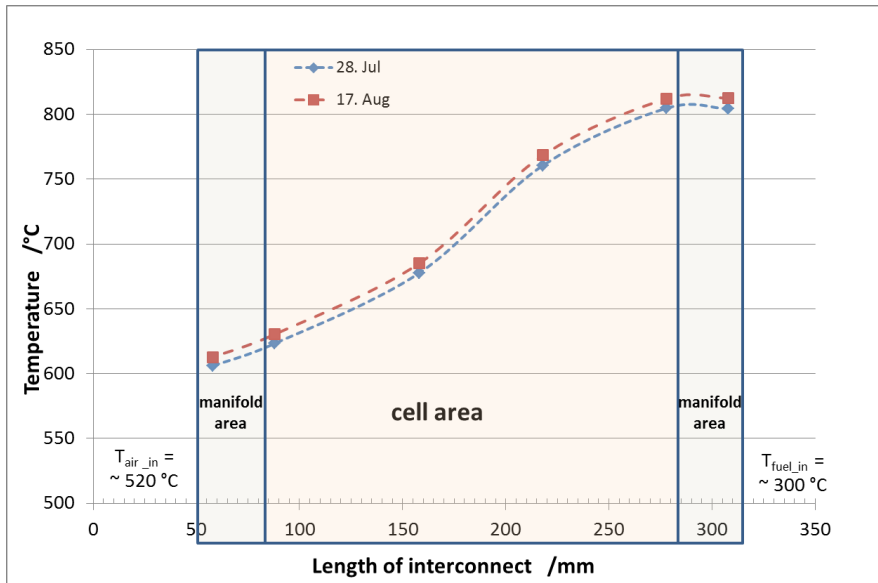


Fig. 23: F”2036-08: Temperature distribution in one cell level in the center of the stack at 5 kW DC power (measured at a depth of 10 mm in the interconnector)

Due to a disturbance in the device periphery, an uncontrolled shutdown occurred, which damaged one of the cells. This meant that the experiment had to be discontinued after approximately 1,170 operating hours.

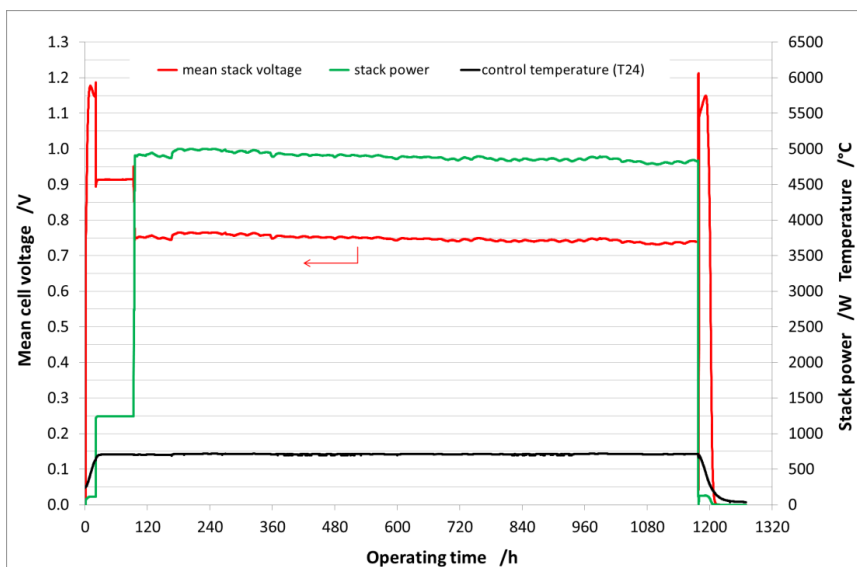


Fig. 24: F''2036-08: behavior with hydrogen and 80 % fuel utilization at 0.5 Acm^{-2} as a function of the operating time

3.1.3 Staff members and fields of activity

Name	Tel. (02461-61-) Email	Field of activity
Prof. L. Blum	6709 l.blum@fz-juelich.de	Head of Solid Oxide Fuel Cells
A. Al-Masri	3774 a.al-masri@fz-juelich.de	Simulation of SOFC stacks, CFD and FEM
R. Deja	5291 r.deja@fz-juelich.de	System simulation, development and testing of SOFC system components
M. Engelbracht	4652 m.engelbracht@fz-juelich.de	System simulation, development and testing of SOFC system concepts
Dr. Q. Fang	1573 q.fang@fz-juelich.de	Head of SOFC Electrochemical Measuring Technology, electrochemistry, testing and analysis
M. Frank	1573 ma.frank@fz-juelich.de	System simulation, development and testing of rSOC system concepts
I. Hoven	4053 i.hoven@fz-juelich.de	Electrical engineering, measurement data acquisition and systems control

Dr. V.N. Nguyen	8393 v.n.nguyen@fz-juelich.de	Chemical process engineering, development and testing of system components
Fr. U. de Haart	5170 u.de.haart@fz-juelich.de	Testing of SOFC stacks and test evaluation
Dr. M. Peksen	8732 m.peksen@fz-juelich.de	Simulation of stacks and high-temperature system components, CFD and FEM
Ro. Peters	4664 ro.peters@fz-juelich.de	Head of SOFC Systems Engineering, component development, system design, system engineering and system testing
Y. Yan	5487 y.yan@fz-juelich.de	SOFC, Electrochemical Measuring Technology, testing of SOFC stacks and test evaluation

3.1.4 Important publications, doctoral theses and patents

Publications in peer-reviewed journals

Fang, Q., Berger, C.M., Menzler, N.H., Bram, M., Blum, L.

Electrochemical characterization of Fe-air rechargeable oxide battery in planar solid oxide cell stacks

Journal of Power Sources 336 (2016) 91-98

Peters, R., Deja, R., Engelbracht, M., Frank, M., Nguyen, V.N., Blum, L., Stolten, D.

Efficiency analysis of a hydrogen-fueled solid oxide fuel cell system with anode off-gas recirculation

Journal of Power Sources 328 (2016) 105-113

Blum, L., de Haart, L.G.J., Malzbender, J., Margaritis, N., Menzler, N.H.

Anode-Supported Solid Oxide Fuel Cell Achieves 70 000 Hours of Continuous Operation *Energy Technology* 4 (8) (2016) 939-942

Nguyen, V.N., Deja, R., Peters, R., Blum, L.

Methane/steam global reforming kinetics over the Ni/YSZ of planar pre-reformers for SOFC systems

Chemical Engineering Journal 292 (2016) 113-122

Engelbracht M., Peters, Ro., Blum, L., Stolten D.

Analysis of a Solid Oxide Fuel Cell System with Low Temperature Anode Off-Gas Recirculation

Journal of The Electrochemical Society, 162 (9) (2015) 982-987

Blum L., Batfalsky P. Fang Q., de Haart L. G. J., Malzbender J., Margaritis N., Menzler N. H., Peters Ro.

SOFC Stack and System Development at Forschungszentrum Jülich

Journal of The Electrochemical Society, 162 (10) (2015) 1199-1205

Fang, Q., Blum, L., Peters, Ro., Peksen, M., Batfalsky, P., Stolten, D.

SOFC stack performance under high fuel utilization

International Journal of Hydrogen Energy 40 (2015) 1128-1136

Nguyen, V.N., Blum, L.

Syngas and Syngas from H₂O and CO₂: Current Status

Chem. Ing. Tech. (2015) 87, No. 00, 1–23

Engelbracht M., Peters, Ro., Blum, L., Stolten D.

Comparison of a fuel-driven and steam-driven ejector in solid oxide fuel cell systems with anode off-gas recirculation: Part-load behavior

Journal of Power Sources 277 (2015) 251-260

Fang Q., Blum L., Menzler N. H.

Performance and degradation of solid oxide electrolysis cells in stack

Journal of The Electrochemical Society, 162 (8) (2015) 907-912

Peters, Ro., Deja, R., Blum, L., Nguyen, V.N., Fang Q., Stolten, D.

Influence of operating parameters on overall system efficiencies using solid oxide electrolysis technology

International Journal of Hydrogen Energy 40 (2015) 7103-7113

Peksen, M., Al-Masri, A, Peters, Ro., Blum, L., Stolten, D.

3D multiscale-multiphysics SOFC modelling status at the Institute of Electrochemical Process Engineering

ECS Transactions, 68 (1) (2015) 2861-2866

Peksen, M.

Numerical thermomechanical modelling of solid oxide fuel cells

Progress in Energy and Combustion Science 48 (2015) 1-20

Peksen, M.

3D CFD/FEM analysis of thermomechanical longterm behaviour in SOFCs: Furnace operation with different fuel gases

Journal of Hydrogen Energy 40 (2015) 12362-12369

Peksen, M., Meric, D., Al-Masri, A, Stolten, D.

A 3D multiphysics model and its experimental validation for predicting the mixing and combustion characteristics of an afterburner

Journal of Hydrogen Energy 40 (2015) 9462-9472

Important patents

Patent applications:

Principal inventor	PT	Description
M. Engelbracht	1.2760	A process for producing a protective gas

Patents granted:

Principal inventor	PT	Description
Dr. W. A. Meulenbergh.	1.2366	A membrane power plant and a method for operating such a system
Dr. M. Peksen	1.2474	Fuel cell modules

3.2 Fuel processing systems

3.2.1 Objectives and fields of activity

The availability of hydrogen is a prerequisite for the use of fuel cells in mobile and stationary applications. An option for passenger cars, buses, and fleets of vehicles in the delivery sector is to combine electric motors with hydrogen-driven fuel cells. However, the infrastructure for hydrogen as a future energy carrier first has to be established. In future, hydrogen will be produced from renewable and solar power using electrolysis. With a pressure tank of 700 bar, a range of approx. 350–400 km can be achieved. Such ranges are insufficient for trucks, ships, and aircraft. Due to the poor storage properties of liquid and gaseous hydrogen compared to today's fuels (i.e. gasoline, kerosene, and diesel), liquid fuels are preferable for the aforementioned areas of application. The tank system as a whole with its mass- and volume-specific power densities must be considered in analyses. The aforementioned energy carriers are mainly produced today from the fossil primary energy carrier crude oil. In the long term, some of the liquid energy carriers currently required could be produced from biomass or synthesized from carbon dioxide and hydrogen.

Carbon dioxide from industrial off-gases and renewable hydrogen represent the basis for the production of electrofuels, a process often termed "*Power-to-Fuel*". Potential fuels include n-alkanes from Fischer–Tropsch synthesis, alcohols, various ethers and n-alkanes, cycloalkanes, and aromatics from an oligomerization process. In addition to using hydrogen for fuel cell vehicles, this represents a further integration of renewable energy in the transport sector – and a reduction of our dependence on oil. Renewable hydrogen can thus also find its way into goods and passenger transport using ships, aircraft, and trucks. Synthetic fuels furthermore permit engine efficiencies to be improved and limited emissions to be reduced.

Fuel cells are not available in the power classes needed for drive trains in maritime applications or aviation (i.e. larger than 1 MW_e). In driving mode, the diesel engines used in the truck sector are extremely efficient and have a high mass- and volume-specific power density. When idling, a power of 3–5 kW_e is generated to operate air conditioning or electrical heating as well as to supply electrical devices on board. Under these load conditions, diesel engines have an efficiency of only 10–15 %; special power units – small internal combustion engines – have slightly better efficiencies of 20–30 %. In aviation, on-board power on the runway and sometimes at the gate is generated by auxiliary power units with efficiencies of approx. 20%.

At IEK-3, research in the field of fuel processing concentrates on reforming middle distillates, the desulfurization of kerosene, and system development for on-board power supply in combination with HT-PEFCs. Reformers are also being developed for high-temperature SOFCs. All areas of work are supported by relevant modeling. Important tools are CFD simulations on the institute's own cluster and system simulations using the Simulink program in order to optimize the dynamic performance under load changes and for starting strategies.

3.2.2 Important results

3.2.2.1 Catalysts for autothermal reforming

As part of a doctoral project concluded in 2015, different catalysts (Rh/ γ -Al₂O₃, Rh/La-Al₂O₃, Rh/CeO₂, Rh/Gd-CeO₂, Rh/ZrO₂ and Rh/Y-ZrO₂, as well as Pt, Ru, Ni, PtRh, and PtRu on γ -Al₂O₃) were synthesized, comprehensively characterized using well-established methods (TDS, TPR, TPO, N₂ adsorption, TGA, TEM), and extensively investigated experimentally with respect to autothermal reforming of hydrotreated vegetable oils and fossil-based diesel fuels. It was found that Rh-based catalysts display the highest catalytic activity and stability. A general schematic for various mechanisms of deactivating catalysts was derived from the results obtained and published in the *Journal of Power Sources* in 2016 (Fig. 25). Sintering effects, carbon-containing deposits (fouling), and solid-state reactions were identified as major reasons for catalyst deactivation. One focus of the experiments characterizing the fresh and aged catalyst samples was their temperature-programmed reduction. In these experiments, the consumption of hydrogen (the reducing agent) is a measure of the catalysts' ability to take up and release electrons. This ability is the basic prerequisite for their catalytic activity. In these experiments, the fresh and aged Rh-containing samples displayed by far the best redox properties, which correlated very closely with their outstanding catalytic activity and stability.

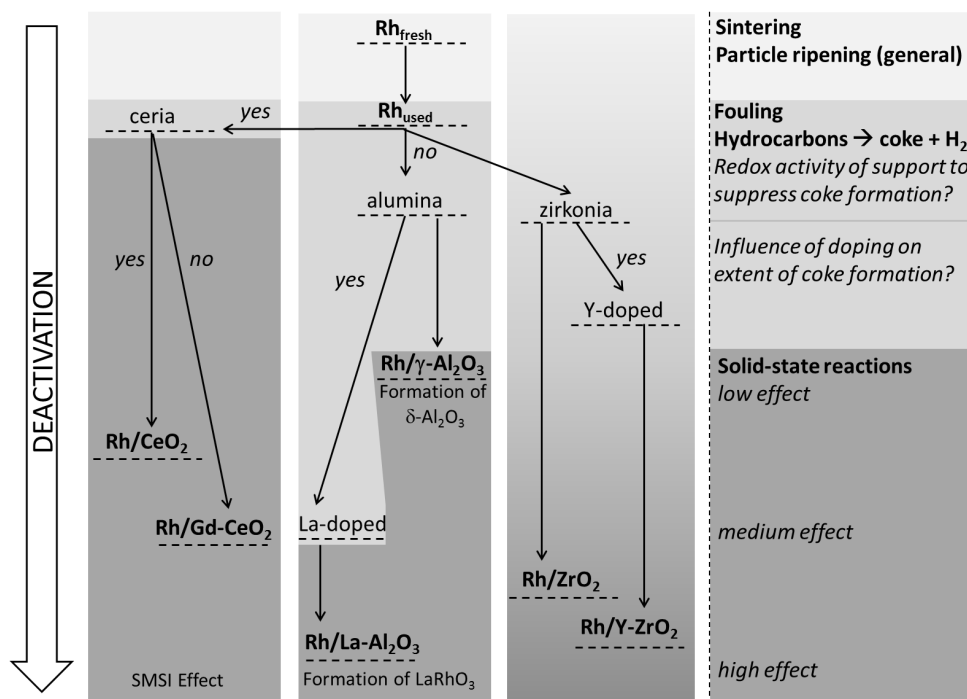


Fig. 25: Schematic of deactivation routes and mechanisms of different types of catalysts for autothermal reforming of liquid hydrocarbons

3.2.2.2 Diesel injection system

As part of the ADELHEID project funded by the federal state of North Rhine-Westphalia (NRW), a fast-closing valve and a diesel pump were developed and manufactured by GSR Ventiltechnik and Thomas Magnete, respectively, according to the specifications for a 28 kW_{th} diesel reformer. Fig. 26 shows the results of spray pattern analyses obtained by using the selected arrangement of the fuel-injection device comprising the pump, a reservoir, a pressure regulator, the fast opening/closing magnetic valve, and the pressure swirl nozzle before integration into the ATR AH2. The image series in Fig. 26 has a time interval of 75 µs at 13300 fps for each image.

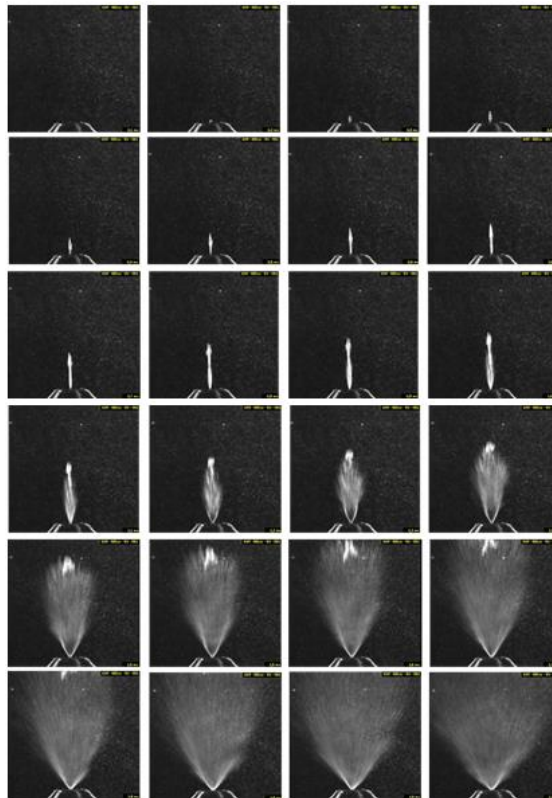


Fig. 26: Series of video stills recorded by the high-speed camera at a frame rate of 13,300 fps during pulsed operation of the fuel injection device. The pressure swirl nozzle is situated at the bottom. The formation of the spray pattern is shown

The spray pattern formed in 1.5–2 ms. It is important that a liquid jet no longer occurs after less than 1 ms. The development of the pump and magnetic valve in combination with the technical layout was therefore successfully implemented. For a good-quality spray pattern, a constant operating pressure of 40–50 bar is ideal. A storage pressure of 50 bar was set for the measurements in Fig. 26. The repetition rate was 16 2/3 Hz, corresponding to 60 ms per stroke. The effective minimal load was 10 %. The theoretically conceivable load of 5 % could not be achieved. A load of 10 % was only possible to a limited extent because the spray was of low quality.

3.2.2.3 Reformer development

All generations of autothermal reformers developed at IEK-3 in the past few years have in common that they are equipped with a pressure swirl nozzle for the injection of cold diesel fuel. They all have a fuel evaporation chamber, in which fuel is vaporized and mixed with superheated steam and part of the air. During fuel cell system operation, the steam is produced by the catalytic burner. It is heated in a superheater to the required temperature of more than 400 °C using the waste heat of the product gas stream from the reformer. The other part of the volume flow of air is conducted into the reformer via the air inlet. In the mixing chamber, air is mixed with the steam and the vaporized fuel. The central component of every reformer developed by IEK-3 is the catalyst. In most cases, it consists of a bimetallic RhPt species applied to a $\text{Al}_2\text{O}_3\text{-CeO}_2$ washcoat, which is in turn applied to a monolithic cordierite substrate.

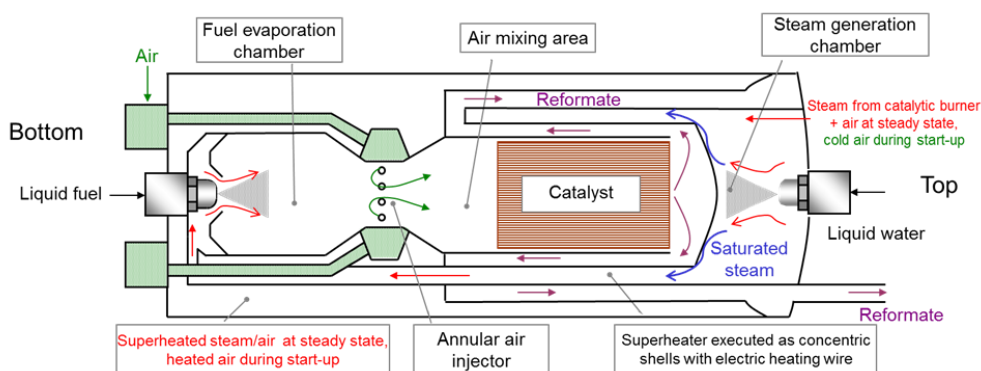


Fig. 27: Basic structure of the latest reformer generation designed by IEK-3, ATR 12

The latest reformer developed by IEK-3, ATR 12, Fig. 27 is a further development of ATR AH2. The improvements to ATR AH2 in comparison to previous reformer generations consist of an additional pressure swirl nozzle for the injection of cold water, as well as a corresponding steam generation chamber. This means that an external processing component (mixer) for supplying steam is no longer necessary. Furthermore, the cross-sectional area of the ATR AH2 superheater – through which a considerable amount of air is fed to the reformer – was enlarged while simultaneously reducing its length. The pressure drop caused by the superheater was thus significantly reduced. These advantages concerning the design of the autothermal reformer are not decisive if the operation of the reformer is considered in isolation. They only play a role with respect to the entire fuel cell system since they reduce the parasitic losses caused by the air compressor and significantly simplify the system layout. This strategy of taking into consideration important technical requirements from the point of view of the entire fuel cell system was consistently continued in the design and construction of ATR 12. The technical design of the superheater was substantially modified and further improved. The previously used coiled tubing for the transfer of waste heat from the reformate to the mass flow of saturated steam was replaced by concentric shells into which turbulence inserts were introduced in order to improve the heat transfer properties. This modification aimed at a further reduction of pressure drops in this part of the reformer and a homogenization of the media flows as they enter the fuel evaporation chamber. The concentric shells also offer sufficient room for an electric heating

wire to be integrated. This modification permits the reformer to be started up in a quick and autonomous manner.

3.2.2.4 Start-up and power-down strategies

Based on experimental results in the literature, the start-up process of ATR AH2 was examined with respect to the formation of undesirable by-products such as ethene, ethane, propene, and benzene. These substances had in the past been shown to be precursors of carbonaceous deposits on the catalyst surface, which also decrease catalytic activity. Fig. 28 shows the media flows and resulting concentrations during a conventional start-up. It begins with a large volume flow of air at a temperature of 450 °C and a mass flow of steam at $T = 350$ °C being fed into the vaporization and mixing chambers of the reformer. Subsequently, the volume flow of air is considerably reduced to 2 m³/h while a mass flow of 3.2 kg/h of steam is fed in. Both measures were taken in order to avoid hotspots caused by exceeding oxygen concentrations during fuel feed-in. In the next step, an amount of diesel fuel was added that corresponds to 50 % reformer load. Fig. 28 shows that considerable amounts of by-products were formed during this start-up process. Thus, the concentrations of ethene and propene, for example, amounted to 2100 ppmv and 3600 ppmv, respectively. As a consequence, elaborate test series led to the start-up process being modified so that the air volume flow was no longer sharply reduced to 2 m³/h but to only 4 m³/h. This roughly corresponds to the volume flow in the stationary operating state of ATR AH2 at 50% load. Thus, the formation of the aforementioned by-products was almost completely inhibited. A similar technique was applied to the shut-down strategy.

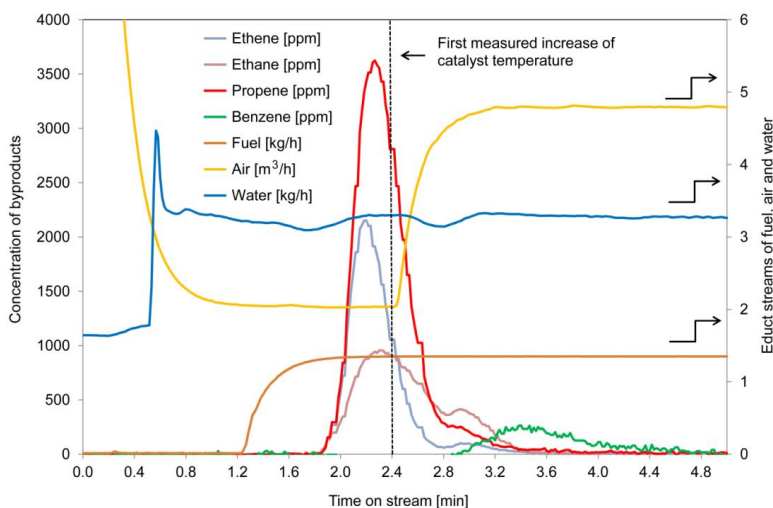


Fig. 28: The concentrations of ethene, ethane, propene, and benzene in the reformat of ATR AH2, mass flows of diesel and water, and the air volume flow during conventional start-up

3.2.2.5 Wasser-Gas-Shiftreaktor

Experiments were conducted under stationary conditions in order to analyse the activity and stability of two commercial catalysts for the water-gas shift reaction. Fig. 29 shows the results of these investigations under high-temperature shift conditions at an inlet temperature of

410 °C. Both catalysts displayed an almost constant CO conversion rate close to the thermodynamic equilibrium over the operating time of 24 h. The average conversion rates amounted to 53.2 % for catalyst A and 55 % for catalyst B. CO conversion was also individually analysed in the first and the last two hours of operation. The difference between the triangles and the squares indicates whether operation was stable or unstable.

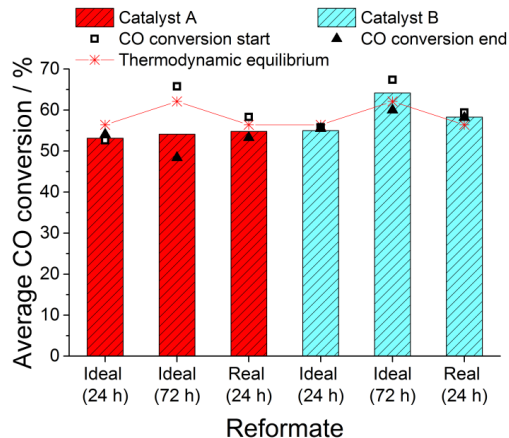


Fig. 29: CO conversion at stationary operation under HTS conditions with ideal and real reformat; comparison between catalysts A and B ¹

As can be seen in the Fig. 29, both catalysts work in a very stable manner if the reformat is ideal. The results from the 24 h and the 72 h test of catalyst A differ; this may be caused by a slightly different temperature level, on the one hand, and by the diverging operating time, on the other hand, but is also due to sample variability. For the real reformat, catalyst A achieved an average CO conversion of 54.8 %. In this experiment, the catalyst deactivated from initially 58.3 % to 53.3 %. Despite this, the real reformat displayed no significant influence on catalyst stability. Catalyst B achieved an average conversion of 58.3 % at almost unchanged activity throughout the operating period. In comparison with the ideal reformat, this indicates a negligible influence of the 220 ppmv higher hydrocarbons. In the experiments with real reformat, the hydration of alkenes into alkanes was observed. These side reactions did not seem to negatively influence catalyst B under the test conditions. Irrespective of the reformat quality, the operation of catalyst B was nearly stable. However, with slight changes in the operating temperature, the catalyst operation was more stable over a period of 24 h than over 72 h. In comparison, the degradation behavior of catalyst A is more difficult to interpret due to the increased sample variability.

¹ D. Krekel, Betriebsstrategien für Brenngaserzeugungssysteme zur Anwendung in HT-PEFC-Hilfsstromaggregaten, doctoral thesis at RWTH Aachen University, date of oral examination: 9 December 2016.

3.2.2.6 PEFC system development focusing on fuel processor

As part of the EU-funded FCGEN project (fuel cell based power generation), an international consortium pursued the objective of developing and testing in the laboratory a fuel cell system based on PEFC and autothermal reforming of standard diesel fuel. An important aspect of such a system is the fuel processor, which serves to produce a hydrogen-rich gas flow (reformat) of sufficient quality, which can then be fed into the fuel cell anode. Quality requirements included, on the one hand, that the concentration of non-methane hydrocarbons (NMHCs: ethene, ethane, propene, benzene, etc.) in the reformat ideally be zero and, on the other hand, that the concentration of CO be less than 25 ppmv and that of sulfur less than 1 ppmv. Additionally, the molar flow of hydrogen should be large enough to achieve net electric power of at least 3 kW in the fuel cell. Design aspects such as weight, volume, and costs also had to be taken into careful consideration. IEK-3 coordinated and scientifically headed the fuel processor work package of this project. The following main components were required for the fuel processor: the autothermal reformer is a key component of fuel processing since in it a reaction of diesel fuel, air, and steam produces the hydrogen-containing reformat. The catalytic burner has two functions: on the one hand, it has to convert all combustible components of the off-gas from the anode (H_2 , CO, CH_4) into CO_2 and H_2O . On the other hand, it must be designed in such a way that it can transfer the reaction heat of combustion to the mass flow of water by means of an internal heat exchanger. This produces saturated steam, which is superheated in the internal heat exchanger of the reformer. Intensive tests for FCGEN at IEK-3 experimentally showed that both reactors reliably fulfilled their described functions. The H_2S trap is located in the direction of flow behind the reformer; it reduces the sulfur concentration in the reformat to less than 1 ppmv. The reactors for the water-gas shift reaction and the preferential oxidation of CO are located downstream. Both reactors in tandem have the function of reducing the concentration of CO in the reformat to less than 1 ppmv. Experimental tests conducted within the scope of FCGEN confirmed this.



Fig. 30: FCGEN system with electric power of 3–5 kW; the fuel cell section is visible on the left, and the right-hand side shows the fuel processor

The right-hand side of the above photo (Fig. 30) shows the complete fuel processor after assembly and commissioning. On the left side, the fuel cell and its peripherals can be seen. The experimental testing of all components of the fuel cell system in interaction with each other showed the successful operation of the entire system. The reformer produced a

reformat of the required quality outlined above. The fuel cell system generated electric power in the range of 3 kW.

3.2.3 Staff members and fields of activity

Name	Tel. (02461-61-) Email	Field of activity
Prof. Dr. R. Peters	4260 ra.peters@fz-juelich.de	Head of Fuel Processing and Systems
Dr. J. Pasel	5140 j.pasel@fz-juelich.de	Head of Chemistry for Fuel Processing
Dr. R. C. Samsun	4616 r.c.samsun@fz-juelich.de	Head of Systems Engineering for On-Board Power Supply
A. Tschauder	4547 a.tschauder@fz-juelich.de	Reactor development, reforming, system design
J. Meißner	4306 j.meissner@fz-juelich.de	Catalytic combustion, CO fine cleaning
S. Schemme	2779 s.schemme@fz-juelich.de	Future fuels, process and systems analysis of electrofuels
M. Decker	5322 ma.decker@fz-juelich.de	Future fuels, liquid energy carriers for ships, aircraft, and trucks
S. Weiske	5322 s.weiske@fz-juelich.de	Future fuels, DME synthesis methods, reactor modeling

3.2.4 Important publications, doctoral theses, and patents

Publications in peer-reviewed journals

Pasel, J.; Wohlrab, S.; Rotov, M.; Lohken, K.; Peters, R.; Stolten, D.
Routes for deactivation of different autothermal reforming catalysts
Journal of Power Sources 325 (2016) 51-63

Dolanc, G.; Pregelj, B.; Petrovčič, J.; Pasel, J.; Kolb, G.
Control of autothermal reforming reactor of diesel fuel
Journal of Power Sources 313 (2016) 223-232

Liu, Y.; Lehnert, W.; Janßen, H.; Samsun, R.C.; Stolten, D.
A review of high-temperature polymer electrolyte membrane fuel-cell (HT-PEMFC)-based auxiliary power units for diesel-powered road vehicles
Journal of Power Sources 311 (2016) 91-102

Meißner, J.; Pasel, J.; Peters, R.; Samsun, R. C.; Tschauder, A.; Stolten, D.
Elimination of by-products of autothermal diesel reforming
Chemical Engineering Journal 306 (2016) 107-116

Samsun, R.C.; Krupp, C.; Baltzer, S.; Gnörich, B.; Peters, R.; Stolten, D.
A battery-fuel cell hybrid auxiliary power unit for trucks: Analysis of direct and indirect hybrid configurations
Energy Conversion and Management 127 (2016) 312-323

Krekel, D.; Samsun, R.C.; Pasel, J.; Prawitz, M.; Peters, R.; Stolten, D.

Operating strategies for fuel processing systems with a focus on water-gas shift reactor stability

Applied Energy 164 (2016) 540-552

Samsun, R.C.; Krupp, C.; Tschauder, A.; Peters, R.; Stolten, D.

Electrical start-up for diesel fuel processing in a fuel-cell-based auxiliary power unit

Journal of Power Sources 302 (2016) 315-323

Meißner, J.; Pasel, J.; Samsun, R. C.; Peters, R.; Stolten, D.

Start-Up and Load-Change Behavior of a Catalytic Burner for a Fuel-Cell-Based APU for Diesel Fuel

Fuel Cells 15, 1 (2015) 15–26

Pasel, J.; Samsun, R. C.; Tschauder, A.; Peters, R.; Stolten, D.

A novel reactor type for autothermal reforming of diesel fuel and kerosene

Applied Energy 150 (2015) 176–184

Pasel, J.; Samsun, R. C.; Peters, R.; Stolten, D.

Fuel cell systems with reforming of petroleum-based and synthetic-based diesel and kerosene fuels for APU applications

International Journal of Hydrogen Energy 40 (2015) 6405–6421

Krekel, D.; Samsun, R.C.; Pasel, J.; Prawitz, M.; Peters, R.; Stolten, D.

Investigation of operating parameters in conjunction with catalyst deactivation of the water-gas shift reactor in a fuel cell system

ECS Transactions 65 (1) (2015), 99–114.

Publications in books

Peters, R.

Fuel Processing for Utilization in Fuel Cells,

in Hydrogen Science and Engineering : Materials, Systems, Processes and Technologies, First Edition. Stolten, D.; Emonts, B., (Eds.), 2016, Wiley-VCH, Weinheim, p. 173-216

Samsun, R.C.

Global development status of fuel cell vehicles

in Fuel Cells: Data, Facts, and Figures, First Edition. Stolten, D.; Samsun, R.C.; Garland, N., (Eds.), 2016, Wiley-VCH, Weinheim, p. 39-60

Samsun, R.C.

Fuels for APU applications

in Fuel Cells: Data, Facts, and Figures, First Edition. Stolten, D.; Samsun, R.C.; Garland, N., (Eds.), 2016, Wiley-VCH, Weinheim, p. 185-196

Peters, R.

Reforming Technologies for APUs,

in Fuel Cells: Data, Facts, and Figures, First Edition. Stolten, D.; Samsun, R.C.; Garland, N., (Eds.), 2016, Wiley-VCH, Weinheim, p. 208-224

Samsun, R.C.

PEFC for APU applications

in Fuel Cells: Data, Facts, and Figures, First Edition. Stolten, D.; Samsun, R.C.; Garland, N., (Eds.), 2016, Wiley-VCH, Weinheim, p. 225-234

Peters, R.

Heutige und zukünftige Kraftstoffe für Brennstoffzellen in der Luftfahrt, in Brennstoffzellen in der Luftfahrt

in Brennstoffzellen in der Luftfahrt. Peters, R. (Ed.), 2015, Springer Vieweg, Berlin, p. 7-100

Pasel, J.

Technische Entwicklung, Bau und Test von Brenngaserzeugungskomponenten

in Brennstoffzellen in der Luftfahrt. Peters, R. (Ed.), 2015, Springer Vieweg, Berlin, p. 181-234

Meißner, J; Tschauder, A.

Reaktorentwicklung und Konstruktion

in Brennstoffzellen in der Luftfahrt. Peters, R. (Ed.), 2015, Springer Vieweg, Berlin, p. 235-280

Samsun, R.C.

Entwicklung und Charakterisierung eines Gesamtsystems

in Brennstoffzellen in der Luftfahrt. Peters, R. (Ed.), 2015, Springer Vieweg, Berlin, p. 281-332

Peters, R. und Westernberger, A.

Brennstoffzellensysteme als Bestandteil eines multifunktionalen Systems,

in Brennstoffzellen in der Luftfahrt. Peters, R. (Ed.), 2015, Springer Vieweg, Berlin, p. 333-404

Peters, R.; Meißner, J.; Pasel, J.; Samsun, R.C.; Stolten, D.

Verbundvorhaben ELFA Effiziente Luftfahrzeuge, Brennstoffzellensysteme zur Energieeffizienz, BREZEN - Teilprojekt: Kerosinaufbereitung,

Schriften des Forschungszentrums Jülich, Reihe Energie & Umwelt, Band 302, 2016. ISBN 978-3-95806-114-9

Doctoral theses

Löhken, K.

Aktivitätsuntersuchungen und Methoden zur Regeneration von Katalysatoren für die autotherme Reformierung von Dieselmotorkraftstoffen

Schriften des Forschungszentrums Jülich, Reihe Energie & Umwelt, 288 (2015), ISBN 978-3-95806-093-7

Krupp, C.

Computerunterstützte Auslegung eines Brennstoffzellen-Batterie-Hybridsystems für die Bordstromversorgung

Schriften des Forschungszentrums Jülich, Reihe Energie & Umwelt, 309 (2015), ISBN 978-3-95806-124-8

Important patents

Patents granted:

Principal inventor	PT	Description
Dr. Z. Pors	1.2272	A method for vaporizing a liquid fuel and mixing chamber for carrying this out
Prof. R. Peters	1.2188	A method for processing fuel

3.3 High-temperature polymer electrolyte fuel cells

3.3.1 Objectives and fields of activity

High-temperature polymer electrolyte fuel cells (HT-PEFCs) based on phosphoric-acid-doped polybenzimidazole membranes have an operating temperature of 150–180 °C. Due to the high temperature level, they have a high CO tolerance, which makes them ideal for operation in combination with reformers. In contrast to Nafion-based polymer electrolyte membrane fuel cells (PEFCs), gases do not need to be humidified externally to ensure the protonic conductivity of the membrane, assuming an adapted flow distributor is present in the cells. Another advantage of HT-PEFC technology is due to the considerable temperature difference between the stack and the ambient temperature, which facilitates a more compact cooling concept than is the case in conventional PEFC systems.

Despite all of these advantages, the acid still has to be prevented from being discharged from the membrane – operating conditions where liquid water can form in the cells must therefore be avoided. Operation in low temperature ranges should therefore be avoided. This must be taken into account by operating strategies and the specific areas of application.

In parallel to the cell and stack developments at IEK-3, in particular physico-chemical interactions within the membrane electrode assembly (MEA) are being investigated. There has been a boost to innovation in cell and stack development, away from graphitic and towards metallic bipolar plates (Fig. 31).

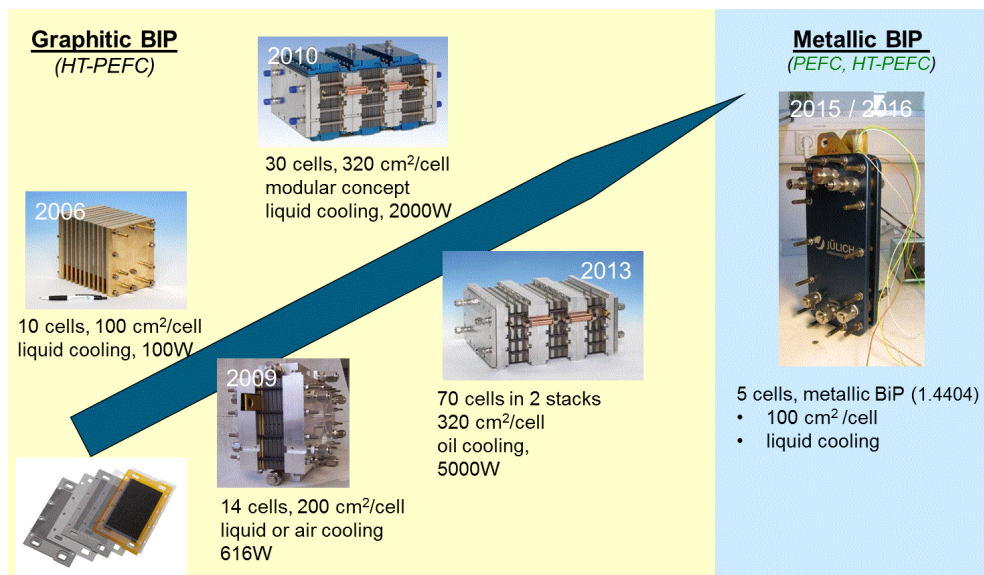


Fig. 31: HT-PEFC stack development at IEK-3: the left-hand side shows stacks with graphitic bipolar plates, the right-hand side a stack with metallic bipolar plates

In addition, the major priorities of modeling and simulation have become more pronounced in the past few years. To describe HT-PEFC cells and entire cell stacks, models were developed using the open source simulation tool OpenFOAM. Detailed simulations of mass transport in porous gas diffusion layers were performed using the lattice Boltzmann software

tool JULABOS developed at IEK-3. Analytical fuel cell models for describing impedance phenomena complete these activities.

The need for an expansion of R&D activities towards conventional PEFCs also became apparent in the years 2015 and 2016. The focus is on the experimental investigation and the mathematical description of two-phase flow phenomena both in the flow channels and in the porous cell components.

3.3.2 Important results

3.3.2.1 HT-PEFC stack development

In the field of stack development, there has been a transition away from graphitic towards metallic bipolar plates. This step meant that the weight of the stack was reduced by 70 % and its volume by 40 %. This work was conducted within the scope of the BMWi-funded project RoBiPo ("Robuste Bipolarplatten für HT-PEFC", "robust bipolar plates for HT-PEFCs", funding reference no: 03ET2030F) and in collaboration with the industrial partners Enymotion, Gräbener Maschinentechnik, Wickeder Westfalenstahl, DiaCCon, and Polyprocess Kunstharzverarbeitung.

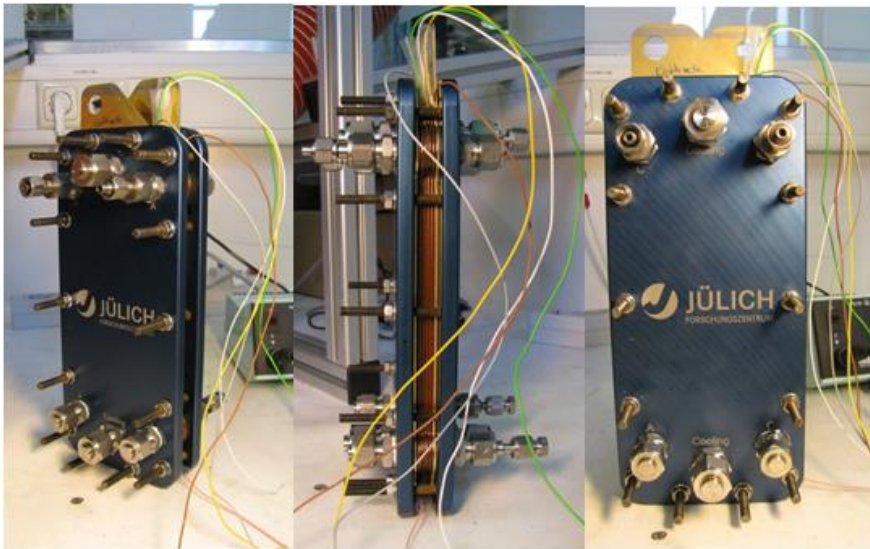


Fig. 32: Exterior views of the 5-cell test stack with cables for tapping the voltage of the individual cells

For the proof of functionality of the metallic bipolar plates developed within the scope of this project, a stack was constructed at IEK-3. The required additional stack components were also dimensioned, designed, and manufactured at Jülich. Planar, rectangular aluminium end plates 10 mm in thickness were produced. The stack is braced with 14 tie rods distributed around the circumference; they are screwed into one end plate and a defined load is applied to them via the second end plate using nuts and disc springs. Fig. 32 shows several views of the completely assembled stack before installation in the test stand. Further visible elements

include the screws in the end plates used to connect the gas and coolant lines as well as the colored cables for tapping the voltage of the individual cells.

Fig. 33 shows further photos of the stack being installed in IEK-3's test stand (manufactured by Hydrogenics). A number of the tubes are already thermally insulated with fiberglass mats. Connecting cables to the measurement equipment (temperatures, voltages) as well as the thicker load cables can also be seen.

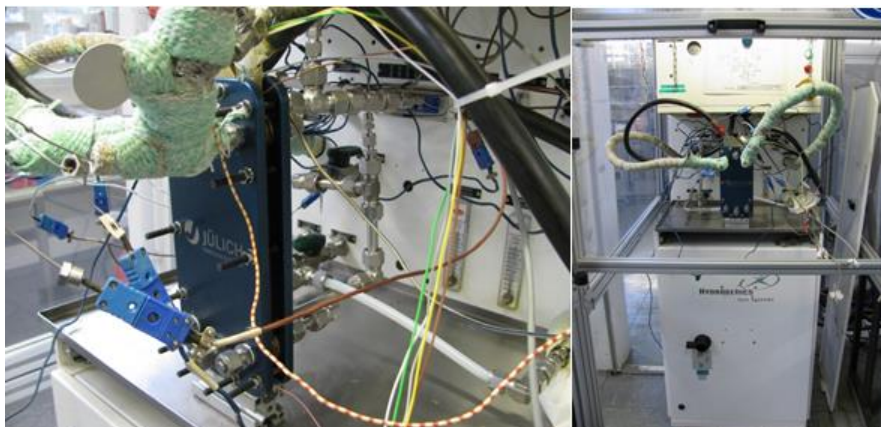


Fig. 33: Installation of the stack in the test stand; the stack and some of the lines are not yet thermally insulated

After heating the stack to its nominal operating temperature of 160 °C using recirculated coolant (Fragotherm S-15-A, manufactured by Fragol, polyglycol basis), the preheated gases (hydrogen and air) were fed in. Approximately one hour after initial commissioning, the first polarization curve was determined. The result is shown in Fig. 34. The selected operating parameters are shown in the legend on the right-hand side in Fig. 34. The diagram shows the polarization curves for all five cells in the stack separately. What is striking at first glance is that the voltages of cells 1 and 5 (which are located at the edges of the stack) are significantly lower than those of the other three cells. A possible explanation for this is that the stack was not thermally insulated during these measurements and that the cells at the edges were operated at a lower temperature due to the additional heat dissipation via the aluminium end plates. In hydrogen–air operating mode, an average current density of 0.5 A/cm² and a cell voltage of 0.55 V were achieved. At 0.9 A/cm², the average cell voltage amounted to 0.45 V. This corresponds to a specific power of approximately 0.4 W/cm². For an HT-PEFC stack, this is a very good value.

After an operating time of approximately 25 h at a constant current density of 0.2 A/cm², another polarization curve was determined in the hydrogen–air operating mode. Fig. 35 shows the results. Overall, the voltage levels are 20–40 mV lower than in the first polarization curve. The maximum power density of 0.38 W/cm² was measured at 1 A/cm².

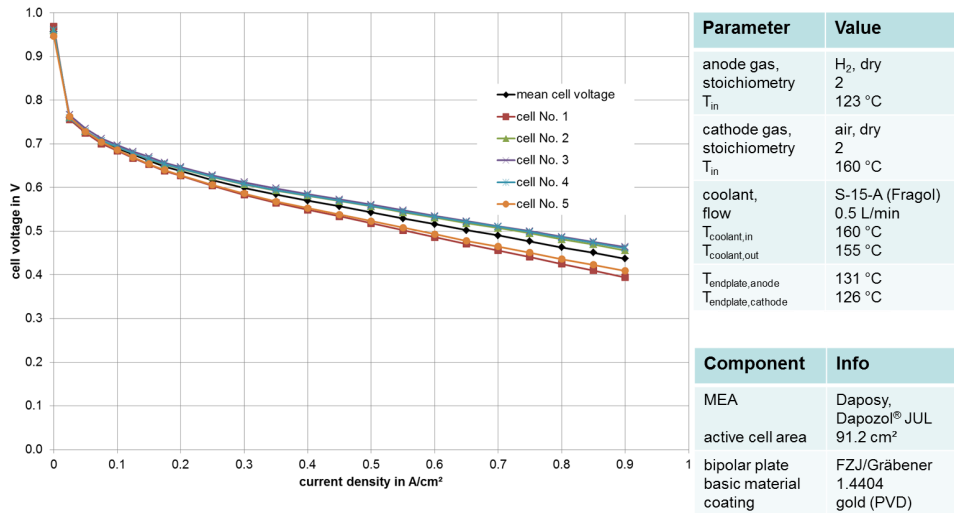


Fig. 34: Polarization curves in hydrogen–air operating mode for all five individual cells in the stack, directly after installation and one-hour running-in phase

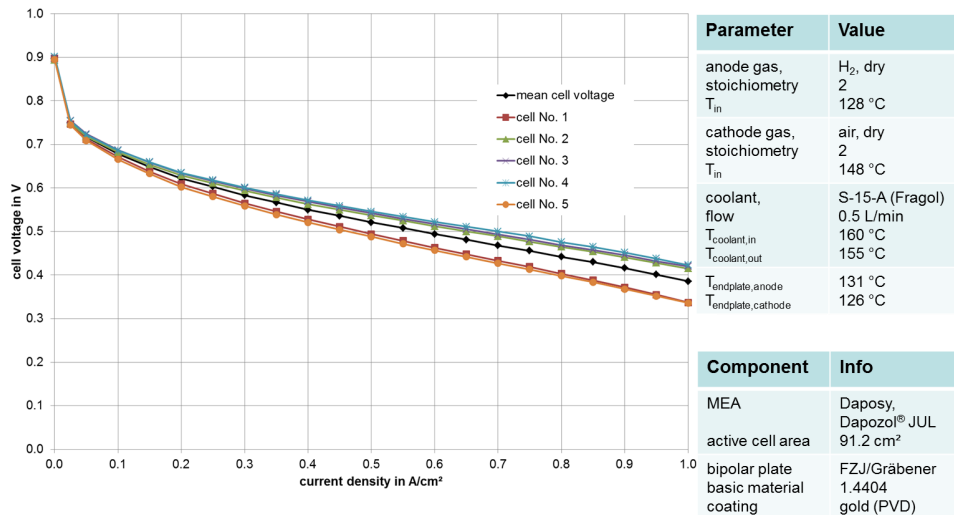


Fig. 35: Polarization curves in hydrogen–air operating mode for all five individual cells in the stack after 25 hours of operation

Subsequent to this, a diesel-based synthetic reformat was used as fuel. The reformat consisted of 32 % hydrogen and 1 % carbon monoxide. The remainder is nitrogen. In this synthetic reformat, nitrogen represents the sum of all inert gases present in similar proportions in real reformat (H₂O, N₂, and CO₂). Due to the high hydrogen dilution, the presence of 1 % CO, and the dryness of the gas, this fuel is a “worst-case reformat”. The polarization curves after a stack operating period of 43 h are shown in Fig. 36. As is to be expected, the current–voltage characteristics are significantly below the curves for hydrogen operation. At 0.5 A/cm², an average of 0.45 V per cell is achieved. At 0.65 A/cm², the first cell voltage falls below the set limit of 0.35 V, at which the polarization curve is automatically

terminated. The average specific cell power at this operating point amounts to 0.25 W/cm². For a first stack test, this is a very promising result.

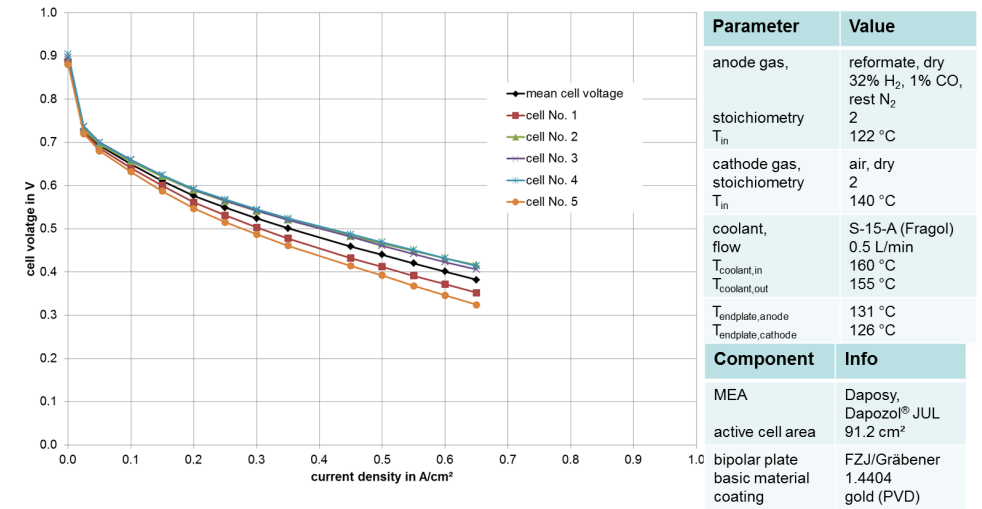


Fig. 36: Polarization curves for reformate–air operation for all five individual cells in the stack, after an operating period of 43 h

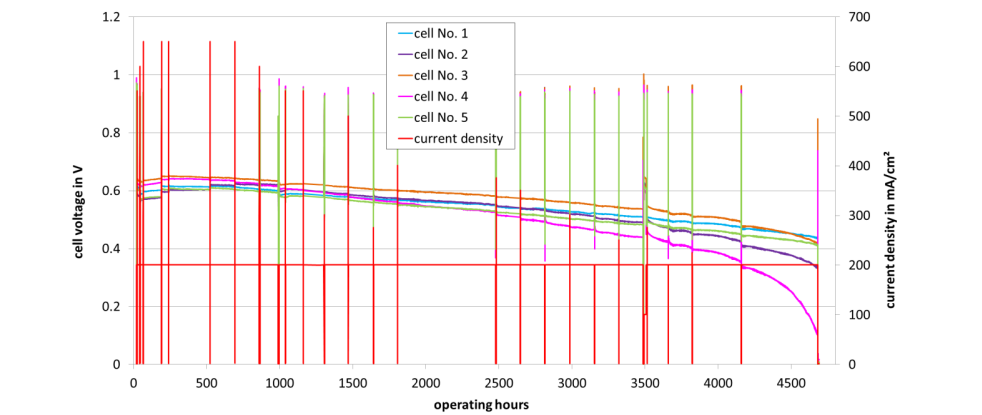


Fig. 37: Long-term test of the five-cell short stack, H₂–air operation, $\lambda_A = \lambda_C = 2$, $T_{coolant, in} = 160\text{ °C}$, $i = 0.2\text{ A/cm}^2$

Subsequent to the first performance characterizations in the form of the polarization curve measurements for the hydrogen–air as well as the reformate–air operating mode shown above, the short stack was set to continuous operation at a constant current density of 0.2 A/cm². The further operating conditions and the voltage curve over time of the five cells is shown in Fig. 37.

The vertical lines in the diagram mark the points in time at which polarization curves were recorded. Several phases can be discerned in the voltage curves:

- Up to approximately 200 hours of operation, the cell voltage increased on average by approximately 50 mV, starting from approximately 0.6 V. In this initial period of stack

operation, the phosphoric acid in the area of the MEA components is redistributed, which can improve the protonic conductivity and therefore cell performance.

- The further cell voltage curves are marked by a continuous decrease. After 2500 hours of operation, the average cell voltage amounts to approximately 0.55 V.
- The differences in the temporal voltage drops of the five individual cells is striking. This process begins at a comparatively low voltage in cells 1 and 5 (cells at the edge of the stack), which can be explained by the increased heat dissipation of the cells at the edge and thus the slightly lower cell temperature. The voltage gradient drops of these cells until the end of operation are, however, the lowest. At the end of operation, cells 1 and 5 have the highest voltages.
- The end of operation of the short stack is reached after 4700 h. The lifetime test was terminated when one of the cells (cell 4) reached a cell voltage of 0.1 V. The voltage drop of cell 4 is the sharpest by far. There is as yet no plausible explanation for this, but a *post mortem* analysis may provide clues.

3.3.2.2 CFD simulation

Although an external humidification of the gases is not necessary for HT-PEFCs, the conductivity of the phosphoric-acid-doped PBI membrane depends on humidity (IEK-3 Report 2015). The water content of the electrolyte (phosphoric acid) is a function of the water vapor partial pressure in the flow channels and determines the ohmic resistance of the cell. The distribution of the product water between anode and cathode permits additional conclusions to be drawn on the state of the electrolyte during fuel cell operation. Therefore, a simulation package was developed as part of a project funded by the federal state of North Rhine-Westphalia (FLEXSIM, funding reference no: 313-EF-2019A), which permits the computational fluid dynamics of fuel cells to be simulated, taking the water distribution into consideration. **Fig. 38** (left-hand side) shows a typical individual HT-PEFC, which was used for basic characterization at IEK-3. It has an active cell surface of approximately 17 cm². The gas is distributed on the anode side and the cathode side by a threefold meandering structure. **Fig. 38** (right-hand side) shows this meandering structure as well as a section of the simulation lattice of the air channel with GDL.

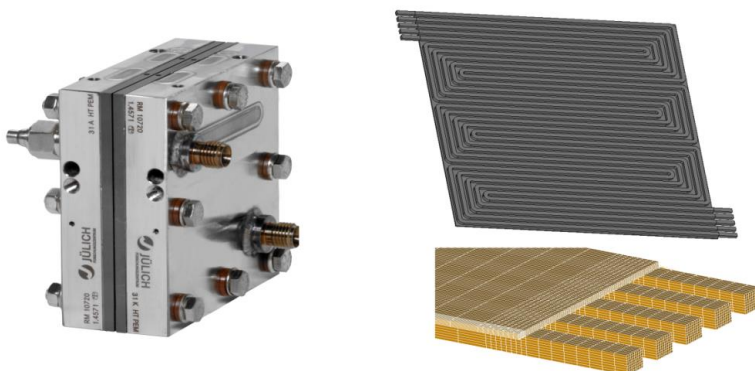


Fig. 38: Individual HT-PEFC (left) and meandering flow distributor as well as a section of the simulation lattice from the computational fluid dynamics (right)

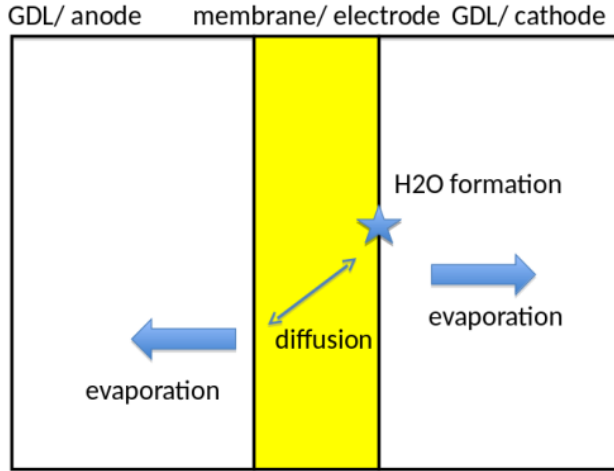


Fig. 39: Schematic of the water distribution in an HT-PEFC

In this model, the electrochemical reactions relative to area take place at the interface between anode and cathode. The modeling of the water distribution includes the following steps: calculation of the local amount of product water, diffusion within the electrolyte, vaporization at the interface between catalyst and anode/cathode compartment. These processes are schematically shown in Fig. 39.

Coupling the computational fluid dynamics with the electrochemistry and the model of the water distribution provides results with the spatially resolved distribution of current density and gas species. Fig. 40 shows the distribution of the normalized mass flow (mass fraction) of gaseous water at the interface between catalyst and anode/cathode at a selected operating point as an example. Water is formed electrochemically at the cathode. It is clearly visible that a similar water vapor distribution can also be observed at the anode due the diffusion through the electrolyte.

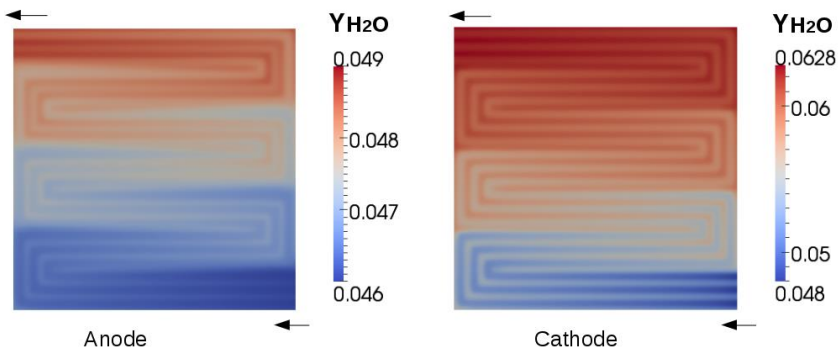


Fig. 40: Local distribution of the mass fraction of water vapor (160 °C, 101,325 Pa, stoichiometry air/H₂ = 2/2)

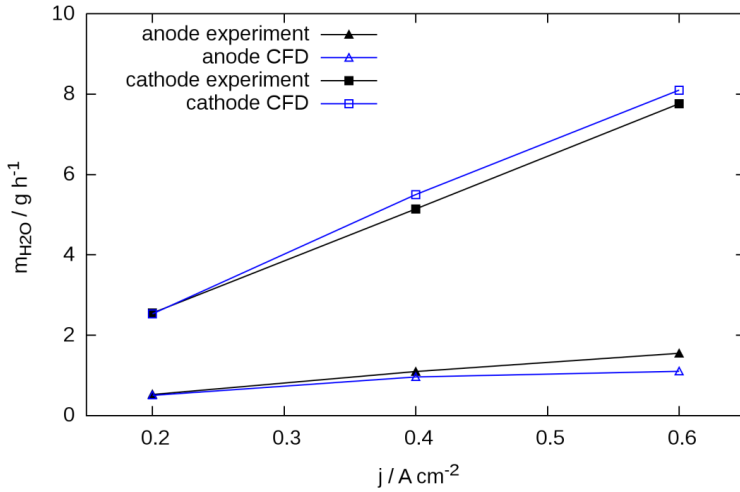


Fig. 41: Mass flow of water vapor at the anode and the cathode side as a function of the current density – comparison between simulation and experiment

A comparison with the experiment shows that the distribution of the water in the exhaust gas flow of anode and cathode can be accurately reproduced (see Fig. 41).

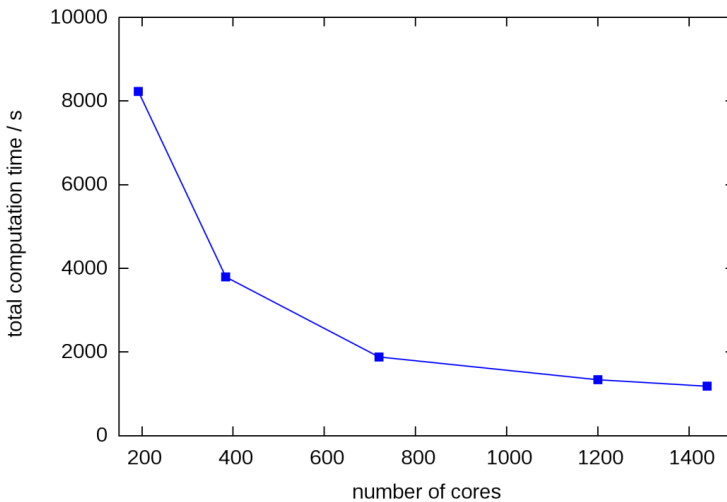


Fig. 42: Actual computation time as a function of the processor cores used

The simulations were run on the JARA HPC infrastructure. An example of the necessary computation time as a function of the computer cores is shown in Fig. 42. The scaling shows that it is not expedient to increase the number of processors to more than 700 in this example. These simulations were conducted within the scope of the JARA HPC project JARA0070 by RWTH Aachen University.

3.3.3 Staff members and fields of activity

Name	Tel. (02461-61-) Email	Field of activity
Prof. Dr. W. Lehnert	3915 w.lehnert@fz-juelich.de	Head of High-Temperature Polymer Electrolyte Fuel Cells
Prof. Dr. M. Andersson (Gast)	9074 m.andersson@fz-juelich.de	CFD with OpenFOAM, Volume of Fluid
Prof. Dr. S. Beale	8856 s.beale@fz-juelich.de	CFD with OpenFOAM, cell and stack level
Fr. Y. Cai	6484 y.cai@fz-juelich.de	Electrochemical half-cell investigations
Q. Cao	1923 q.cao@fz-juelich.de	CFD with OpenFOAM on cell level
D. Froning	6676 d.froning@fz-juelich.de	Lattice Boltzmann simulations in porous components
B. Hussain	8626 m.hussain@fz-juelich.de	Coating of metallic bipolar plates
P. Irmischer	9803 p.irmischer@fz-juelich.de	Stack mechanics
Dr. H. Janßen	5082 h.janssen@fz-juelich.de	Head of HT-PEFC Stack Development
A. Kulikovskiy, PhD, DSci	5396 a.kulikovskiy@fz-juelich.de	Development of analytical and numerical fuel-cell models
Fr. S. Krönauer	9576 s.kroenauer@fz-juelich.de	Coating of metallic bipolar plates
Fr. S. Lee	1923 s.lee@fz-juelich.de	CFD with OpenFOAM on cell level
R. Li	96924 r.li@fz-juelich.de	Corrosion of metallic bipolar plates
Y Lin	9036 y.lin@fz-juelich.de	HT-PEFC membranes
Sh. Liu	8626 Shu.liu@fz-juelich.de	HT-PEFC electrodes
Y. Rahim	6029 y.rahim@fz-juelich.de	HT-PEFC stack
Dr. U. Reimer	3537 u.reimer@fz-juelich.de	Head of HT-PEFC Modeling and Simulation
Y. Shi	1902 y.shi@fz-juelich.de	PEFC water management
Fr. B. Schumacher	5406 b.schumacher@fz-juelich.de	Development of designs for test stands for HT-PEFCs, testing of HT-PEFCs
Dr. V. Weißbecker	9576 v.weissbecker@fz-juelich.de	Coating of metallic bipolar plates
Prof. L. Xu (Gast)	9074 l.xu@fz-juelich.de	Modeling of dynamic fuel-cell behavior

J. Yu	2989 j.yu@fz-juelich.de	Lattice Boltzmann simulations in porous components
S. Zhang	96465 s.zhang@fz-juelich.de	CFD with OpenFOAM, cell and stack level
Fr. W. Zou	9399 w.zou@fz-juelich.de	Modeling of dynamic fuel-cell behavior

3.3.4 Important publications, doctoral theses and patents

Publications in peer-reviewed journals

U. Reimer, B. Schumacher, W. Lehnert

Accelerated degradation of high-temperature polymer electrolyte fuel cells – discussion and empirical modeling

J. Electrochemical Soc. 162 (2015) F153-F164

C. Tötzke, I. Manke, G. Gaiselmann, J. Böhner, B. Müller, A. Kupsch, M. P. Hentschel, V. Schmidt, J. Banhart, W. Lehnert

A Dedicated Compression Device for High Resolution X-ray Tomography of Compressed Gas Diffusion Layers

Review of scientific instruments, 86 (2015) 043702

C. Korte, F. Conti, J. Wackerl, P. Dams, A. Majerus, W. Lehnert

Uptake of Protic Electrolytes by Polybenzimidazole-Type Polymers –Adsorption Isotherm and Electrolyte/Polymer Interactions

Journal of Applied Electrochemistry 45 (2015) 857-871

T. Arlt, W. Lüke, N. Kardjilov, J. Banhart, W. Lehnert, I. Manke

Monitoring the hydrogen distribution in Poly(2,5-benzimidazole)-based (ABPBI) membranes in operating High Temperature Polymer Electrolyte Fuel Cell using H-D contrast neutron imaging

J. Power Sources 299 (2015) 125-129

SB Beale

Mass transfer formulation for polymer electrolyte membrane fuel cell cathode

International Journal of Hydrogen Energy 40 (2015), 11641-11650

T Reshetenko, A Kulikovsky

PEM Fuel Cell Characterization by Means of the Physical Model for Impedance Spectra

Journal of The Electrochemical Society 162 (2015), F627-F633

AA Kulikovsky, P Berg

Positioning of a Reference Electrode in a PEM Fuel Cell

Journal of The Electrochemical Society 162 (2015), F843-F848

AA Kulikovsky

Potentials Near a Curved Anode Edge in a PEM Fuel Cell: Analytical Solution for Placing a Reference Electrode

Journal of The Electrochemical Society 162 (2015), F1191-F1198

AA Kulikovsky

One-dimensional impedance of the cathode side of a PEM fuel cell: Exact analytical solution

Journal of The Electrochemical Society 162 (2015), F217-F222

AA Kulikovsky, O Shamardina

A model for PEM fuel cell impedance: Oxygen flow in the channel triggers spatial and frequency oscillations of the local impedance

Journal of The Electrochemical Society 162 (2015), F1068-F1077

AA Kulikovsky

A simple and accurate fitting equation for half of the faradaic impedance arc of a PEM fuel cell

Journal of Electroanalytical Chemistry 738 (2015) 108-112

AA Kulikovsky

Analysis of Damjanović kinetics of the oxygen reduction reaction: Stability, polarization curve and impedance spectra

Journal of Electroanalytical Chemistry 738 (2015) 130-137

P Berg, AA Kulikovsky

A model for a crack or a delaminated region in a PEM fuel cell anode: analytical solutions

Electrochimica Acta 174 (2015) 424-429

K. Wippermann, J. Wackerl, W. Lehnert, B. Huber, C. Korte

2-Sulfoethylammonium trifluoromethanesulfonate as an Ionic Liquid for High Temperature PEM Fuel Cells

J. Electrochem. Soc. 163 (2016) F25-F37

U. Reimer, J. Ehlert, H. Janßen, W. Lehnert

Water distribution in high temperature polymer electrolyte fuel cells

Int. J. Hydrogen Energy 41 (2016) 1837-1845

Y. Liu, W. Lehnert, H. Janßen, R.C. Samsun, D. Stolten

A review of high-temperature polymer electrolyte membrane fuel-cell (HT-PEMFC)-based auxiliary power units for diesel-powered road vehicles

J. Power Sources 311 (2016) 91-102

D. Froning, J. Yu, G. Gaiselmann, U. Reimer, I. Manke, V. Schmidt, W. Lehnert

Impact of compression on gas transport in non-woven gas diffusion layers of high temperature polymer electrolyte fuel cells

J. Power Sources 318 (2016) 26-34

C. Tötze, G. Gaiselmann, M. Osenberg, T. Arlt, H. Markötter, A. Hilger, A. Kupsch, B.R. Müller, V. Schmidt, W. Lehnert, I. Manke

Influence of hydrophobic treatment on the structure of compressed gas diffusion layers

J. Power Sources 324 (2016) 625-636

A. Niemöller, P. Jakes, S. Kayser, Y. Lin, W. Lehnert, J. Granwehr

3D printed sample holder for in operando EPR spectroscopy on high temperature PEM fuel cells

Journal of Magnetic Resonance 269 (2016) 157-161

J. Gostick, M. Aghighi, J. Hinebaugh, T. Tranter, M.A. Hoeh, H. Day, A. Bazylak, A. Burns, W. Lehnert, A. Putz

OpenPNM: A Pore Network Modeling Package

Comput. Sci. Eng. 18 (2016) 60

M. Andersson, S. Beale, M. Espinoza, Z. Wu, W. Lehnert
A review of cell-scale multiphase flow modeling, including water management, in polymer electrolyte fuel cells
Applied Energy 180 (2016) 757–778

M. Khanef, O. Holderer, O. Ivanova, W. Lücke, E. Kenzinger, M.S. Appavou, R. Zorn, W. Lehnert,
Structure and proton dynamics in catalytic layer for HT-PEFC
Fuel cells 16 (2016) 406–413

M. Fazeli; J. Hinebaugh; Z. Fishman; Ch. Tötze; W. Lehnert; I. Manke, A. Bazylak
Pore network modeling to explore the effects of compression on multiphase transport in polymer electrolyte membrane fuel cell gas diffusion layers
J. Power Sources 335 (2016) 162–171

T Reshetenko, A Kulikovsky
Comparison of two physical models for fitting PEM fuel cell impedance spectra measured at a low air flow stoichiometry
Journal of The Electrochemical Society 163 (2016), F238–F246

AA Kulikovsky
PEM Fuel Cell Impedance at Open Circuit
Journal of The Electrochemical Society 163 (2016), F319–F326

T Reshetenko, A Kulikovsky
Variation of PEM Fuel Cell Physical Parameters with Current: Impedance Spectroscopy Study
Journal of The Electrochemical Society 163 (2016), F1100–F1106

AA Kulikovsky
A simple physics-based equation for low-current impedance of a PEM fuel cell cathode
Electrochimica Acta 196 (2016) 231–235

AA Kulikovsky
Non-Pt Catalyst Layer Operation in a PEM Fuel Cell: A Variable-thickness Regime
Fuel Cells 16 (2016), 754–759

Publications in books

W. Lehnert, U. Reimer, H. Janßen
Hochtemperatur-Polymerelektrolyt-Brennstoffzellen
In: R. Peters (Eds.), Brennstoffzellensysteme in der Luftfahrt, Springer Vieweg, Springer Verlag Berlin Heidelberg 2015, pp 101–144

H. Janßen, A. Bendzulla, W. Lehnert
Stackentwicklung Hochtemperatur-Polymerelektrolyt-Brennstoffzellen
In: R. Peters (Eds.), Brennstoffzellensysteme in der Luftfahrt, VDI-Springer, Springer Vieweg, Springer Verlag Berlin Heidelberg 2015, pp 145–180

H. Janßen, J. Supra, W. Lehnert
Chapter 20, Stack Concepts for High Temperature Polymer Electrolyte Membrane Fuel Cells
In: Jens Oluf Jensen, David Aili, Hans Aage Hjuler, Qingfeng Li, High Temperature Polymer Electrolyte Fuel Cells- Approaches, Status and Perspectives, Springer (2016) pp 441–457

C. Korte, F. Conti, J. Wackerl, W. Lehnert

Chapter 8, Phosphoric acid and its interactions with polybenzimidazole type polymers

In: Jens Oluf Jensen, David Aili, Hans Aage Hjuler, Qingfeng Li, High Temperature Polymer Electrolyte Fuel Cells- Approaches, Status and Perspectives, Springer (2016) pp 169-194

W. Lehnert, L. Lücke, R. C. Samsun

High Temperature Polymer Electrolyte Fuel Cells

In: D. Stolten, R.C. Samsun, N. Garland, Fuel Cells, Data Facts and Figures, Wiley-VCH (2016) pp 235-247

Doctoral theses

Weißbecker, V.

Korrosionsverhalten metallischer Bipolarplatten von Hochtemperatur-Polymer-elektrolyt-Brennstoffzellen

Schriften des Forschungszentrums Jülich, Reihe Energie & Umwelt, 357 (2016), ISBN 978-3-95806-205-4

Important patents

Patent applications:

Principal inventor	PT	Description
Dr. A.A. Kulikovskiy	1.2690	A method for determining over-voltages in fuel cells
Dr. A.A. Kulikovskiy	1.2700	A method for determining over-voltages in fuel cells
A. Schulze Lohoff	1.2766	A coating for electrical contact and method for producing this

3.4 Direct methanol fuel cells

3.4.1 Objectives and fields of activity

Liquid energy carriers such as methanol have the advantage of being simple to handle and having a high energy density. In contrast to hydrogen, an energy carrier frequently used for fuel cells, methanol does not require pressurized gas tanks, which are disproportionately heavy and large especially for small quantities of hydrogen. In addition, the storage tanks can be refilled quite simply, similar to gasoline or diesel. The fact that some substances are liquid at environmental conditions can be attributed to their intermolecular interactions due to their complex chemical structure. However, it also means that they cannot be electrochemically converted as easily and quickly as hydrogen. Thus, direct methanol fuel cells require larger amounts of catalysts and their power density and efficiency is lower. Direct methanol fuel cells are therefore particularly suitable when moderate power levels of up to some kW have to be maintained over long operating times without refilling, or if the system is mobile and the fuel must thus be carried on board. Therefore, the main fields of application which IEK-3 focuses on are small mobile applications such as the field of material handling or uninterruptable power supply (UPS), particularly at remote locations where frequent refilling is impracticable.

3.4.2 Important results

3.4.2.1 Direct methanol fuel cells with flowing electrolytes

As part of his Horizon 2020 individual fellowship, Prof. C. Ozgur Colpan from Dokuz Eylül University in Izmir, Turkey, spent three months at IEK-3 as a visiting scientist together with his colleague Dr. David Ouellette. Within the scope of Prof. Ozgur Colpan and Dr. David Ouellette's research stay, extensive experimental investigations were conducted in the field of direct methanol fuel cells (DMFCs) with flowing electrolytes. Conventional DMFCs have the disadvantage that methanol permeates from the anode to the cathode, where the methanol is not only wasted without being utilized but also blocks the cathode catalyst, which reduces the efficiency and the performance of the DMFC. Thanks to the flowing electrolyte, any methanol entering the electrolyte is removed before reaching the cathode. Prof. Colpan and Dr. Ouellette had already investigated the concept by means of extensive simulations and initial experiments. The aim of their research stay was to experimentally confirm the potential of the concept using the extensive experience at IEK-3 in the operation of DMFCs and the determination of methanol permeation.

For these measurements, specialized measuring cells made of a special sulfuric-acid-resistant steel were manufactured at Forschungszentrum Jülich based on the visiting scientists' design. Two existing test stands at IEK-3 equipped for measuring methanol permeation were adapted for operation with sulfuric acid as a flowing electrolyte.

The measurements conducted at Jülich with these cells show that methanol permeation can indeed be considerably reduced depending on methanol concentration and current density.

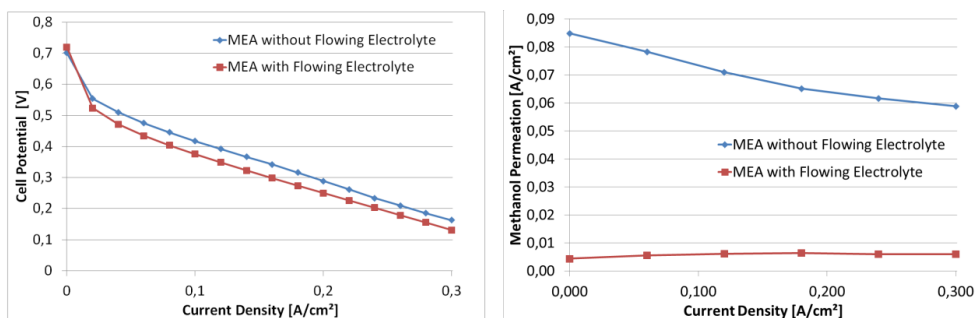


Fig. 43: Characteristic curves (left) and methanol permeation (right) of MEAs with and without flowing electrolytes (70 °C, 1M methanol)

Fig. 43 shows the behavior of MEAs with and without flowing electrolytes. Both MEAs consist of two semi-MEAs, each composed of a membrane (Nafion® 115) and an anode or cathode. In one case, the two semi-MEAs are directly pressure-bonded to each other, in the other case, they are separated by a 175 µm porous channel through which 2M sulfuric acid flows. The characteristic curves are largely parallel, but slightly offset from each other. The parallel plot indicates that the ohmic resistance of the cell with the flowing electrolyte is not significantly higher than that of the other. The expected increase in cell voltage due to inhibited methanol oxidation at the cathode can, however, only be observed during currentless operation. The slightly decreased cell voltage of the cell with the flowing electrolyte is probably caused by a minor amount of sulfuric acid which passes through the membrane, reaching the electrodes.

The difference in methanol permeation is particularly apparent: in the MEA with flowing electrolyte, the permeation is reduced by at least 90 % relative to the normal MEA. This leads to a significantly higher methanol utilization. At a current density of 0.12 A/cm² and without the flowing electrolyte, the amount of methanol lost through oxidation at the cathode could be used to produce 0.071 A/cm², so that the methanol utilization is only 63 %. With the flowing electrolyte, the loss is reduced to 0.006 A/cm², increasing the methanol utilization to 95 %. At the highest current density tested, 0.3 A/cm², methanol utilization is as high as 98 %.

In a system working autonomously, however, the methanol removed by the sulfuric acid must be recovered so that the significantly increased methanol utilization can be exploited to increase the overall efficiency. The results of these measurements have been published in detail².

3.4.2.2 Testing new catalyst materials

A significant part of the costs of a DMFC system is due to the relatively large amounts of noble metal catalyst material needed in the DMFC. It is therefore important to investigate

² Colpan, C.O., Ouellette, D., Glösen, A. Müller, M., Stolten, D.: Reduction of methanol crossover in a flowing electrolyte-direct methanol fuel cell. International Journal of Hydrogen Energy (2017) DOI: 10.1016/j.ijhydene.2017.01.004

catalyst coatings which use smaller amounts of noble metal loading as well as to research new catalysts with better performance and of which lesser amounts are thus needed. Hierarchically structured catalysts from the Hamburg Center for Applied Nanotechnology (CAN) have proven particularly promising as candidates for the cathode. Using as little as 30 $\mu\text{g}/\text{cm}^2$ platinum led to acceptable cell performance, in contrast to commercially available catalysts. Fig. 44 shows the characteristic curves of MEAs with hierarchically structured cathodes and with the same amount of commercial catalyst.

For comparison, the characteristic curve of a commercial catalyst whose current density was multiplied by six is also shown; as can be seen, this characteristic curve approximately corresponds to that of the hierarchically structured cathode. Thus, approximately six times the electricity can be generated using the same amount of catalyst material.

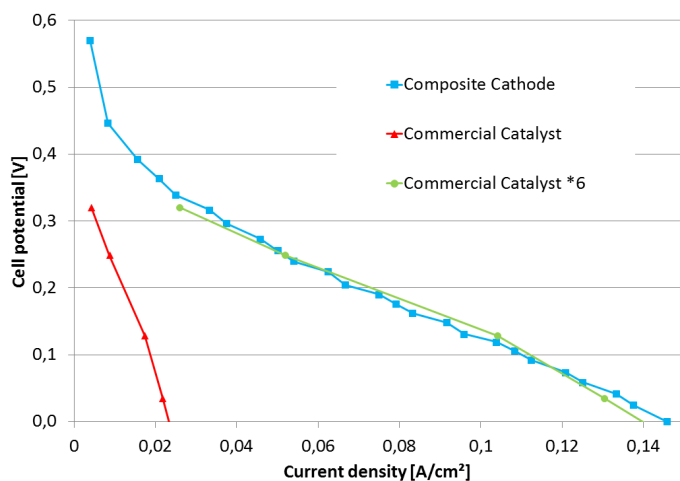


Fig. 44: Characteristic curves of MEAs with hierarchically structured cathode (blue), and a cathode with the same amount of commercial catalyst material (red). For comparison the chart also shows the current density of an MEA with six times the amount of commercial catalyst (green)

The performance is lower than that of standard MEAs – however the latter require about 100 times the amount of platinum for their cathodes. Judging from the results of this initial test, it is to be expected that in order to achieve the same performance as commercial catalysts, a significantly smaller amount of platinum will be required. This cannot, however, be easily verified at the present time since hierarchically structured cathodes are still complex to produce. a collaborative project, founded by the BMBF has been started – involving CAN, Universität Hamburg, and Smart Fuel Cells as a user – in order to optimize these catalysts, automate their production, and evaluate their performance³.

Moreover, new catalysts are constantly being tested by different research groups in order to reduce the amount of noble metals needed in fuel cells. In addition to the cathode catalysts mentioned above, anode catalysts in particular are also being investigated.

³ Hierarchische Komposit-Nanopartikelsysteme zur Anwendung in Brennstoffzellen – Entwicklung und kontinuierliche Herstellung (HiKAB), Förderkennzeichen (FKZ): 03ET1435C - HiKAB

3.4.2.3 Field test of a DMFC system for emergency power supply for NRW police digital radio system

From January to November 2016, a field test of a DMFC UPS system was successfully conducted in collaboration with the NRW police. The collaboration concerned securing an uninterruptable power supply (UPS) for a digital radio system used by the police. It was operated with direct methanol fuel cells (DMFCs). Over the course of the test phase, the module (see Fig. 45) was able to secure emergency power operation for the required period of 72 hours.



Fig. 45: Project partners at the police digital radio system location with the DMFC UPS system

It was particularly encouraging that the system was able to provide the required power both in winter at temperatures below 0 °C and in summer at more than 35 °C. The module intended to cover emergency power supplies for authorities and organizations with security and safety tasks (BOS) was made up of two DMFC systems with 2 kW power each, connected to the feed-in for the radio system's emergency power supply via an inverter. The two DMFC systems had been constructed within the scope of the Helmholtz Validation Fund and integrated into an outdoor container for the field test. The container was set up at the BOS radio facility and connected to the digital radio system according to the following schematic (see Fig. 46):

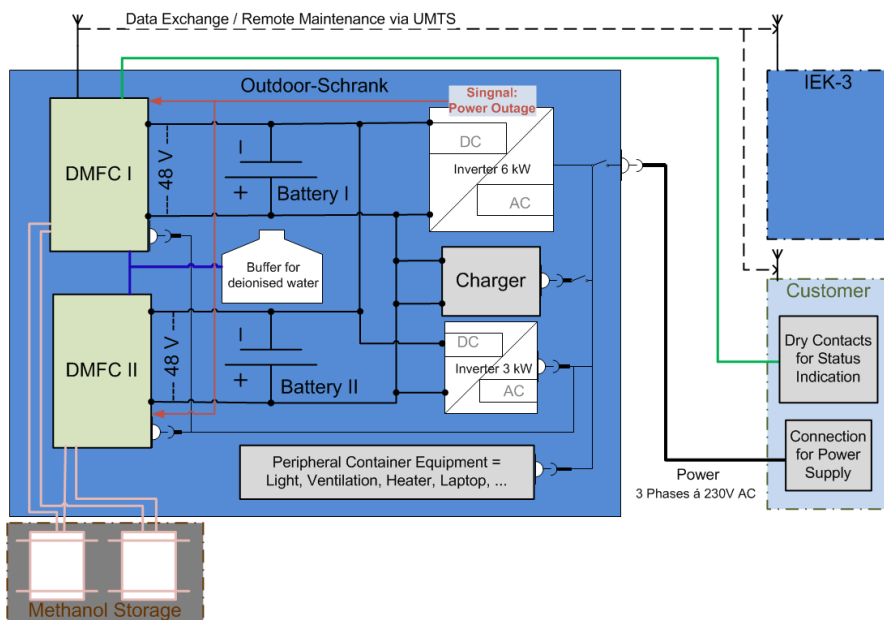


Fig. 46: Schematic structure of the DMFC UPS system

System boundary		Design stack		Stack			
		BOL	EOL	RW 117 Indoor, best performance	RW 118 Outdoor, best performance	RW 117 Indoor, 15.02.2015 test at FC power	RW 118 Outdoor, 26.11.2015 IBN USV container
Power	W	3.900	2.400	3.831	3.750	1.840	2.050
Length	dm	2,7	2,7	2,7	2,7	2,7	2,7
Width	dm	3,8	3,8	3,8	3,8	3,8	3,8
Height	dm	2,1	2,1	2,1	2,1	2,1	2,1
Volume	Liter	21,5	21,5	21,5	21,5	21,5	21,5
Power density	W/L	181,01	111,39	177,79	174,03	85,40	95,15

Table 5: Power density DMFC USV stacks

As part of a master's thesis, the field test was examined with respect to energy efficiency and aging behavior of the fuel cells. With an efficiency of more than 28 %, the set-up satisfied expectations. The aging of the fuel cells amounted to 2-5 $\mu\text{V/h}$ relative to calendar time, meaning that the project aim of 1.5 $\mu\text{V/h}$ was not quite achieved. The operating experience with the system reveals that it is well-suited for application in uninterruptable power supply systems. The system and the control software were optimized during practical application and improvements were suggested for future systems. In terms of the energy density, the

PoF milestone (M 3.1-22) was thus fulfilled with the stacks used. Table 5 shows that the mark of 100 W/liter was exceeded.

Michael Cieslik from the state office for central police services in Duisburg monitored the project from the user perspective and coordinated the tests for the police. His summary was positive: "The successful conclusion of the project is an express recommendation to continue developing the prototype of the Jülich fuel cell system and to bring it to market maturity, for example for emergency power supplies."

Further current research projects at IEK-3 contribute to reducing the costs of such systems, for example by developing new materials for the membrane–electrode unit, the core component of every fuel cell. Novel coating techniques for the bipolar plates are also being investigated. Both projects could contribute to using smaller amounts of noble metals, thus reducing the costs. IEK-3 thus possesses extensive know-how that can be transferred to industrial partners for potential future commercial fabrication of DMFC systems.

3.4.3 Staff members and fields of activity

Name	Tel. (02461-61-) Email	Field of activity
Dr. M. Müller	1859 mar.mueller@fz-juelich.de	Head / coordinator
Dr. A. Glösen	5171 a.gloesen@fz-juelich.de	MEA development
M. Hehemann	5431 m.hehemann@fz-juelich.de	System development
R. Keller	4124 r.keller@fz-juelich.de	Control development
W. Zwaygardt	2103 w.zwaygardt@fz-juelich.de	Stack development

3.4.4 Important publications, doctoral theses, and patents

Publications in peer-reviewed journals

Schulze Lohoff, A.; Günther, D.; Hehemann, M.; Müller, M.; Stolten, D
Extending the lifetime of direct methanol fuel cell systems to more than 20,000 h by applying ion exchange resins,
International Journal of Hydrogen Energy, 41 (2016), 15325-15334

Publications in books

Müller, M.
Fuel Cell Forklift Systems,
in Fuel Cells: Data, Facts, and Figures, First Edition. Stolten, D.; Samsun, R.C.; Garland, N., (Eds.), 2016, Wiley-VCH, Weinheim, p. 323-333

Other publications

Important patents

Patent applications:

Principal inventor	PT	Description
Dr. A.A. Kulikovsky	1.2644	A direct-alcohol fuel cell with effective CO ₂ removal, as well as methods for operating such a system

Patents granted:

Principal inventor	PT	Description
Dr. K. Wippermann	1.2318	Methods for the electrochemical activation of fuel cells
Dr. M. Stähler	1.2326	Emissions control for a fuel cell and a fuel cell stack
Dr. M. Müller	1.2331	Fuel cell systems and methods for controlling these
Dr. A. A. Kulikovsky	1.2426	A catalyst layer for use in a fuel cell and a method for its production
Dr. A. A. Kulikovsky	1.2544	Direct methanol fuel cells and methods of operation
Dr. A. A. Kulikovsky	1.2601	Method for characterizing the catalyst structure in a fuel cell, as well as a fuel cell design suitable for this purpose
Dr. J. McIntyre	1.2616	Low temperature fuel cells and methods for operating these

3.5 Water electrolysis

3.5.1 Objectives and fields of activity

The two groups Electrochemistry Electrolysis and Process Engineering Electrolysis develop industrial-scale electrolyzers with polymer electrolyte membranes (PEMs) in cooperation with leading industrial enterprises in this field. Cutting costs and increasing lifetime and power density are central aims. New types of membranes are being developed for PEM electrolysis to replace the 175–200 μm thick, extruded Nafion membranes currently used, which do not possess sufficient mechanical or chemical stability for use in the planned industrial systems under pressures exceeding 50 bar. Another objective is to reduce, and ideally completely replace, the metals from the platinum group – iridium, ruthenium, and platinum – which are commonly used today with a loading of around 4 mg/cm^2 for catalytic reactions. For PEM electrolysis to be economically feasible in the long term on a GW scale for the storage of large quantities of energy produced from renewable power, a 90 % reduction is needed in the quantity of platinum group metals used, combined with an increase in the overload capacity of membrane electrode assemblies to more than 6 W/cm^2 as well as a long-term stability of 40,000 hours or more. Another work package develops new cost-effective materials and coating techniques for metallic separator plates and current collectors with the aim of cutting the costs associated with these components, which presently account for 48 % of stack costs.

3.5.2 Important results

3.5.2.1 Development of advanced porous structures for electrolysis

As part of an institute-spanning project, advanced porous structures for electrolyzers are developed together with IEK-1 and industrial partners. The required geometric and mechanical parameters are defined at IEK-3, while IEK-1 is responsible for the sinter-metallurgical manufacture of the layers. The materials sintered at IEK-1 are then built into a standard cell with an effective area of 17.64 cm^2 at IEK-3 using commercial catalyst-coated membranes (CCMs) supplied by Greenerity.

Polarization curves were recorded at a temperature of 80 °C. Subsequently, an impedance spectrum was recorded for each cell. The results of impedance-spectroscopic investigations were then presented and discussed. For the IEK-1 parameter study, spherical as well as amorphous titanium particles with particle fractions of less than 45 μm were sintered at four different temperatures (800 °C, 900 °C, 1000 °C, 1200 °C). In order to determine the influence of sample thickness on cell performance, samples 250 μm and 500 μm in thickness were produced.

As can be seen in Fig. 47, the cells of the current collectors sintered at 1200 °C display mass transport limitations at an earlier stage, irrespective of the thickness of the current collectors and the shape of the titanium particles. The curves shown in black display a kink at 0.5 A/cm^2 . If the current density is further increased, the voltage rises sharply. The performance of cells with current collectors sintered at low temperatures is higher. Low sintering temperatures permit a higher porosity, leading to higher current densities of around 2.6 A/cm^2 at a voltage of 2 V.

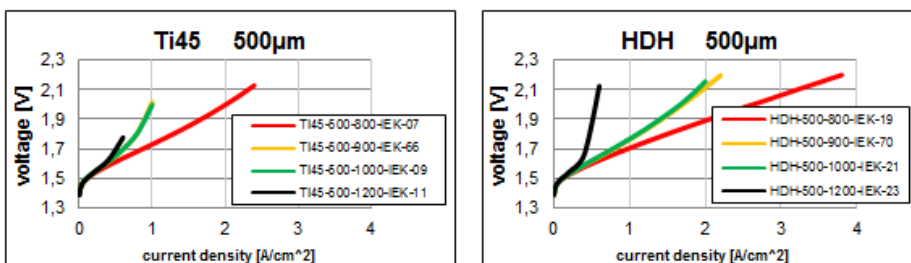


Fig. 47: Polarization curves of 500 μm samples from the parameter study (800 $^{\circ}\text{C}$, 900 $^{\circ}\text{C}$, 1000 $^{\circ}\text{C}$, 1200 $^{\circ}\text{C}$)

Within the scope of the sinter study, the thickness of one of the current collector types was varied and the polarization curves at various sample thicknesses compared to each other. The initial samples were produced from amorphous (HDH) titanium powder at a sintering temperature of 1000 $^{\circ}\text{C}$. The sample thickness varied from 150 μm to 650 μm .

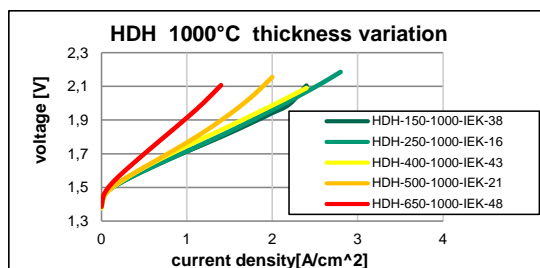


Fig. 48: Polarization curves of HDH titanium samples at a sintering temperature of 1000 $^{\circ}\text{C}$ (150 μm , 250 μm , 400 μm , 500 μm , 650 μm)

Fig. 48 shows the U-I curves of the samples from the thickness variation study. The figure shows that cell performance decreases with increased current collector thickness. However, the curves of the current collectors with thicknesses of 150–400 μm display only slight deviations from each other, so that the difference in thickness has no major influence in this range. It can thus be concluded that current collectors should have a thickness of less than 400 μm for optimal performance.

Furthermore, the influence of the titanium powder fractions of current collectors was investigated with regard to cell performance. Spherical titanium particles with particle fractions of < 45 μm , 45–75 μm , and 75–100 μm were used. These were compared to amorphous particles with particle fractions of < 45 μm . The polarization curves are shown in Fig. 49.

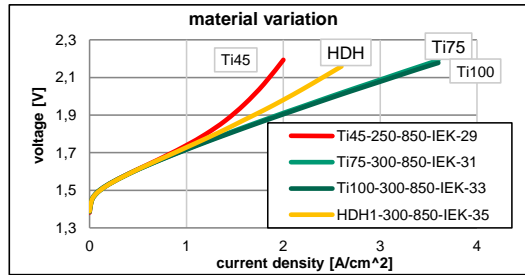


Fig. 49: Polarization curves of samples of titanium powder size variation sintered at 850 °C with a thickness of approximately 300 µm; spherical particles of < 45 µm fraction (Ti45); particle fraction 45–75 µm (Ti75); particle fraction 75–100 µm (Ti100); amorphous particles < 45 µm (HDH)

The Ti45 sintered foil has the lowest porosity (29 %) and the poorest performance. The two current collectors Ti75 and Ti100 have almost the same porosity (48 % and 49 %) and the U–I curves are almost identical. The current collector sintered from amorphous titanium particles has the highest porosity (51 %), but not the best performance. The pore shape in current collectors is thus much more important than the overall porosity. Further measurements are necessary in order to determine the pore shape resulting from the powder shape and sintering temperature.

Furthermore, titanium and stainless-steel expanded metals were tested with four different mesh sizes. The sinter plates and expanded metals were placed on top of each other and contacting was ensured only via pressure. The difference in thicknesses was compensated by means of an adapted sealant.

The expanded metals were included and tested directly between MEA and flow field plate, as schematically shown in Fig. 50 a). As a comparison to this measurement, a sintered foil was included and tested between MEA and expanded metal in order to improve the electric contacting. The schematic structure can be seen in Fig. 50 b).

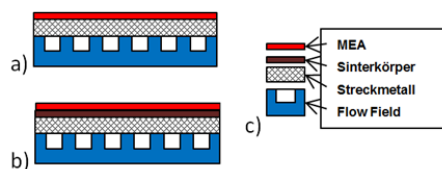


Fig. 50: Schematic cell structure: a) MEA in direct contact with expanded metal, b) sintered foil included between MEA and expanded metal c) cell components

The polarization curves of the cells with expanded metal are depicted in Fig. 51. Stainless-steel expanded metals (blue curves) generally have a poorer influence on cell performance than titanium expanded metals (red curves). If expanded metals are incorporated so that they are in contact with the MEA, finer mesh leads to improved performance since the electric current can flow through the mesh nodes. An additional porous sintered plate inserted between MEA and expanded metal ensures improved contacting and thus flatter characteristic curves. The characteristic curves of the individual variations of cells with expanded metals and sintered plates are very close to each other. A tendency is hardly recognizable.

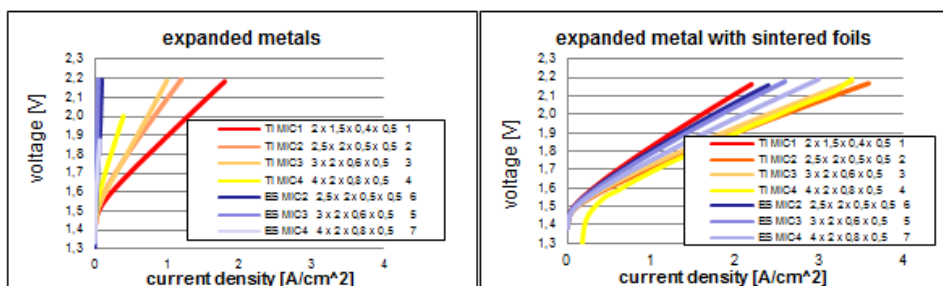


Fig. 51: Polarization curve for expanded metals: in direct contact with the CCM (left); with a sintered foil between CCM and expanded metal (right)

The expanded metals can be used as supports for sintered foils. They represent a good compromise between electrical contacting, media supply, and mechanical stability.

Impedance spectroscopy provides additional information on the resistances and reaction processes within a cell. Slow processes in an electrolysis cell, such as those that occur during mass transport or accumulation, arise mostly in the low-frequency range of the spectrum. Fast processes, such as charge transport or chemical reactions, contribute to the high-frequency range of the spectrum. The quantitative evaluation of impedance spectra is realized via a mathematical description of the system using a model equivalent circuit. An example of one of the equivalent circuits used is shown in Fig. 52. The parameters of this model are adapted until it corresponds to the measured data (curve fitting). The following parameter values are then determined from the model parameters:

- the ohmic series resistance (R_1), which depends mainly on the membrane resistance (ion conduction) but can also include contact resistances
- the kinetic resistance (R_2), e.g. charge transfer resistance of the electrochemical reactions at the electrodes
- the capacitance (CPE) corresponds to the double-layer capacitance/pseudocapacitance
- L1 is an artifact caused by the measurement setup, particularly cable inductance

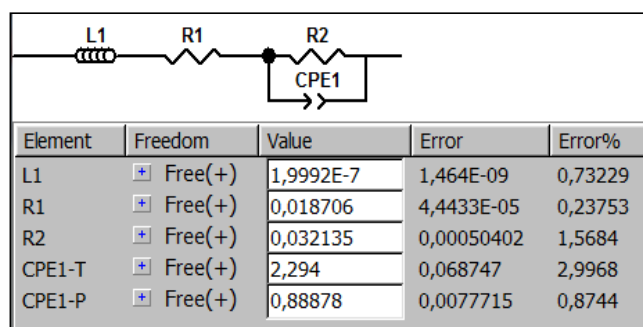


Fig. 52: Equivalent circuit shown for the example Ti100-300-850-IEK-33

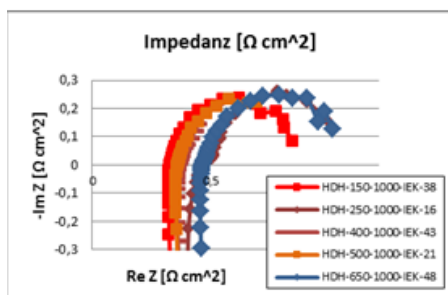


Fig. 53: Selection of measured impedance spectra

The impedance spectra (Fig. 53) were measured at 0.7 A; therefore, they do not provide any information on transport limitation. The series resistance (R_1) can be read out from the curve's point of intersection with the transverse axis. The values in Table 6 show the statistical scatter which can be explained by the varying degrees of sample oxidation during storage and preparation before insertion into the cell and the experiment itself.

Material name		Ohmic series resistance	Kinetic resistance	Capacitance
		[mΩcm ²]	[mΩcm ²]	[F/cm ²]
Variation in thickness	HDH-150-1000-IEK-38	324,7	544,5	0,093
	HDH-250-1000-IEK-16	459,2	685,5	0,056
	HDH-400-1000-IEK-43	360,6	485,1	0,098
	HDH-500-1000-IEK-21	356,2	538,8	0,096
	HDH-650-1000-IEK-48	460,2	623,3	0,085

Table 6: Impedances for various thicknesses of the sintered body

The kinetic resistance (R_2) is determined from the width of the semicircle using the evaluation programme; it provides information on the electrochemical reaction at the electrodes. As is the case with the series resistance, the kinetic resistance values in Table 6 show a statistical scatter. There are no outliers, but also no tendency; the values are close to each other, which indicates good reproducibility for the tests. The area-normalized capacitance values are close to 0.1 F/cm², which is typical of the CCM used. The MEAs used for the electrochemical test were very similar during the measurement and displayed similar aging.

Within the scope of the project, experiments were also conducted to determine the tensile strength and the elastic modulus of sintered titanium foils. The experiments were performed using samples of both types of titanium powder (spherical and spattered). Samples of both powder types were available with sintering temperatures between 800 and 1200 °C. Ti45 was in a porosity range of 10–33 % and HDH in a range of 10–55 % (see Fig. 54). The tensile strength was determined using samples 1 mm in thickness. The elastic modulus was

derived from the stress–strain values obtained in a tensile test. The tensile strength ranged from 18 N/mm² to 593 N/mm² and the elastic modulus from 72 N/mm² to 2204 N/mm².

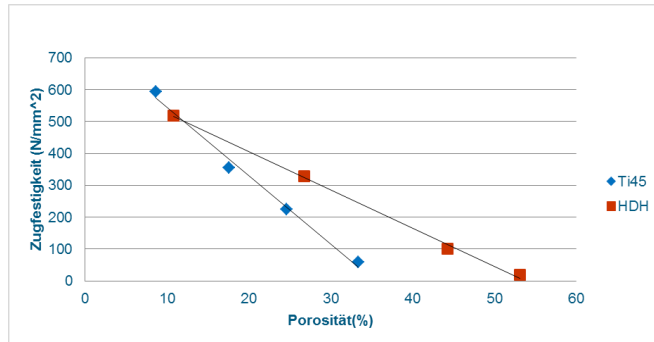


Fig. 54: Tensile strength in relation to porosity

Stress–strain diagrams revealed that higher sintering temperatures and lower porosity are associated with increased deformability. A considerably increased strain to failure, i.e. ductility, was striking in Ti45 starting at a sintering temperature of 1000 °C, whereas HDH did not display a massive increase in ductility. Overall, Ti45 displayed a much increased deformation capability compared to HDH at the same sintering temperature and porosity.

In addition, an experiment (see Fig. 55) was conducted that took into consideration the superposed tensions exerted on the sintered body during differential-pressure electrolysis. Within the scope of this flow-field experiment, the samples were pressed against a slit simulating the flow field of the bipolar plates.

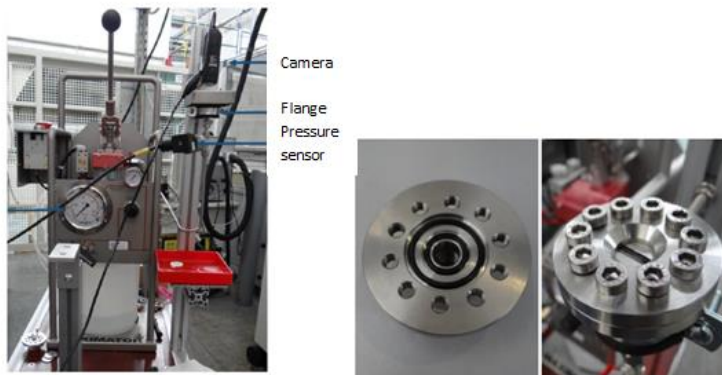


Fig. 55: Experimental setup of the flow-field experiment (left) and test cell (right)

The samples tested in the flow-field experiment were 250 µm and 500 µm thick. Their failures can be classified according to three different mechanisms: three of the material failures were ideally brittle, two ideally ductile, and all others displayed a brittle fracture with a proportion of plasticity (see Fig. 56).



Fig. 56: Types of failure of sintered bodies

3.5.2.2 Development of electrolysis systems

The industrial-scale production of hydrogen using power-to-gas plants imposes demanding requirements on the identification of the optimal operating and dimensioning parameters of the plant. From a technical point of view, it is high efficiency, in particular, that is the decisive parameter for economic operation. The subject of analysis was therefore an energetic consideration of a power-to-gas plant with a PEM electrolysis system for the industrial-scale production of hydrogen (see Fig. 57). The specific energy consumption of the electrolyzer and the corresponding cause–effect relationships were first identified. The relevant investigations were then conducted for the entire plant, taking into consideration the following process steps: performance conditioning, electrolysis, gas dehumidification, and gas compression. Optimal operating parameters for the electrolyzer and the entire plant were successfully identified. Using these results, a potential analysis was then conducted in order to estimate the energy demand of future power-to-gas plants.

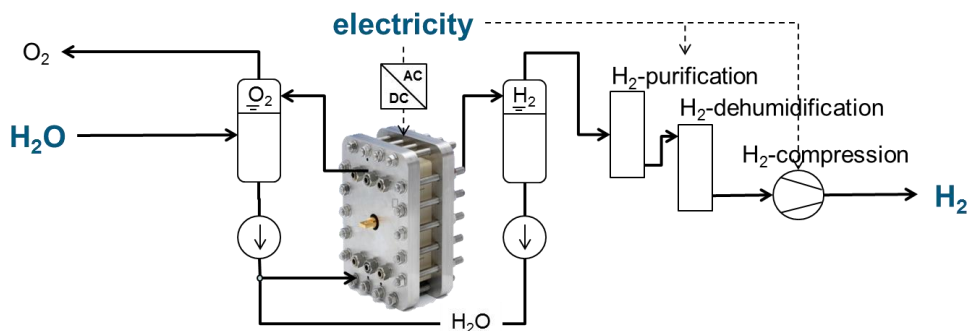


Fig. 57: Schematic of the electrolysis system

The results were presented on the basis of a model which comprised the electrolyzer including the representation of the polarization curves and the process steps of performance conditioning, gas dehumidification, and gas compression. The polarization curve modeling was parameterized with an individual cell using measurement data. The permeation processes via the membrane as well as heat transmission at the stack and system components were taken into account.

The energetic consideration of the electrolyzer (see Fig. 58) was first conducted in a system with an idealized membrane. Thus, the cause–effect relationships could be examined

independently of the losses occurring, revealing that the thermal power for operating ranges with low pressure levels and high temperatures represents a large fraction of the total output. These heat losses were mainly attributed to the vaporization of water in the product gas flows. It was possible to considerably reduce the thermal work by raising the pressure by only a few bar. It was also shown that lowering the temperature can also be beneficial for current densities below 1 A/cm² (see Fig. 58). An examination of the electrolyzer with a real membrane showed that permeation losses are dominant for low current densities below 1 A/cm², while above this operating point, the losses due to ion transport account for a larger share. Optimizing the membrane thickness in the relevant operating range above 1 A/cm² thus leads to a reduced membrane thickness of up to 50 µm.

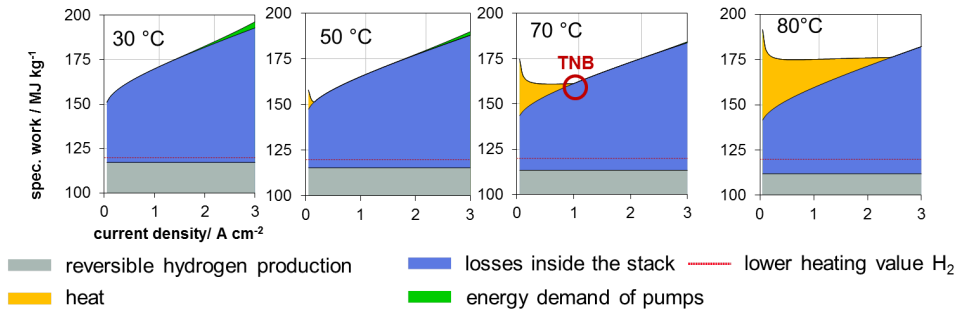


Fig. 58: Specific energy required for providing hydrogen at various operating temperatures

The examination of the electrolyzer in the context of the plant reveals the distribution of the specific energy requirements, with the electrolyzer requiring the largest amount of energy. Directly coupling the energy consumption of the power electronics to the system's consumption results in the second largest share in the overall energy consumption, at 8 %. These large shares are reached primarily in the low partial-load range below 1 A/cm² since the efficiency of the power electronics is considerably reduced here. The gas dehumidification performed after electrolysis requires less than 1 % of the overall energy consumption. This results, on the one hand, from the upstream gas cooling, which removes a large part of the steam from the product gas in an almost energy-neutral manner. On the other hand, the adsorption dehumidification system has to be designed in such a way that the regeneration gas can be recirculated, so that mass losses of the hydrogen produced can be prevented. A maximum share of 5 % is required for gas compression. This share can be reduced by increasing the pressure on the cathode side. However, the electrolyzer also requires more energy due to the work necessary for the volume change. Additionally, the permeation losses also rise with the pressure level of electrolysis. Depending on the operating point and cell performance, the optimal pressure range is thus 2–10 bar.

The optimization measures of the above investigations thus led to an increase in efficiency by 6 percentage points in the technically relevant load range of 1–3 A/cm². This is achieved by reducing the ionic losses. An increase of the maximum efficiency to more than 71 % is thus not possible. However, the potential analysis shows that future developments could reduce the activation losses of the individual cells, potentially increasing the efficiency across the entire load range. A maximum efficiency of the electrolyzer of approximately 81 % can thus be achieved. At the maximum current density of 3 A/cm², efficiency is reduced to

approximately 69 %. In future, the operation of the entire plant will thus be possible at efficiencies of 69–72 %. The major results are summarized in the following.

- At the current state of the art, electrolyzer efficiencies of 56–74 % (relative to the heating value of hydrogen) are possible. The greatest losses are caused by overpotentials in the stack. This applies particularly to the technically relevant operating range of 1–3 A/cm². For operating conditions at low pressures and high temperatures, the losses due to thermal work increase considerably. This increase results from the large share of steam in the product gas and the necessary vaporization enthalpy. Pressure operation of the electrolyzer is characterized by losses due to permeation processes. These losses reduce the efficiency of a potential internal compression of the hydrogen in the electrolyzer.
- Further process steps in the context of a plant reduce the electrolyzer efficiency to 53–66 % at the current state of the art. With a relative share of up to 94 %, the electrolyzer represents the greatest energy consumer. In order to condition the performance, a relative share of up to 8 % is necessary. The mechanical compression of the hydrogen requires a relative share of maximal 5 %. If the gas dehumidification is effected with regeneration flow recirculation, then a relatively small amount of power is consumed, amounting to less than 1 %.
- This optimized operational management can increase the efficiency even at the current state of the art. Efficiencies in the relevant operating range can thus be increased by up to 6 percentage points. This is mainly achieved by an optimized design of the membrane. This reveals that for operation above 1 A/cm², thin membranes of 50 µm thickness are preferable. The current state of the art uses 200 µm thick membranes. The use of thin membranes in order to increase the efficiency results from the high ionic losses at increasing current densities. The use of thin membranes requires the optimum pressure level of the electrolysis to be adjusted to 2–10 bar. The decreasing mechanical stability of the membrane is a limitation.
- Developments on the cell level, i.e. the reduction of overpotentials, can in future lead to increased efficiencies. The electrolyzer efficiency can thus be increased to above 80 % if the activation losses are reduced. Efficiencies of 68–72 % are thus possible for the entire plant. Reducing the losses caused by permeation, in contrast, leads to minor efficiency increases in the relevant operating range of 1–3 A/cm².

3.5.3 Staff members and fields of activity

Name	Tel. (02461-61-) Email	Field of activity
Dr. M. Müller	1859 mar.mueller@fz-juelich.de	Head/coordinator, multiphase flow
Dr. W. Lücke		Head of the electrochemical electrolysis department
Dr. M. Carmo	5590 m.carmo@fz-juelich.de	Head of the MEA development group
Dr. M. Stähler	2775 m.staehler@fz-juelich.de	Head of the MEA production group

D. Borah	6365 d.borah@fz-juelich.de	Flow simulation
C. Bordin	9381 c.bordin@fz-juelich.de	Mechanics
E. Borgardt	3079 e.borgardt@fz-juelich.de	Stack development, stack mechanics
A. Burdzik	2574 a.burdzik@fz-juelich.de	MEA manufacturing
S. Cheriyan	2094 s.cheriyam@fz-juelich.de	Analytics
N. Commerscheidt	3464 n.commerscheidt@fz-juelich.de	Stack manufacture, cell tests
S. Fischer	4478 st.fischer@fz-juelich.de	MEA development
I. Friedrich	1948 i.friedrich@fz-juelich.de	MEA manufacturing
Dr. A. Glösen	5171 a.gluesen@fz-juelich.de	Use of polymeric materials
D. Günther	2378 d.guenther@fz-juelich.de	Electrochemical characterization, quality assurance of processes
M. Hehemann	5431 m.hehemann@fz-juelich.de	Systems development, modeling, and testing
T. Höfner		MEA development
D. Holtz	2956 d.holtz@fz-juelich.de	MEA development
R. Lambertz	6695 r.lambertz@fz-juelich.de	Flow visualization, modeling, 3D topography
Dr. M. Langemann	9759 m.langemann@fz-juelich.de	Corrosion, coating, stack development
P. Paciok		MEA development
O. Panchenko	3079 o.panchenko@fz-juelich.de	Development and characterization of porous layersSchichten
C. Rakousky		MEA development
L. Ritz	5725 l.ritz@fz-juelich.de	Mechanics
S. Saba	9568 s.saba@fz-juelich.de	Economic viability of electrolysis systems
M. Schalenbach		MEA development
F. Scheepers	2177 f.scheepers@fz-juelich.de	MEA manufacturing
A. Schulz	8965 a.schulz@fz-juelich.de	MEA manufacturing
R. Wegner	4832	System and stack manufacture

W. Zwaygardt
2103
r.wegner@fz-juelich.de
w.zwaygardt@fz-juelich.de

Stack development and
characterization

3.5.4 Important publications, doctoral theses, and patents

Publications in peer-reviewed journals

Schalenbach, M.; Tjarks, G.; Carmo, M.; Lüke, W.; Müller, M.; Stolten, D.;
Acidic or Alkaline? Towards a New Perspective on the Efficiency of Water Electrolysis
Journal of the Electrochemical Society, 163 (2016), F3197-F3208

Schulze Lohoff, A.; Poggemann, L.; Carmo, M.; Müller, M.; Stolten, D.;
Enabling High Throughput Screening of Polymer Electrolyte Membrane (PEM) Water Electrolysis Components via Miniature Test Cells
Journal of the Electrochemical Society, 163 (2016), F3153-F3157

Langemann, M.; Fritz, D.L.; Müller, M.; Stolten, D.;
Validation and Characterization of Suitable Materials for Bipolar Plates in PEM Water Electrolysis
International Journal of Hydrogen Energy, 40 (2015), 11385-11391

Publications in conference volumes

Müller, M.; Tjarks, G.; Schalenbach, M.; Stolten, D.;
Efficiency of Electrolysis - How Transport Processes in Micro Scale Influence the Performance of Whole Systems
In Proc.: 21st World Hydrogen Energy Conference 2016, Zaragoza, Spain

Höh, M.; Banhart, J.; Fritz, D.; Lehnert, W.; Arlt, T.; Manke, I.; Müller, M.; Lin, Y.; Kardjilov, N.; Ehlert, J.;
Investigation of Two-Phase Flow in Polymer Electrolyte Membrane Water Electrolysis Using Neutron Radiography
In Proc.: Symposium for Fuel Cell and Battery Modeling and Experimental Validation MODVAL 13, Lausanne, Switzerland, 2016

Alexander Spies, Michael A. Hoeh, Tobias Arlt, Nikolay Kardjilov, David L. Fritz, Jannik Ehlert, John Banhart, Manuel Münsch, Antonio Delgado, Alexander Hahn, Ingo Manke, Werner Lehnert
Visualization of the two-phase flow inside a polymer electrolyte membrane water electrolysis cell using neutron radiography
In Tagungsband: "Lasermethoden in der Strömungsmesstechnik", 8. – 10. September 2015, Dresden

Important patents

Patent applications:

Principal inventor	PT	Description
Dr. M. Müller	1.2770	Electrolysis cells and method for operating them

3.6 Process and systems analysis

3.6.1 Objectives and fields of activity

The research priority of the interdisciplinary department is energy-related process and systems analysis. The year 2016 was characterized by an extensive restructuring of the activities of Process and Systems Analysis (VSA). In addition to developing from a specialist team into an independent department, human resources were expanded from eight to 13 employees, with a strongly increasing tendency. This also led to research topics being focused and expanded, supplemented by the following areas (see also chapter 5.5):

- Mobility
- Infrastructures and sector coupling
- Stationary energy systems

The new activities are accompanied by projects concerning a future CO₂-neutral energy system, including the Helmholtz Energy System 2050 initiative⁴, the virtual institute “Strom zu Gas und Wärme”⁵ (“Electricity into gas and heat”), and the Kopernikus Power-to-X project⁶.

The aims of VSA include identifying the potential of these innovative technologies to reduce greenhouse gas emissions as well as defining technical requirements for infrastructural elements as a starting point for future R&D measures.

VSA is currently developing energy strategies to fulfil the greenhouse gas reduction targets of the German Federal Government by designing and dimensioning alternative supply structures (e.g. power-to-X concepts) for a cross-sector Energiewende. Technology-based systems analyses can thus no longer be reduced to the evaluation of hydrogen applications in the entire system alone; in contrast, they comprise the neutral evaluation of all potential technologies. For this purpose, extensive models and methods are being developed.

3.6.2 Important results

3.6.2.1 METIS packages

The joint consideration and coupling of various sectors (energy, industry, households, and transport) is termed sector coupling and is one research field essential to achieving the greenhouse gas reduction targets (cf. chapter 5.5). Two possible methods are considered for the modeling of sector coupling: a closed model environment, on the one hand, and a model environment comprising several partial models, on the other hand (see Fig. 59).

⁴ https://www.helmholtz.de/en/research/energy/energy_system_2050/

⁵ <http://strom-zu-gas-und-waerme.de/>

⁶ <https://www.kopernikus-projekte.de/projekte/power-to-x>



Fig. 59: Different model environments for modeling sector coupling; left-hand side: closed modeling environment; right-hand side: various partial models

The aim of the closed modeling environment is to represent all sectors and technologies in one structure. It is used in order to determine a trend and includes simplifications in certain boundary conditions, permitting the calculations to be performed on computers with limited computing power. An example of such a simplification is a low spatial resolution, where all production and consumption profiles can be added up in one node. The aim of model environments composed of different partial models is to compensate the disadvantage of spatial resolution. For example, a partial model could analyze household consumption in great detail and pass on the results to a current flow model, which would then represent the grid and thus the current flow in detail. These calculations, however, require high computing power. Both modeling approaches are relevant and should be applied in accordance with the research issue in question.

The modeling of sector coupling requires high computing power and the development of new algorithms. The methodological development of the new model is based on a combination of models created by students and doctoral researchers who worked at Jülich's IEK-3 in recent years. It can thus be considered as one model consisting of various partial models (cf. Fig. 59, right-hand side). These models currently work with different development environments, but efforts are being undertaken to transfer the models into the Python programming language. This project was named METIS (Models for Energy Transformation and Integration Systems).

Data management for METIS is realized through a MSSQL database, which provides a data management system across several hard drives and optimized data retrieval. All data used in the study, including the hourly time series of the residual load for the federal states and municipalities, are stored in this database. Furthermore, individual wind turbines at different locations in Germany are included in the constructed scenarios.

3.6.2.2 Aging analyses of fossil-fired power plants

Extrapolating existing fossil-fired power plants in the models is essential for energy and electricity market projections. For this purpose, "technical lifespans" are assumed in many investigations. Using such assumptions as well as the knowledge of the commissioning years of individual power plant blocks, the decommissioning years for individual facilities can be deduced. The capacity of fossil-fired power plants can thus be assumed to decrease in a future period. Such projections are in turn used to estimate the future demand for newly constructed capacities. The technical lifespan is thus an important control variable. Many studies rely on figures based on experience when estimating lifetimes, without specifying these more closely, however. Using the fossil-fired power plants decommissioned in Germany over the past 35 years as an example, an ex post analysis shows how the lifetimes

of power plants have changed⁷. The analyses contribute to providing a basis for and classifying the lifespan estimates of existing and future energy projections.

For this purpose, ex post analyses were conducted on the basis of facilities decommissioned in the past 35 years. These analyses show that the lifetime of fossil-fired power plants has significantly increased during the past 3 decades. While for hard coal, it amounted to a power-output-based average of 33 years between 1990 and 1999, this value has increased to approximately 41 years during the past one-and-a-half decades. The hard-coal-fired power plants listed for decommissioning by the Federal Network Agency exhibit a comparable value of more than 42 years. A similar development can also be observed in power plants fired with lignite, oil, or gas.

In many electricity-market models, a correlation is assumed between efficiency development and the age of the power plant; this is then used for the projections of power-plant efficiency values. The efficiencies determined by means of regression analyses are in turn transferred to real power-plant blocks in many electricity-market models. Several existing power plants for which detailed data are available were used as examples to analyze whether and to what extent such a transfer is permissible.

The efficiency analyses indicate that the transferability of efficiencies extrapolated from regression analyses must be very critically examined for electricity-market analyses aiming to be accurate on the level of individual blocks. Determining efficiencies is particularly difficult with regard to estimating the influence of retrofitting measures on the efficiency of a power plant. The analyses show that the difference between calculated and real efficiencies can amount to several percentage points. It must be assumed that such differences have a considerable influence on merit-order analyses.

3.6.2.3 Hydrogen supply chains with alternative storage systems

Renewable energies will play a major part in future energy systems featuring low CO₂ emissions. In addition to the industrial-scale development of renewable energies in the electricity and heat sector, the planned emission reduction of 80–100 % by 2050 will also require enormous volumes of storage capacity. Furthermore, low-emission fuels must be identified for the transport sector. Hydrogen offers the option of interlinking the electricity with the mobility sector by storing surplus energy from renewable electricity generation in the form of hydrogen and subsequently serving as a fuel in fuel cell vehicles⁸. Due to the temporal and spatial discrepancy between production and utilization as a fuel, an infrastructure will be needed in order to store the hydrogen and to transport it to filling stations.

Currently, hydrogen is primarily transported and stored in its pure form as a compressed gas or cryogenic liquid. Since neither technology has the desired properties yet in terms of handling, thermodynamic properties, energy demand, and costs, alternative technologies are repeatedly the subject of scientific investigations. The objective of work carried out at VSA is to develop a model to compare various technologies along the entire chain in order to identify potential fields of application.

⁷ Markewitz, P., Robinius, M., Stolten, D., Wie alt werden fossil gefeuerte Kraftwerke?. 10. Internationale Energiewirtschaftstagung "Klimaziele 2050: Chance für einen Paradigmenwechsel?". 2017.

⁸ Robinius, M. Strom- und Gasmaktdesign zur Versorgung des deutschen Straßenverkehrs mit Wasserstoff RWTH Aachen University. 2015: Forschungszentrum Jülich GmbH Zentralbibliothek, Verlag. p. 255.

For this purpose, a point-to-point model was developed according to the methodology in Yang & Ogden (2007)⁹. In addition to the already examined systems of hydrogen provision, this model also includes alternative technologies. The use of liquid organic hydrogen carriers (LOHCs) as an element of the hydrogen supply chain could represent an alternative to the current state of the art. For industrial-scale energy systems, it is furthermore conceivable that the use of different storage technologies for storage and transport could lead to economic advantages. In order to take this into consideration, an energy conversion between storage and transport was modelled.

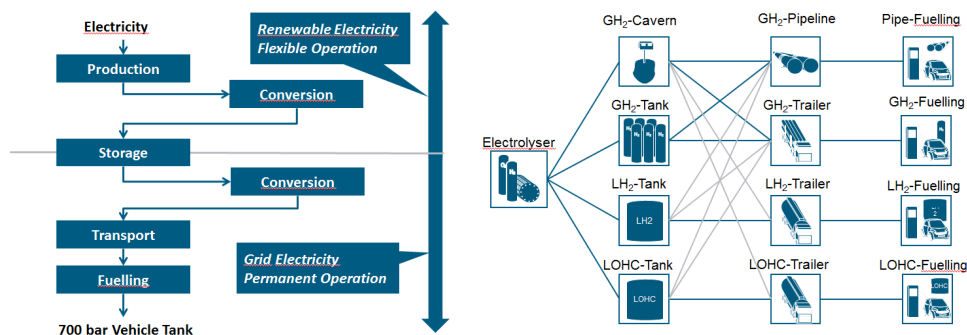


Fig. 60: Left-hand side: structure of the model; right-hand side: pathways investigated

In order to improve comparability, all supply pathways are assumed to include central and therefore industrial-scale hydrogen production from renewable electricity via electrolysis as well as a filling station with a 700 bar fuel pump as a consumer. The left-hand side of Fig. 60 shows the model structure and the subdivision into individual modules. Flexible plants are assumed for hydrogen production and conversion, which can seasonally store hydrogen from fluctuating renewably generated electricity that cannot be used on the grid side at the time of generation. Electricity provision via infrastructure components downstream of large-scale storage is assumed to be effected like the current EU electricity mix. The right-hand side of Fig. 60 shows the pathways investigated. The pathways without and with additional conversion between storage and transport are shown in blue and gray, respectively.

Fig. 61 shows the calculated specific costs of hydrogen at filling stations as a function of transport distance and overall demand. Similarly to the results obtained by Yang & Ogden (2007), the most cost-efficient areas arise from storage and transport technology. Among the assumptions, LOHC pathways are preferable particularly with low overall hydrogen demand (< 20–40 tH₂ per day). For short transport distances and increasing demand, transportation of gaseous hydrogen via trucks in combination with salt caverns is the most cost-efficient option. With higher demand and longer distances, the combination of pipeline and cavern leads to the lowest supply costs. Supplying hydrogen in liquid form is not applied in these

⁹ Yang, C. and J. Ogden, Determining the lowest-cost hydrogen delivery mode. International Journal of Hydrogen Energy, 2007. 32(2): p. 268-286.

assumptions. This is due to the high costs incurred by the liquefaction of hydrogen, composed of high investment costs as well as high operating costs.

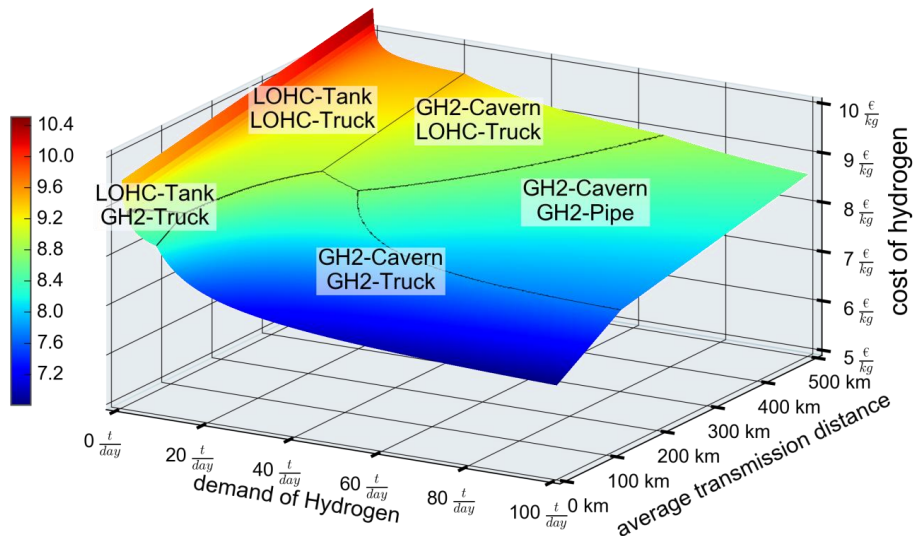


Fig. 61: Hydrogen provision costs at filling stations as a function of overall demand and transport distance

The present results show that there is application potential for the LOHC technology in a future hydrogen economy. With rising hydrogen demand, however, pipeline systems are advantageous with regard to the supply costs investigated here. The use of LOHC on an industrial scale has not yet been field-tested so that questions – for example on the long-term stability, the provision of energy for dehydrogenation, or hydrogen purity – cannot yet be answered satisfactorily.

3.6.2.4 Cost-optimal supply systems for a fully self-supporting single-family home

There is currently a trend in the residential building sector towards partly autonomous systems based on photovoltaics (PV) and battery storage. In the long term, fully self-supporting electricity and heat supplies are conceivable. One of the first fully self-supporting buildings was inaugurated in Switzerland in June 2016¹⁰. Against this backdrop the question arises of how large the potential of these systems is, which cover 100 % of their own requirements and are thus no longer dependent on the general electricity supply or energy carrier delivery (e.g. natural gas, oil, or biomass). For this purpose, VSA determined costs and designs of self-supporting supply systems for single-family homes and identified suitable technologies¹¹.

¹⁰ Diermann, R., *Ohne Netz - Erstes völlig energieautarkes Mehrfamilienhaus der Welt fertiggestellt*, in *Wirtschaftswoche*. 2016.

¹¹ Kotzur, L. et al. *Kostenoptimale Versorgungssysteme für ein vollautarkes Einfamilienhaus*. 10. Internationale Energiewirtschaftstagung "Klimaziele 2050: Chance für einen Paradigmenwechsel?". 2017.

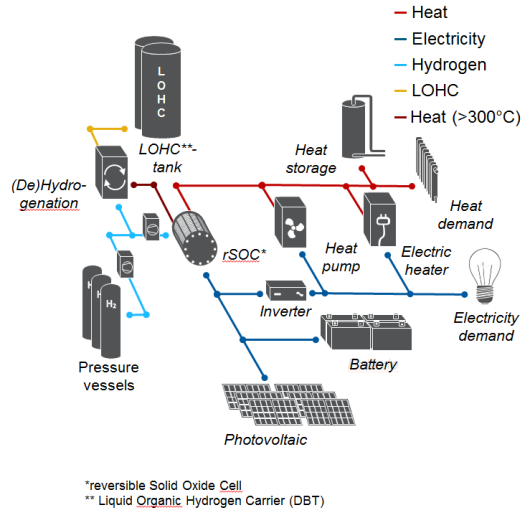


Fig. 62: The supply system investigated

A mixed-integer linear program (MILP) was compiled, which models the energy supply system of a residential building. The aim is to determine a cost-optimal technology configuration for heat and electricity supply for 8760 h per year. Technologies taken into account for the reference system include photovoltaics modules, batteries, heat pumps, immersion heaters, and heat storage systems. Potential system extensions include an electrolyzer, a hydrogen pressure store, and a fuel cell. In addition to alternative hydrogen conversion, the potential technology portfolio is expanded to include a reversible solid-oxide fuel cell (rSOC), which can be operated as an electrolyzer or as a fuel cell. As an alternative way of storing hydrogen, the model also has the option of integrating a system using liquid organic hydrogen carriers (LOHCs), consisting of hydrogenation and dehydrogenation units as well as an LOHC tank. This system is shown in Fig. 62.

As shown in Fig. 63, the supply system of the residential building was optimized for various system configurations. The sole use of batteries as a storage technology results in the most expensive system for 100 % self-sufficiency and represents the reference case. Utilizing hydrogen as a storage medium reduces the system costs by 20 %, with the use of a rSOC leading to a 24 % reduction. The building's heating requirements can be fully covered by waste heat from the fuel cell. The use of LOHC as a storage medium reduces the system costs further, to 44 % of the reference costs. The heat is here supplied by a heat pump, since the waste heat of the rSOC is used for the dehydrogenation of the LOHC. Furthermore, if a battery is connected to the system, another significant reduction can be achieved for the hydrogen system. Thanks to interim storage in the battery, the hydrogen system can be operated in a more constant manner throughout the year and can thus specifically convert more hydrogen. Consequently, the most cost-efficient fully self-supporting system can be realized with the combined use of rSOC, LOHC, and a battery.

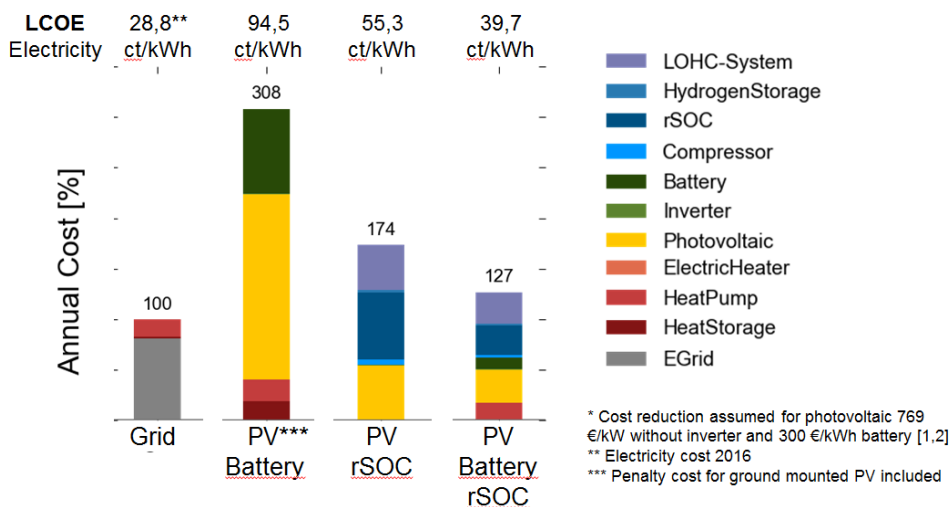


Fig. 63: Resulting composition of system costs, where the costs of the pure battery system were set as the reference value, i.e. at 100 %

3.6.3 Staff members and fields of activity

Name	Tel. (02461-61-) Email	Field of activity
Dr. M. Robinius	3077 m.robinius@fz-juelich.de	Head of Process and Systems Analysis
Dr. T. Grube	5398 th.grube@fz-juelich.de	Group leader Mobility
Dr. P. Markewitz	6119 p.markewitz@fz-juelich.de	Scientific responsibility for the field of stationary energy systems
D. Caglayan	5396 d.caglayan@fz-juelich.de	Concept of a pan-European solution for sector coupling via hydrogen
P. Heuser	9742 p.heuser@fz-juelich.de	Techno-economic analysis of a global hydrogen infrastructure
L. Kotzur	6689 l.kotzur@fz-juelich.de	Cost-optimal supply systems for houses
P. Lopion	1923 p.lopion@fz-juelich.de	Sector-coupling potential analyses for Germany
M. Reuss	9153 m.reuss@fz-juelich.de	Alternative hydrogen supply pathways
S. Ryberg	4064 s.ryberg@fz-juelich.de	Modeling of the European residual load at different development degrees of renewable energies

K. Syranidis	9156 k.syranidis@fz-juelich.de	Analysis of electricity not usable on the grid side at different development levels of the grid
Y. Wang	3742 yu.wang@fz-juelich.de	Membrane-based gas separation processes in energy technology
L. Welder	96992 l.welder@fz-juelich.de	Spatially and temporally highly resolved model environments
Dr. L. Zhao	4064 l.zhao@fz-juelich.de	Membrane-based gas separation processes in energy technology

3.6.4 Important publications, doctoral theses, and patents

Publications in peer-reviewed journals

Otto, A. ; Grube, T. ; Schiebahn, S. ; Stolten, D.

Closing the loop: Captured CO₂ as a feedstock in the chemical industry

Energy & environmental science 8(11), 3283 - 3297 (2015) [10.1039/C5EE02591E]

Publications in conference volumes

Otto, A. ; Grube, T. ; Ortwein, A. ; Zunft, S. ; Kaiser, J. ; Schneider, E. ; Tänzer, G. ; Schneider, C. ; Krönauer, A.

Wärme und Effizienz für die Industrie

In Proc.: FVEE Jahrestagung, Berlin, Germany, 3 Nov 2015 - 4 Nov 2015

Robinius, M. ; Stolten, D. ; Grube, T. ; Schiebahn, S.

Methodische Aspekte der Systemanalyse zur Energiewende

In Proc.: DPG-Jahrestagung 2016, Regensburg, Germany, 7 Mar 2016 - 7 Mar 2016

Robinius, M. ; Schiebahn, S. ; Grube, T. ; Stolten, D.

An Energy Concept to Supply the Transport Sector with Hydrogen from Renewable Energy Sources

In Proc.: 21st World Hydrogen Energy Conference 2016, Zaragoza, Spain, 13 Jun 2016 - 16 Jun 2016

Otto, A. ; Grube, T. ; Robinius, M. ; Stolten, D.

The Role of Hydrogen in an Environmental and Economical Synthesis of Organic Chemicals

In Proc.: 21st World Hydrogen Energy Conference 2016, Zaragoza, Spain, 13 Jun 2016 - 16 Jun 2016

Kotzur, L. ; Markewitz, P. ; Robinius, M. ; Stolten, D.

Kostenoptimale Versorgungssysteme für ein vollautarkes Einfamilienhaus

In Proc.: 10. Internationale Energiewirtschaftstagung IEWT Wien 2017, Vienna, Austria, 15 Feb 2017 - 17 Feb 2017

Doctoral theses

Robinius, M.

Strom- und Gasmärktedesign zur Versorgung des deutschen Straßenverkehrs mit Wasserstoff

Schriften des Forschungszentrums Jülich, Reihe Energie & Umwelt, 300 (2015), ISBN 978-3-95806-110-1

Otto, A.

Chemische, verfahrenstechnische und ökonomische Bewertung von Kohlendioxid als Rohstoff in der chemischen Industrie

Schriften des Forschungszentrums Jülich Reihe Energie & Umwelt, 268 (2015), ISBN 978-3-95806-064-7

Important patents

Patent applications:

Principal inventor	PT	Description
H. Notzke	1.2704	Membrane modules

3.7 Physicochemical principles / electrochemistry

3.7.1 Objectives and fields of activity

In the physicochemical fuel cell laboratory, the basic structure–activity relationships of complex processes in electrochemical energy converters are investigated to identify ways of improving them. The focus is on physicochemical properties and the electrochemical behaviour of components and model cells. Various in situ and ex situ methods are used:

- Imaging analysis techniques (SEM/EDX, optical microscopy), catalyst characterization using spatially resolved MS
- Spectroscopic methods (Raman, IR)
- Thermochemical and mechanical analysis techniques (TGA, DSC, elasticity/expansion measurements, BET, densitometry (gas pycnometer), (standard) porosimetry, contact angle measurements)
- Electrochemical analysis techniques (EIS, CV, conductivity), rotating disc and micro electrodes

Existing methods are adapted depending on the tasks at hand and new methods are established as required. In addition to examining the suitability of mechanical and thermomechanical conditions for application in fuel cells, another aim is to explain fundamental microscopic mechanisms of the redox kinetics of the electrodes and ion transport in the electrolyte membranes.

3.7.2 Important results

3.7.2.1 Ionic liquids as alternative electrolytes for the HT-PEFC

The physicochemical and electrochemical investigations on proton-conducting ionic liquids (PILs) as alternative electrolytes for HT-PEFC were continued. In addition to 2-sulfoethylammonium trifluoromethanesulfonic acid [2-Sea][TfO], which was developed three years ago, a new PIL was prepared and characterized: the N-methyl derivative [2-Sema][TfO], which contains a N,N-(2-sulfoethyl-methyl)-ammonium cation (see **Fig. 64**).

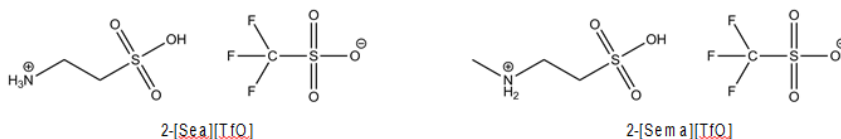


Fig. 64: Molecular structure of the investigated ionic liquids (PILs)

The bulk properties of these PILs were determined, as well as their ion conductivity and viscosity. The properties of the interface between the PIL electrolyte and a platinum electrode, such as the kinetics of the oxygen reduction and the double layer capacitance, were

also investigated. Since water is produced at the cathode in HT-PEFCs, all PILs were blended with 0 – 6 wt% water.

The following new results have been obtained for a system with a polycrystalline platinum electrode and an electrolyte composed of [2-Sea][TfO] and 5 wt% water since the last report¹². (i) the strong coupling between specific conductivity and dynamic viscosity indicates a vehicular proton transport, (ii) the temperature-dependent kinetics of the oxygen reduction reaction correlates with a competitive adsorption of [2-Sea][TfO] and water, (iii) with increasing temperature, the ordering in the adsorbate structure of the [2-Sea]⁺ and [TfO]⁻ ions on the platinum surface decreases and the co-adsorption of water molecules on the platinum surface increases.

The influence of up to 6 wt% water on the behaviour of the electrolytic double layer between the new PIL electrolyte [2-Sema][TfO] and a polycrystalline platinum electrode was investigated. The most important results of an analysis of series impedances are the following: (i) the representation as a complex capacitance results in spectra with up to four capacitive processes (see Fig. 65), *i.e.* two at high and two at low frequencies (fast/slow processes), (ii) the activation energy of the fast capacitive processes in the double layer corresponds to that of ion transport in the bulk electrolyte, (iii) the slow capacitive processes correlate with Faraday's reactions such as hydrogen or platinum oxidation.

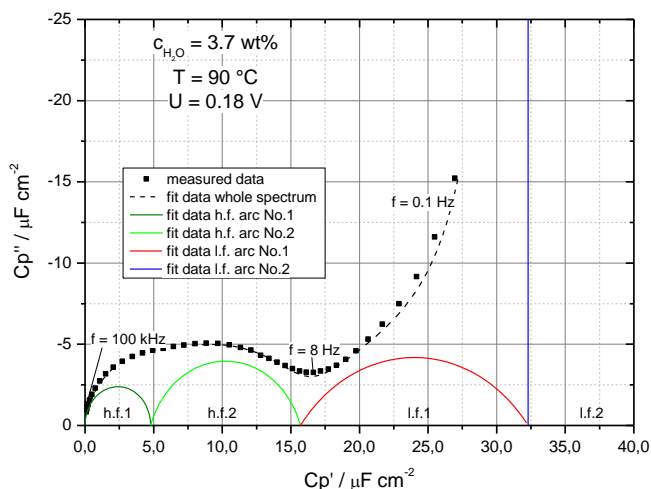


Fig. 65: Plot of the complex capacitance of the platinum-[2-Sema][TfO] phase interface using the example of 3.7 wt% water content

Also using the [2-Sema][TfO] electrolyte, the influence of the water content (1.3 – 4.4 wt%) on the kinetics of oxygen reduction reaction (ORR) on polycrystalline platinum electrodes was investigated. For this purpose, the hanging meniscus variant of a rotating platinum disc electrode was used (HM-RDE). The following results were obtained: (i) the limiting currents obtained from the current/voltage measurements at different rotation velocities comply with the Levich equation, (ii) the current densities of ORR were extracted from Koutecký-Levich

¹² K. Wippermann, J. Wackerl, W. Lehnert, B. Huber, C. Korte, Journal of The Electrochemical Society, 163 (2016) F25-F37.

plots and depicted as a Tafel plot (see Fig. 66), (iii) the current densities of the ORR showed no clear dependence on water content, (iv) the Tafel factors are close to the theoretical value of 144 mV/decade (at a temperature of 90 °C), (v) on average, the current density of the ORR using [2-Sema][TfO] as protic electrolyte is higher by a factor of three in comparison to 95 wt% phosphoric acid.

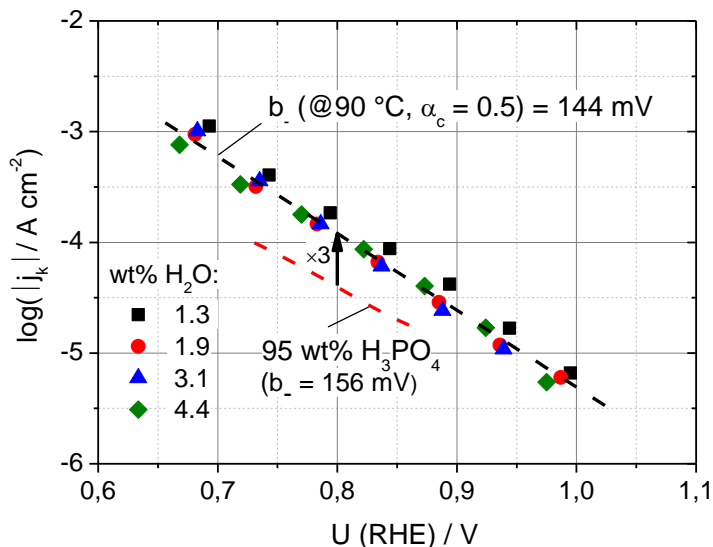


Fig. 66: Tafel plots of the oxygen reduction at platinum in [2-Sema][TfO] with 1.3–4.4 wt% water compared to 95 wt% phosphoric acid

3.7.2.2 Charge transfer between liquid and solid Li^+ electrolytes

In post-Li-ion battery systems like Li-S or Li- O_2 cells, the separation of the anodic and the cathodic part of the liquid electrolyte by a solid electrolyte membrane to opens new possibility to improve the cell setup. This will allow the use of different electrolytes for each side, so that they can be better tailored for the specific conditions.

The incorporation of a solid ion conductor might cause additional potential drops at the liquid electrolyte-solid electrolyte interfaces and in the solid electrolyte itself, because of interface charge transfer processes and the lower conductivity of the solid electrolyte compared to the liquid electrolyte. Because of the lack of literature data on solid/liquid electrolyte charge transfer kinetics, experimental studies on DC polarization of solid electrolyte-liquid electrolyte interfaces were performed. A symmetrical eight-electrodes-cell (6 potential probes + 2 current loaded electrodes) for spatially resolved electrochemical measurements was used. It consists of three compartments: i) liquid electrolyte, ii) solid electrolyte and iii) liquid electrolyte. The compartments with the liquid electrolyte, LiPF_6 in 1:1 w/w ethylene carbonate (EC)/dimethyl carbonate (DMC), are equipped with two electrochemical lithiated Pt-wires as electrochemical potential probes for Li^+ ions. The solid electrolyte $\text{Li}_{6.6}\text{La}_3\text{Zr}_{1.6}\text{Ta}_{0.4}\text{O}_{12}$ (LLZO:Ta) is directly contacted with two Li-wires as potential probes, see Fig. 67 a):

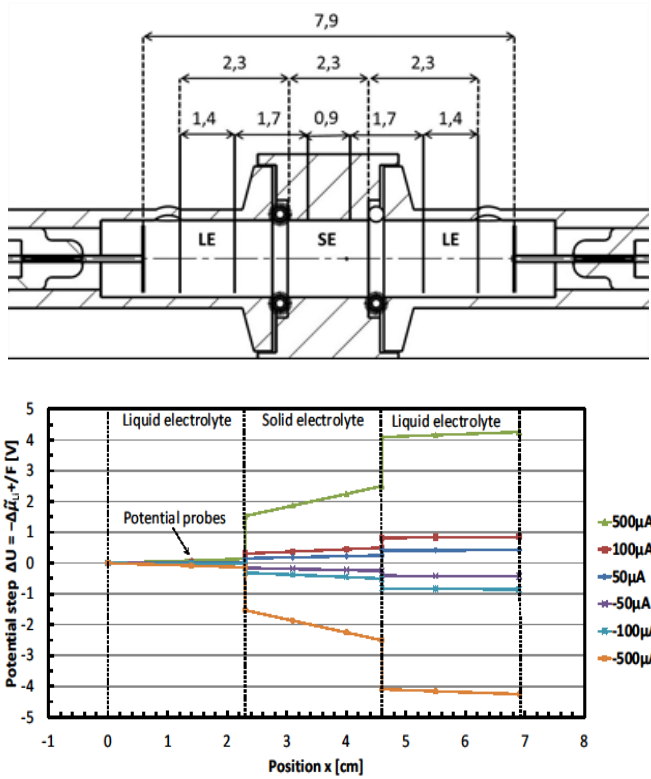


Fig. 67: a) Schematic setup of a DC polarization cell (above)
b) plot of the electrochemical potential gradients of Li^+ ions in a cell with a EC/DMC + 0.1 mol l^{-1} $LiPF_6$ liquid electrolyte and a $Li_7La_3Zr_2O_{12}$ solid electrolyte vs. position x in the cell for different polarisation currents (below), extrapolated from the measured voltages of the six potential probes

When polarising the cell with various current densities j , the stationary electrochemical potential differences of Li^+ ions, $\Delta \tilde{\mu}_{Li^+}/F$ ($= U$, electric potential drop), across the solid electrolyte-liquid electrolyte interfaces are determined by extrapolating the measured values of the Li^+ potential probes in each compartment to the interfaces, see Fig. 67 b).

In the case of small electrochemical potential differences $\Delta \tilde{\mu}_{Li^+}/F$ of at maximum ± 1 V across the solid liquid interface and Li^+ concentrations c_{Li^+} between 10^{-1} and 2 mol l^{-1} , nearly symmetric and s-shaped $\Delta \tilde{\mu}_{Li^+}/F$ vs. j -curves can be measured, see Fig. 68 a). Only at very small concentrations c_{Li^+} down to 10^{-3} mol l^{-1} the functional course becomes considerably asymmetric, indicating a transport limitation (depletion of Li^+ -ions at the interface).

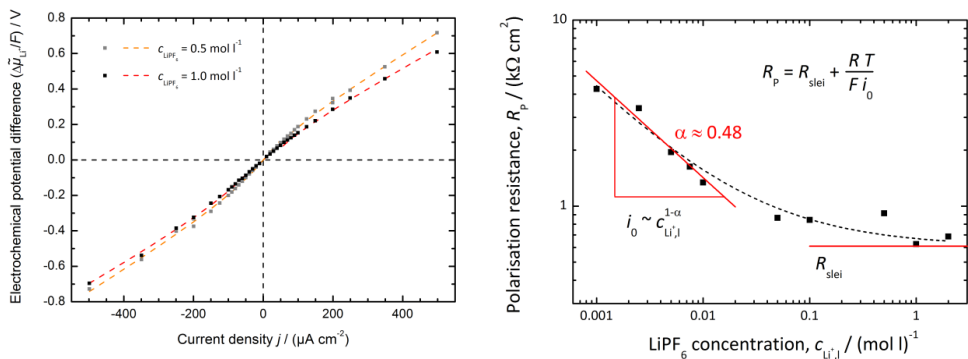


Fig. 68: a) Electrochemical potential difference $\Delta\tilde{\mu}_{Li^+}/F$ of Li^+ ions across the solid electrolyte-liquid electrolyte interface vs. current density j
b) log-log plot of the polarisation resistance $R_p = d(\Delta\tilde{\mu}_{Li^+}/F) / d c_{Li^+}$ vs. $LiPF_6$ concentration c_{Li^+}

The (areic) polarisation resistance R_p can be obtained from the slope at $j = 0$ in $\Delta\tilde{\mu}_{Li^+}/F$ vs. j plots. In Fig. 68 b) R_p is plotted as a function of the Li^+ concentration in the liquid electrolyte. The polarisation resistance R_p is reaching a lower limit for Li^+ concentrations c_{Li^+} above $0.1 mol l^{-1}$. In the case of lower Li^+ concentrations, the polarisation resistance R_p decreases with increasing Li^+ concentrations by power law. In a log-log plot a slope of -0.52 can be determined, i.e. $R_p \propto c_{Li^+}^{-0.52}$.

Abe and Sagane et al. conclude (from temperature dependent AC measurements) on the presence of an activated desolvation/solvation process for the ionic transfer^{13,14}. Busche et al. assume the presence of a poor ionic conducting solid-liquid electrolyte interphase (SLEI) formed by decomposition/degradation reactions between the solid and the liquid electrolyte¹⁵. The measured s-shaped course of the $\Delta\tilde{\mu}_{Li^+}/F$ vs. j curves can be well described by assuming a serial connection of a constant ohmic interphase resistance R_{SLEI} due to a poor conducting solid-liquid electrolyte interphase and a current dependent resistance due to a thermally activated ion transfer kinetic, considering the observations of Abe, Sagane and Busche et al.:

$$j = j_0 \left[\exp \left(\alpha \frac{\Delta\tilde{\mu}_{A^{z+},D}}{RT} \right) - \exp \left((1-\alpha) \frac{\Delta\tilde{\mu}_{A^{z+},D}}{RT} \right) \right] \text{ und } j = -\frac{1}{R_{SLEI}} \frac{\Delta\tilde{\mu}_{A^{z+},SLEI}}{zF}$$

$$\Delta\tilde{\mu}_{A^{z+},if} = \Delta\tilde{\mu}_{A^{z+},D} + \Delta\tilde{\mu}_{A^{z+},SLEI}$$

A thermally activated ion transfer process (formally) obeys a Butler-Volmer like expression for the current density, introducing an exchange current density j_0 and a charge transfer

¹³ T. Abe, F. Sagane, M. Ohtsuka, Y. Iriyama, Z. Ogumi, J. Electrochem. Soc., 152 (2005), A2151-A2154

¹⁴ F. Sagane, T. Abe, Z. Ogumi, J. Phys. Chem., C 113 (2009), 20135-20138

¹⁵ M. R. Busche, T. Drossel, T. Leichtweiss, M. Falk, M. Schneider, M. L. Reich, H. Sommer, P. Adelhelm, J. Janek, Nat. Chem., 8 (2016), 426-434

coefficient α . This model yields a concentration dependent specific polarisation resistance $R_p \propto c_{A^{z+},LE}^{1-\alpha}$ with R_{SLEI} as a limiting value:

$$R_p = \frac{RT}{zF j_0} + R_{SLEI} \quad \text{mit} \quad j_0 \propto c_{A^{z+}}^{1-\alpha}$$

Hereby, $c_{A^{z+},LE}$ is the concentration of the mobile A^{z+} cation in the liquid electrolyte (LE) and z the charge number. The pre-exponential factors for the charge transfer between liquid and solid electrolyte and vice versa are denoted with $k_{LE/SE}^0$ and $k_{SE/LE}^0$ and the activation energy with ΔG^\ddagger . The activated ionic transfer process takes place within a distance of d . The concentration of mobile cations $c_{A^{z+},SE}$ in the solid electrolyte (SE) is virtually constant.

Fitting the $\Delta\tilde{\mu}_{Li^+}/F$ vs. j plots, depicted exemplarily in Fig. 68 a, with the introduced model yields a concentration dependent exchange current density j_0 and a constant charge transfer coefficient α of ~ 0.5 and interphase resistance R_{SLEI} of $\sim 400 \Omega \text{ cm}^{-2}$. For a Li_+ concentration of $c_{Li^+} = 1 \text{ mol l}^{-1}$ the exchange current density j_0 can be estimated to about $60 \mu\text{A cm}^{-2}$.

Fitting the model to the R_p vs. c_{Li^+} plot, depicted in Fig. 68 b, yields an interphase resistance R_{SLEI} of $600 \Omega \text{ cm}^2$ and a charge transfer coefficient α of 0.4 . Both findings are comparable to the values obtained from directly fitting the $\Delta\tilde{\mu}_{Li^+}/F$ vs. j plots. In Fig. 68 b the interphase resistance R_{SLEI} appears as the plateau value at high Li^+ concentration and the charge transfer coefficient $1 - \alpha$ as the exponent of the power law at low concentrations.

The present preliminary DC measurements backup the presence of a poor conducting and current limiting interlayer¹⁵, as well as the presence of an activated process for the ionic transfer^{13,14}. The position of the transition state on the reaction coordinate is fairly symmetric.

3.7.3 Staff members and fields of activity

Name	Tel. (02461-61-) Email	Field of activity
PD. Dr. C. Korte	9035 c.korte@fz-juelich.de	Head of the Physicochemical Fuel Cell Laboratory
A. Everwand	8710 a.everwand@fz-juelich.de	Scanning electron microscopy (SEM/EDX)
P. Jehnichen	1891 p.jehnichen@fz-juelich.de	Aging processes of the high voltage cathode material $LiMn_{1.5}Ni_{0.5}O_4$ for Li batteries
Fr. K. Klafki	1895 k.klafki@fz-juelich.de	Sample preparation for electron microscopy (SEM) and light microscopy
Dr. S. Kuhri	1891 s.kuhri@fz-juelich.de	Raman and IR spectroscopy, imaging techniques
M. Schleutker	1891 m.schleutker@fz-juelich.de	Charge transfer between Li^+ conducting solid and liquid

Dr. J. Wackerl	6228 j.wackerl@fz-juelich.de	electrolytes Physical properties: DSC, TGA, mechanical properties, conductivity
Dr. K. Wippermann	2572 k.wippermann@fz-juelich.de	Electrochemical investigations: Properties of the electric double layer, electrochemical kinetics, spatial resolved analytics, aging processes

3.7.4 Important publications, doctoral theses, and patents

Publications in peer-reviewed journals

- K. Wippermann, J. Wackerl, W. Lehnert, B. Huber, C. Korte
2-Sulfoethylammonium trifluoromethanesulfonate as an Ionic Liquid for High Temperature PEM Fuel Cells
J. Electrochem. Soc., 163 (2016), F25-F37
- J. Keppner, C. Korte, J. Schubert, W. Zander, M. Ziegner, D. Stolten
XRD Analysis of Strain States in Epitaxial YSZ / RE₂O₃ (RE = Y, Er) Multilayers as a Function of Layer Thickness
Solid State Ionics, 273 (2015), 2-7
- F. Conti, F. Bertasi, J. Wackerl, P. Dams, V. Di Noto, W. Lehnert, C. Korte
Phase Diagram Approach to Study Acid and Water Uptake of Polybenzimidazole-Type Membranes for Fuel Cells
ECS Transactions, 72(8) (2016), 157-167
- C. Korte, F. Conti, J. Wackerl, P. Dams, A. Majerus, W. Lehnert
Uptake of Protic Electrolytes by Polybenzimidazole-Type Polymers - Absorption Isotherm and Electrolyte/Polymer Interactions
J. Appl. Electrochem., 45 (2015), 857-871
- T. Bergholz, C. Korte, D. Stolten
Development of Benchmarking-Model for Lithium Battery Electrodes
J. Power Sources, 320 (2016), 286-295

Important patents

Patent applications:

Principal inventor	PT	Description
T. Bergholz	1.2660	An electrolyte system for use in electrochemical components





4

Results

Selected Results

- Lithium batteries for stationary and mobile applications
- Evaluation of carbon dioxide as a raw material in the chemical industry
- Fuel cell / battery hybrid systems for auxiliary power units
- Electrodes with reduced Ir content for PEM electrolysis
- Solid oxide fuel cell system with integrated shielding-gas production
- PRECORS: Spin-off for corrosion-resistant coating technologies

4.1 Lithium batteries for stationary and mobile applications

In addition to a changeover to renewable energy sources for the production of electrical energy, the electrification of the transport sector is essential to reduce greenhouse gas emissions. In order to achieve these objectives, the use of electrochemical storage systems is crucial so that electrical energy can be used directly, without a converter. Against this backdrop, a doctoral thesis was written, developing a model to evaluate the application-specific potential of different electrochemical storage systems in general and their components in particular. The objective was to also deduce and prepare research priorities.

The application-specific evaluation of electrochemical storage systems was carried out using the benchmarking method. Based on a sensitivity analysis for battery electric vehicles (EVs), hybrid electric vehicles (HEVs), and an autonomous four-person household with a photovoltaic storage system, it was deduced that the applications considered exhibit different requirements of the storage system.

- the energy density for storage units in EVs,
- the power density for storage units in HEVs,
- the investment costs and the resource demand for stationary energy storage units,
- the safety features and lifetimes are important for all of these systems.

In addition, target and minimum values as well as prioritization factors for the demands of the applications can be deduced. Based on this, the evaluation of storage systems using characteristic values and the benchmarking method reveals that lithium-ion batteries (LIBs) exhibit the greatest potential for all three applications.

A multitude of different anodes, cathodes, electrolytes, and passive components which can be used in the lithium-ion battery technology were identified. In order to reduce the number of components which has to be considered and to estimate their potential in the resulting batteries, a model for the evaluation is introduced. Based on a literature survey, the influences of the various components on the necessary requirements with respect to energy density, power density, safety, lifetime, costs, and raw materials are described and characteristic limiting values are defined. The electrode active materials influence all of the necessary requirements mentioned. They are evaluated according to the following characteristics:

- for gravimetric and volumetric energy density, the modelled data of 18650-cells with reference electrodes (Si or $\text{Li}_2\text{MnO}_3 \cdot \text{LiNi}_{0.5}\text{Mn}_{0.5}\text{O}_2$) are used,
- the modelled particle radius for a peak discharge pulse in HEVs, the redox potential of the active electrode material, and the electrochemical stability with respect to the electrolyte serve to evaluate the power density,
- for security, the thermal stability of the electrodes in comparison to that of the pure cathode active material is considered with respect to the standard electrolyte,
- the electrochemical stability of the electrolyte with respect to the electrodes, the volume effect, the thermal stability of the cathode active material, and of the anode with respect to the electrolyte are limiting for the lifetime,
- the costs are evaluated based on the specific material costs of the redox-active species contained,
- the resulting charge quantities from the accessible raw material reserves and the annual production are evaluation factors for the raw material.

The electrolytes greatly influence the power density, the safety, and the lifetime of batteries. The following characteristics are considered:

- the thermal stability with respect to graphite anodes as well as the flash point and the boiling temperature serve as a basis for the safety evaluation,
- the power density is primarily influenced by the lithium-ion conductivity and the minimum operating temperature,
- for the lifetime, the electrochemical stability window, the hydrolysis stability, and the corrosion properties with respect to Al are the priorities.

Within the scope of evaluating the passive components, current collectors have noticeably influence the power density, lifetime, and costs of LIBs. The evaluation takes into account the power dissipation in a model cell, alloy formation with Li, anode stability, and raw material prices.

Based on the derived model, the evaluation of components of lithium batteries can be classified into intercalation cathodes and anodes, conversion electrodes, electrolytes, and current collectors. The minimum and target values deduced at the beginning for electrochemical storage in EVs, HEVs, and stationary applications also serve to identify exclusion criteria for the respective components. The quantitative evaluation based on characteristic values results in different relevant cell systems for the applications. The following components are particularly suitable for EVs:

- Combinations of silicon anodes and composite ($\text{Li}_2\text{MnO}_3 \cdot \text{LiNi}_{0.5}\text{Mn}_{0.5}\text{O}_2$) or LNMO cathodes ($\text{LiNi}_{0.5}\text{Mn}_{1.5}\text{O}_4$) achieve the largest ranges in EVs (300–500 km on a cell level) and exhibit low specific costs.
- Alternatively, graphite anodes can be used, which have lower energy densities but a better lifetime evaluation compared to Si.
- Due to the sufficient safety and lifetime evaluation as well as the high power density of gels based on organic solvents, they are advantageous in the cells based on composite cathodes.
- The high cell voltage of LNMO-based systems makes the use of ILs crucial due to their high anode stabilities.
- Cu and Al are the only materials which can be used for anode and cathode current collectors in EVs since they exhibit high electric conductivity, relatively low costs, and sufficient cathode and anode stability windows.

Cell systems for HEVs include the following components:

- Due to the high power density, as well as the high safety and lifetime values, the cell based on LiFePO_4 and $\text{Li}_4\text{Ti}_5\text{O}_{12}$ has the greatest potential for application in HEVs.
- The low cell voltage means that conventional organic solvent electrolytes in combination with their high power density are suitable as an electrolyte system.
- As is the case for EV cells, only the use of Cu and Al in anode and cathode current collectors is feasible.

The following components are needed for cells in stationary systems:

- The relatively high costs and low evaluation factors concerning the reserves of raw materials for $\text{Li}_4\text{Ti}_5\text{O}_{12}$ makes this material unsuitable for stationary applications, contrary to the general view expressed in the literature. Instead, the use of TiO_2 for the anode with LiFePO_4 was evaluated as advantageous for stationary batteries.

- The high lifetime and safety evaluation factors of ILs are factors that make these materials suitable for use in a stationary battery system. Due to the low cell voltage when using LiFePO_4 as cathode material, the use of conventional organic solvent gels or purely organic solvents is of interest. In general, these exhibit lower material costs.
- In addition to the conventional current collector materials Cu and Al, the introduction of stainless steel (SS304) is advantageous since it can be used as a bipolar collector.

Based on the analysis of the lithium battery components, the following research priorities can be identified:

- development of a degradation model for the EV electrodes Li_2MnO_3 , $\text{LiNi}_{0.5}\text{Mn}_{0.5}\text{O}_2$, $\text{LiNi}_{0.5}\text{Mn}_{1.5}\text{O}_4$, Si, and graphite, whose potential is outside the stability window of the electrolyte,
- improvement of the total ionic conductivity and the transport number of high-voltage-stable ILs for application in EVs and stationary systems,

Analysis of literature on various degradation models and aging experiments with laboratory-scale and commercial cells reveals that the diffusion-controlled growth of the solid electrolyte interface (SEI) between anode and electrolyte is frequently the limiting degradation process. Due to the diffusion control there is a parabolic relation between the cell live time, respectively the total transferred electric charge as a sum of all cycles and the capacity decrease (SoH_Q), respectively the resistance increase (SoH_R). In the studies analyzed, a linear correlation is revealed between SoH_R and SoH_Q . The degradation processes that occur in high voltage cathode materials as LNMO are not fully explained in the literature, however, the use of high-voltage-stable electrolytes is essential in order to optimize the lifetime and the safety characteristics of high-voltage cathodes.

Based on the analysis and the benchmarking, the following core statements can be made:

- due to their safety properties and the volumetric energy density, sulfur cathodes are unsuitable for the applications considered,
- lithium and tin anodes as well as LiCoO_2 , LiNiO_2 , $\text{LiNi}_{0.8}\text{Co}_{0.15}\text{Al}_{0.05}\text{O}_2$ (NCA) and $\text{LiNi}_{0.33}\text{Mn}_{0.33}\text{Co}_{0.33}\text{O}_2$ (NMC) also cannot be used due to their safety aspects,
- due to their low conductivity and the formation of contact resistances during cycling, organic and inorganic solid electrolytes are not suitable for use in large-scale cells,
- it is possible to significantly increase the energy density of present LIBs ($\times \sim 2$),
- costs can be significantly reduced by optimizing the raw material parameters of the electrodes,
- new cell concepts require a stabilization of the electrode–electrolyte interface in order to guarantee sufficient lifetime, power density, and safety,
- as soon as an electrolyte is thermodynamically unstable with respect to the potential of the electrode, irreversible degradation reactions occur even after the formation of stabilizing surface layers.

A model for the evaluation of the application-specific potential of electrochemical storage systems in general and their components in particular was successfully implemented and applied.

4.2 Evaluation of carbon dioxide as a raw material in the chemical industry

In its World Energy Outlook 2012¹⁶, the International Energy Agency (IEA) presents scenarios with which the future trends of global energy demand and the associated carbon-dioxide emissions can be estimated with and without implementing CO₂ reduction measures. Fig. 69 shows the measures and their contributions of the 450 Scenario, which are expected to lead to a reduction of 15 billion tonnes of CO₂ by 2035 relative to the New Policies Scenario. The major proportion of CO₂ emissions is planned to be reduced by means of saving electricity, increasing the efficiency of power plants, increasing the energy end-use efficiency, and expanding the application of renewable and nuclear energy (page 241-265 in ¹⁶).

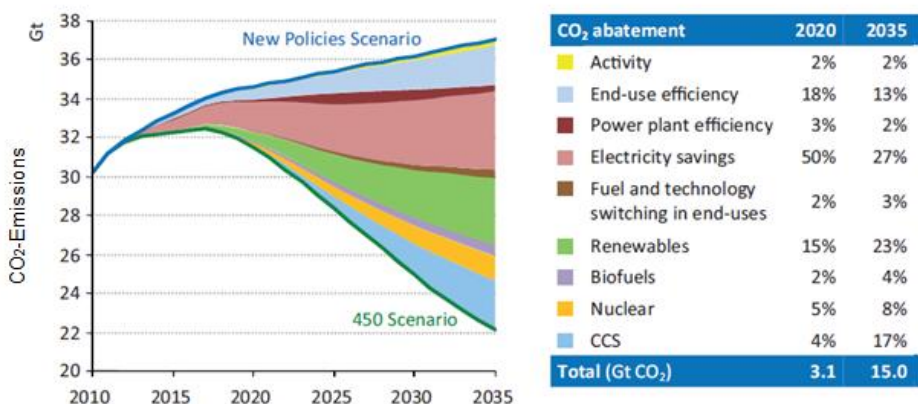


Fig. 69: Decrease in global energy-related CO₂ emissions in the 450 Scenario relative to the New Policies Scenario (page 253 in ¹⁶)
CCS = carbon capture and storage

According to the 450 Scenario, a third of the global electricity demand (10,487 TWh) will be covered by fossil-fired power plant processes. By 2035, approximately 3640 TWh is planned to be provided from fossil-fired power plants, in which the CO₂ will be separated and prevented from entering the atmosphere through geological storage. This technique is also termed “carbon capture and storage” (CCS)¹⁷. CCS is expected to lead to a reduction of CO₂ emissions by 14.3 % (corresponding to 2.1 billion tonnes) by 2035 relative to the New Policies Scenario (page 182 and 251 in ¹⁶). According to the International Energy Agency's Technology Roadmap – Carbon Capture and Storage¹⁸, CCS technologies will not be limited to electricity generation alone. By 2050, 25–40 % of all steel, concrete, and chemistry plants worldwide will be equipped with CCS technology. From 2015 to 2050, this will accumulate to approximately 120 billion tonnes of CO₂ originating from electricity generation and industry and which will have to be stored in geological formations. A general disadvantage of geological storage is the additional costs and additional energy required. The additional

¹⁶ World Energy Outlook 2012, Paris: International Energy Agency, ISBN: 978-92-64-18084-0

¹⁷ Stolten, D., Scherer V. (eds.): Efficient Carbon Capture for Coal Power Plants. WILEY-VCH, Weinheim (2011), ISBN: 978-3-527-33002-7

¹⁸ Technology Roadmap - Carbon Capture and Storage, 2013, International Energy Agency, France

energy demand results from the fact that the CO₂, which after separation is usually present at atmospheric pressure, has to be compressed to at least 100 bar and then transported to the storage locations (page 527-540 in ¹⁷). Furthermore, the geological storage of CO₂ is controversial in Germany and is currently legally limited to 4 million tonnes per year¹⁹.

As an alternative to geological storage, the separated CO₂ could be used as a raw material in the chemical industry, a concept also known as “carbon capture and utilization” (CCU). By using the waste product, its value is increased and the costs and energy demand for storage are avoided. Although CO₂ with its standard formation enthalpy of -393.51 kJ/mol is unreactive, it can be converted into useful products with highly reactive reaction partners such as hydrogen.

The conversion of carbon dioxide into more valuable products can be performed chemically, electrochemically, biochemically, or photochemically (Fig. 70). Depending on the nature of the conversion process, the energy required is supplied thermally, electrically, chemically, or by light. In addition to the preparation of material products, the conversion of CO₂, for example into methane, can also be used as an energy storage solution for renewable energies. This is one option provided by the “power-to-gas” method.

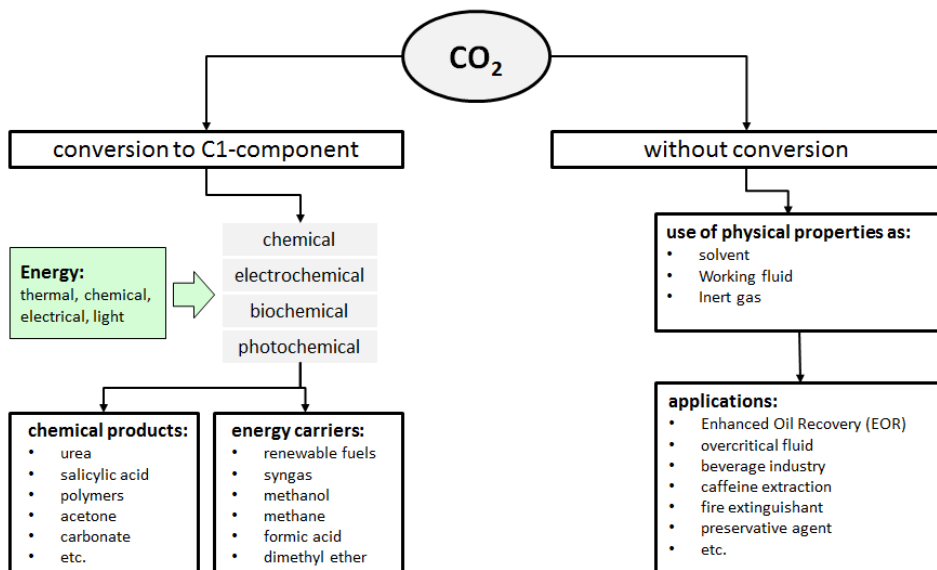


Fig. 70: Potential CO₂ utilization pathways, with and without conversion

The literature lists numerous reactions in which CO₂ is used as a raw material. These range from bulk chemicals with large sales markets such as methanol to numerous fine chemicals and polymers. Such scientific publications are generally concerned only with the viability of the reaction without considering the potential for reducing CO₂ compared to the conventional process or else with the technical and economic feasibility. In systematic investigations in the

¹⁹ Gesetz zur Demonstration der dauerhaften Speicherung von Kohlendioxid (Kohlendioxid-Speicherungsgesetz - KSpG), 17.08.2013, Bundesanzeiger Verlag: <http://www.bmwi.de/BMWi/Redaktion/PDF/Gesetz/gesetzentwurf-ccs-08-2012.property=pdf,bereich=bmwi2012.sprache=de.rwb=true.pdf>

literature which assess potential products and processes based on CO₂, there are still gaps concerning the future potential for climate relevance and industrial and economic viability. The activities of IEK-3²⁰ have therefore contributed to closing these gaps by identifying and subsequently analyzing and assessing suitable CO₂ utilization reactions.

Based on extensive literature research on the possible chemical conversion of CO₂, 123 CO₂-based reactions were compiled. The products resulting from them were divided into 23 bulk chemicals and 100 fine chemicals. Within the scope of a preliminary assessment, the reactions and products were classified according to the CO₂-reduction potential and the economic interest that the chemical industry might have in the resulting products. This assessment was carried out based on selection criteria specifically adapted to bulk and fine chemicals in order to achieve an accurate classification of the substances in a ranking as well as to take into consideration the quality of the data on which the assessment was based. The following criteria were specially developed and considered in the preliminary assessment of the bulk and fine chemicals:

Bulk chemicals	Fine chemicals
- Specific mass of CO ₂ used	- Specific mass of CO ₂ used
- CO ₂ reduction potential	- Production volumes of the substance groups
- Relative added value	- Relative added value
- Independence from fossil raw materials	- Scientific relevance
	- Technical availability

Among the bulk chemicals, the leading CO₂-based reactions result in formic acid, formaldehyde, oxalic acid, methanol, urea, and dimethyl ether; among the fine chemicals, the leading products are methyl carbamate, 3-oxopentane dicarboxylic acid, 2-imidazolidinone, and ethyl carbamate.

A direct comparison of bulk and fine chemicals revealed that the fine chemicals have almost no potential to reduce the mass of CO₂ emissions. The reason for this is that within the European Union, the 23 bulk chemicals considered have the potential to utilize approximately 59 million tonnes of CO₂ per year as a raw material (taking into account the specific amounts of CO₂ used), at a production rate of approximately 78 million tonnes. This corresponds to roughly 1.3 % of the EU's GHG emissions. In contrast, the production volume of fine chemicals (100 fine chemicals, classified into 12 substance groups) amounts to only 4.3 million tonnes per year in the EU. However, it must be taken into account that the produced amounts of these substance groups include not only the 100 fine chemicals considered but all substances from these substance groups that are produced in the 27 EU member states. Taking into account the fact that 0.31 kg_{CO2}/kg_{product} are used on average for the synthesis of the fine chemicals considered, and assuming that the production volume of the 100 fine chemicals considered corresponds to that of the 12 substance groups, these could contribute a maximum of 0.029 % to the reduction of GHG emissions in the EU.

²⁰ Otto, A. Chemische, verfahrenstechnische und ökonomische Bewertung von Kohlendioxid als Rohstoff in der chemischen Industrie, Schriften des Forschungszentrums Jülich, Energie & Umwelt , 268 (2015)

The strength of the fine chemicals is their high relative value creation. For chemical companies releasing small amounts of CO₂, it could therefore be of economic interest to synthesize fine chemicals directly on site due to the high value creation that can be achieved.

For the bulk chemicals formic acid, formaldehyde, oxalic acid, methanol, and dimethyl ether, which best met the criteria from the preliminary assessment, the CO₂-based and the conventional processes were compared directly. Literature-based estimates of the potential that CO₂-based reactions have compared to the conventional processes of reducing CO₂ emissions revealed that oxalic acid and formaldehyde – which were determined to be the products of the ideal CO₂ utilization reactions – do not lead to any reduction of CO₂ emissions according to current knowledge.

For the CO₂-based reactions of methanol and dimethyl ether, which have the potential to reduce CO₂ emissions relative to the conventional process, a simulation-based comparison with the conventional process was conducted.

These simulations of the specially developed CO₂-based processes verified that they permit an industrial-scale implementation of the CO₂-based reactions considered. The comparison with the conventional processes revealed that the CO₂-based processes only lead to a reduction in CO₂ emissions relative to the conventional process if the hydrogen used as a CO reagent is supplied from electrolysis powered by renewable energy. This means that the manner of hydrogen production is crucial in deciding whether the CO₂ utilization process can function as a CO₂ reduction option or if it emits even more CO₂ than the conventional process. Furthermore, the analysis of urea synthesis revealed that this process – although it is viewed as a role model for the industrial-scale utilization of CO₂ – actually emits more CO₂ than is bound during the process. In order for the urea process to achieve a negative CO₂ balance, the hydrogen required for ammonia synthesis would have to be obtained from water electrolysis powered by renewable energy.

For a future implementation of a CO₂-based process, the economic feasibility is also significant in addition to the potential of reducing CO₂ emissions. For this reason, the production costs of the CO₂-based and the conventional process for methanol and dimethyl ether were calculated and compared to each other since they have the greatest CO₂ reduction potential. Considering the current CO₂ emission allowance price of 0.0035 €/kg_{CO2}, the production costs of the CO₂-based methanol and dimethyl-ether processes are 3.3 (1.1 €/kg_{MeOH}) and 2.3 (1.7 €/kg_{DME}) times higher than the respective conventional production process. Even assuming a 10-fold increase of the CO₂ emission allowance price, the specific production costs of the CO₂-based methanol process are 3.1 times as high, and those of the DME process 2.2 times as high as for the conventional process. Only if the CO₂ emission allowance price rises to 0.545 €/kg_{CO2} (for the methanol case) or 0.438 €/kg_{CO2} (for the dimethyl-ether case) will the production costs of the CO₂-based and the conventional processes be on the same level. However, these prices are 125–155 times higher than the current emission allowance prices. The difference between the current emission allowance price and the required CO₂ emission allowance price yields the CO₂ avoidance costs. Considering the current CO₂ emission allowance price, these amount to 0.541 €/kg_{CO2} in the case of the CO₂-based methanol process, and to 0.435 €/kg_{CO2} for the dimethyl-ether process.

For the CO₂-based processes, it was assumed that the CO₂ used as a raw material originates from the flue gas of fossil-fired power plant processes. Alternatively, the CO₂ could

be stored directly in geological formations after separation in the power plant. Under the given boundary conditions, the CO₂ avoidance costs of the CO₂-based methanol and dimethyl-ether synthesis can thus be directly compared with the costs for geological storage. According to a study by McKinsey & Company²¹ the CO₂ avoidance costs for the geological storage of CO₂ in aquifers within Germany amount to 0.006 €/kg_{CO2}. Thus, the costs for CO₂ avoidance via the synthesis of methanol are 90 and those for dimethyl ether almost 73 times higher than the current CO₂ allowance price. The CO₂-based synthesis of methanol and dimethyl ether thus does not represent an economically viable alternative to the geological storage of CO₂. In comparison to the average CO₂ avoidance costs of alternative reduction options, such as the development of renewable energies (0.032 €/kg_{CO2}) or the replacement of lignite by natural gas (0.05 €/kg_{CO2}), the production of methanol and dimethyl ether is not an economically viable alternative to reduce CO₂ emissions. In order to compare the CO₂-based processes with these reduction options, the costs of CO₂ separation in power plants must also be considered.

The high CO₂ avoidance costs in the CO₂-based synthesis of methanol and dimethyl ether are primarily due to the high costs of raw materials to supply hydrogen. The hydrogen must originate from electrolysis powered by renewable energy in order for the CO₂-based processes to achieve a net CO₂ reduction relative to the conventional process. For the calculation of the production costs in this work, wind turbines were assumed to power the electrolysis producing hydrogen, and a price of 5.22 €/kg_{H2} was taken, a value stipulated by the literature. In order for the CO₂-based synthesis of methanol and dimethyl ether to be utilized as a CO₂ reduction option without incurring CO₂ avoidance costs, the price of hydrogen must decrease to 1.22 €/kg_{H2} or 1.76 €/kg_{H2}, respectively. Therefore, in addition to higher CO₂ allowance prices, the price trend of hydrogen produced via electrolysis will determine the future economic implementation of the two CO₂-based processes.

For the future chemical utilization of carbon dioxide as a CO₂ reduction option, the fabrication of bulk chemicals was identified as the most suitable option due to the high production volumes involved. For effective and economic implementation, the reactions must be performed with highly reactive co-reagents produced as cost-effectively as possible with simultaneously low CO₂ emissions. Although the syntheses of fine chemicals will not contribute significantly to reducing CO₂ emissions, they do have great potential for economic implementation.

²¹ Kosten und potenziale der Vermeidung von Treibhausgasemissionen in Deutschland, T. Vahlenkamp, Editor 2007, McKinsey & Company.

4.3 Fuel cell / battery hybrid systems for auxiliary power units

As part of the doctoral thesis entitled “Computer-aided Design of Fuel Cell/Battery Hybrid Systems for Auxiliary Power Units”, a methodology was developed that permits the holistic development of a fuel cell system with diesel reforming, taking into consideration the requirements posed by mobile applications for on-board power supply systems. Balancing the properties of the existing system and these requirements resulted in the following three components: system start-up, system hybridization, and packaging of the fuel processing system. These three subject areas were considered and optimized in an interconnected fashion.

Based on the insights from literature research, a methodological approach was developed. Thermodynamic calculations were applied as a methodology to examine the concepts developed. In a second step, these were supported by dynamic system simulations. The simulations were applied to both the start-up process and the hybridization of the system²². The two models complement each other to form a model of the entire hybrid system. Within the scope of the packaging, additional fluid dynamic simulations were conducted. These were based upon work previously carried out at IEK-3. The models used were also expanded with respect to the dynamic simulation of the preheating processes and the simulation of one of the packages. The fluid dynamic simulations were parallelized in order to reduce the computation time. Experiments with the entire system and various individual components supported the simulation methodology. Using these experiments, the framework conditions were set for the simulations and the methodology was examined.

During the development of the start-up concept, both a thermal and an electric concept were developed. The thermal concept is based on an ignition burner and – in the first heat exchanger – transferring the released heat to air for preheating the fuel processing system, and – in the second heat exchanger – to the heat transfer liquid of the fuel cell. Simulations have shown that for an energy-efficient start-up process, the fuel processing system should not be started until the fuel cell has been preheated. Furthermore, an electric start-up concept was developed, in which air is first heated in order to preheat the system. For the start-up process, water must be vaporized within the reformer. For this purpose, an electric heater was integrated in the ATR 12 reformer, so that the reformer is capable of start-up at 20 % power. After reformer ignition, the heat released in the catalytic burner due to oxidation of the reformat is used to preheat the fuel cell. The simulated preheating time for this start-up process was 31 min, i.e. 13 min shorter than the thermal start-up process.

Furthermore, the start-up process was also modeled by means of two-dimensional fluid-dynamic simulations. For this purpose, various approaches to modeling the porous body were compared to experimental preheating curves. Using the single-zone model to simulate the preheating time led to a deviation of 97 s at 12000 NI/h air and 192 s at 6000 NI/h air until the monolith temperature of 120 °C was reached. In percentages, the deviations amounted to 47 % and 56 %. Using the two-zone model at the same simulation conditions led to a deviation of 3 s at 12000 NI/h air and 5 s at 6000 NI/h air. In percentages, the deviations amounted to as little as 1.5 % relative to the time determined experimentally. For the

²² Krupp, C., Computerunterstützte Auslegung eines Brennstoffzellen-Batterie-Hybridsystems für die Bordstromversorgung, Schriften des Forschungszentrums Jülich, Reihe Energie & Umwelt / Energy & Environment 309, iii, 207 (2016)

dynamic simulation of the entire system, a methodology was developed to couple the individual reactors in one 2D simulation. Using this methodology, the fluid-dynamic model was successfully expanded to include the system components. The model then allowed the influence factors on the preheating process to be investigated in detail. Preheating the system at higher power is advantageous since less heat is transferred to the insulation. In using the ATR 9.2 reformer, the catalytic burner is the limiting component in the preheating process. At 2 kW preheating power and an inlet temperature of 600 °C, the preheating process takes 28 min, and 24 min at 500 °C. The limiting component in the ATR 12 reformer is the monolith. In order to heat the monolith to 320 °C via steam pathway at an inlet temperature of 600 °C, a preheating time of 22 min was calculated, and at 500 °C a preheating time of 24 min. In these cases, the power was a constant 2 kW. Various influencing parameters were investigated in the packaging variant with the ATR 12 reformer. By means of an additional 0.5 kW heating power, the catalytic burner preheating time can be accelerated so that the catalytic burner is no longer the last component to reach the dew point. Heating with steam at a power of 2 kW from this point onwards leads to a delay in preheating. The time necessary for preheating can be slightly accelerated by increasing the power, but this is disadvantageous in terms of energy. The most advantageous start-up process is simultaneously preheating the reformer with a power of 1 kW using air added via the air and steam pathway. In addition, air was supplied to the catalytic burner at a power of 0.5 kW. This procedure meant that in 2D simulations the start-up process for fuel processing in the base case was reduced from 22 min to 9.5 min.

For hybridization, passive and active concepts were investigated. When interconnected as a passive hybrid, the fuel cell voltage was set to the open cell voltage of the battery at the desired power. This concept led to a very minor adaptation of the fuel cell power to between 1667 W and 1968 W in operation. This change can be attributed to the change in battery voltage when the state of charge changes. Due to the minor change of the fuel cell power in this concept, the battery design must be larger, with a minimum of 15 parallel cells. A concept in which the fuel cell completely covers the power requirements up to a certain limit is precluded due to the high dynamic load on the fuel cell. For the active hybrid, various operating strategies were investigated. Operation of the fuel cell at constant power led to the best system efficiency of 29.3 %, but with 15 parallel cells also to the largest battery. Dynamic operation of the fuel processing system means that the battery size can be reduced by up to 87 %. The smallest battery with only 2 parallel cells can be used for very low power requirements in case of dynamic fuel processing in combination with a decrease in fuel utilization. The efficiency in this case decreases to 26.1 %. Furthermore, the influence of the start-up process on hybridization was investigated. Taking into consideration the start-up process leads to a larger battery. The system efficiency thus decreases to 25.3 %. It was revealed that the system should be started, if possible, before power is required and that, if possible, preheating should be effected by means of waste heat from the truck engine. With this quicker start-up process, the efficiency rises to up to 26.2 %. Using waste heat for preheating the fuel cell increases the efficiency to 28.1 %.

Within the scope of the packaging, a simulation methodology was developed in order to model the entire fuel processing package. In order to create the computational mesh, various methods were examined and compared with respect to their suitability for the simulation. For the ATR 9.2 reformer, two hybrid computational meshes were applied: one with exclusively conformal interface interconnection, and one with mostly conformal interface interconnection

but occasional non-conformal interface interconnection. By using the non-conformal interface interconnection, the size of the mesh can be chosen individually for each side of the interface. Conformal interfaces were created at the interfaces for the adjoining surfaces. By duplicating the geometry, these interfaces could be interlinked independently of each other. Subsequently, these surfaces were manually interlinked with the resolver. Using non-conformal interlinkage led to fewer cells and less computation time thanks to the independent choice of mesh sizes. By varying mesh sizes, the number of cells in the ATR 9.2 reformer was reduced from 34.5 million to 6.4 million and 2.9 million, depending on size. The computation time was reduced by 86 % and 92 %, respectively. The results of the simulation were very similar, irrespective of the interlinkage method used. By developing this new interlinkage method, the academic method was translated into a method applicable for optimization. Using the con-conformal interlinkage method, the ATR 9.2 reformer was subsequently simulated together with WGS 4.



Fig. 71: Structure of package 5 with a power class of 10 kW_{el}

Package 5 was designed based on the simulation results of the thermal start-up process. This process is shown in Fig. 71. In this concept, the start burner is flanged directly onto the heat exchanger in order to reduce pressure losses. The start burner heat exchanger is situated immediately adjacent to the reformer in order to minimize the length of the piping between them. The reformat flows from the ATR to the WGS reactor situated next to it and then through the microstructure heat exchanger tested previously. The reformat then reaches the fuel cell and any reformat not converted (residual anode gas) is fully oxidized in the catalytic burner. The reaction heat is used to produce the steam needed for the reformer. As soon as the steam is provided by the catalytic burner, the start burner can be switched off.

The ATR 12 with integrated electric heating wire needed for electric start-up was investigated experimentally. When the reformer is heated at 40 % of the nominal power of the integrated heating wire, the reformer was heated to the temperatures necessary for ignition within 25 min. Furthermore, thanks to these experiments, the concept of internal water evaporation during the start-up process was successfully validated. When water is injected into the reformer, the temperature in the steam pipe decreases only very slightly. Both the thermal mass of the reformer and the heat transfer of the gases released have a positive influence on

the injected water. This concept means that an external vaporizer is no longer necessary during start-up since use is made of the area available in the heat exchanger for evaporating the water. This in turn has a positive impact on the volume and weight of the package. The low thermal mass of the heating wire is also very advantageous for a fast start-up of the system. The ATR 12 reformer can thus be preheated and ignited without any additional external heating. Furthermore, the integrated structure of the reactors was demonstrated using the example of the WGS 6 reactor.

The ATR 12, WGS 6, and CAB 5 reactors are used for the package based on electric start-up. The two-zone model for porous bodies validated as part of the start-up strategy development was used for the transient preheating simulation of package 6. In order to create the computational mesh, the methodology of non-conformal interlinkage was used, with the interlinkage parameters of the mesh study. The preheating process of the package was investigated using the developed three-dimensional model. The system is preheated by three separate pathways simultaneously, whereby the dew point of the reformer monolith is exceeded after 10 min. Once the reformer monolith is preheated, the HTS and catalytic burner monoliths follow suit. The last dew point to be exceeded is that of the LTS monolith, which takes 19 min. These times reflect the results from the 2D simulation. By taking into consideration the in- and outlets, however, the preheating process is considerably delayed. In the 3D simulation, the dew point is only exceeded in all components after 19 min, in contrast to the 9.5 min simulated in the 2D simulation. Due to the required monolith temperature of 320 °C, the reformer is only ready for ignition after 30 min. The large deviation from the 9 min simulated in the 2D simulation can be attributed to the considerable simplification of the connecting pipes.

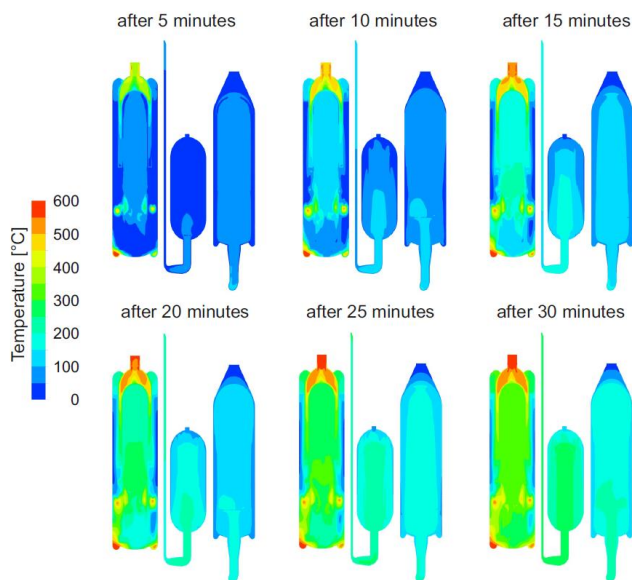


Fig. 72: Temperature profile during the preheating process in the components of package 6

The temperature profiles during the preheating process of the system are shown in Fig. 72. Preheated air is added via the air and steam pathway of the reformer and via the feed line to the catalytic burner. The components downstream from the reformer profit from the heat transferred to the released air by the integrated heat exchanger. Due to this heat transfer, the air is considerably cooler when it reaches the mixing chamber. The air fed in via the air pathway reaches the mixing chamber at a temperature of 300 °C after only 5 min. The fact that the air flows through the thin holes in the sheets and mixes with the cold air means that the air from the air stream cools down considerably, however, so that it takes 15 min before 300 °C is reached in the mixing chamber. Since the catalytic burner only needs to reach a temperature of 120 °C, the power for the added air is selected as 0.5 kW.

By taking into consideration the start-up process, which results from the calculation of the 3D package, the efficiency of the hybrid system decreases to 24.8 % in the case of a preheated fuel cell. This clearly shows that the number and length of connecting pipes, which were disregarded in the 2D simulation, must be reduced considerably.

The methodology developed offers a basis for the development of a compact cylindrical package. Furthermore, a methodology for the dimensioning and evaluation of hybrid systems was developed. Integrating the start-up process in package development, on the one hand, and hybridization, on the other hand, permitted a holistic view of the following components: packaging, start-up process, and hybridization. The overall methodology was applied to the optimization of the current fuel cell system. The overall methodology permits existing as well as new systems to be (further) developed and optimized, thus enabling a multitude of requirements of a mobile system to be met. In summary, the overarching objective of developing a holistic methodology for optimizing the system was accomplished. The methodology was applied to the further development of the existing fuel cell system with diesel reforming.

4.4 Electrodes with reduced Ir content for PEM electrolysis

Current challenges in the field of PEM electrolysis can be grouped under three main aims: i) reduced stack costs, ii) improved stack performance and iii) increased long-term stability under relevant operating conditions. All stack components can be optimized in this respect, including the membrane electrode assembly (MEA), current collectors and bipolar plates.

The noble-metal catalysts are part of the MEA and thus also a component with a considerable influence on stack costs. For a system with a capacity of 40.8 kW, for example, the membrane electrode assembly accounts for around 13 % of the total installation costs²³. This proportion will continue to increase as the size of systems increases into the megawatt range. A reduced use of noble metal catalysts therefore has a positive effect on the investment costs for PEM electrolyzers. However, it is not just the costs of noble metals that must be taken into consideration but also their availability. Iridium is used as a standard catalyst for producing oxygen on the anode. The anode is loaded with 2–6 mgcm² iridium, which is three times as high as the platinum loading of the cathode (0.5–2.0 mg cm²).²⁴ At the same time, the amount of iridium mined per annum (6 tonnes) is around 30 times less than that of platinum (approx. 183 tonnes per annum). To install the electrolysis capacity required in Germany, namely 28 GW according to an energy scenario developed by IEK-3²⁵, a total of 39 tonnes of iridium would be required for the iridium loadings currently used²⁶. This in turn would require about seven times the annual amount currently mined. It can be assumed that such a demand for iridium will lead to price shifts and material shortages. Reducing the amount of iridium needed would therefore have a positive impact on the application of PEM electrolysis for the Energiewende in two respects: on the one hand, the costs per installed capacity would be reduced, and on the other hand, dependence on limited resources would be diminished, which in turn would make it easier to plan the implementation of this technology. However, a precondition for this is that the reduced amount of iridium affects neither the performance nor the long-term stability of the systems.

As part of a doctoral thesis on the long-term stability of polymer electrolyte membrane water electrolysis under reduced iridium loading, two approaches for reducing iridium loading were investigated. In this section, the second approach has been applied, namely a reduced loading of the anode with benchmark catalyst²⁷. In this section, the cells with reduced loading of the anode are presented in terms of their cell performance and then their long-term stability.

²³ Ayers, K. E., Anderson, E. B., Capuano, C., Carter, B., Dalton, L., Hanlon, G., Manco, J. u. Niedzwiecki, M.: 218th ECS Meeting. ECS Transactions. ECS 2010, 3–15

²⁴ Carmo, M., Fritz, D. L., Mergel, J. u. Stolten, D.: A comprehensive review on PEM water electrolysis. *International Journal of Hydrogen Energy* 38 (2013) 12, 4901–4934.

²⁵ Stolten, D., Emonts, B., Grube, T., Weber, M.: Hydrogen as an Enabler for Renewable Energies, in: *Transition to renewable energy systems*, eds. Stolten, D., Scherer, V., Wiley-VCH, Weinheim, Germany (2013), 195-216

²⁶ Carmo, M.: PEM Water Electrolysis - New Approaches Towards Catalyst Separation, Recovery, and Recycling. submitted

²⁷ Rakousky, C., „Langzeitstabile Elektroden mit reduziertem Iridiumgehalt für die PEM-Elektrolyse“, *Schriften des Forschungszentrums Jülich, Reihe Energie & Umwelt / Energy & Environment* 322, ISBN 978-3-95806-147-7 (2016)

4.4.1 Zelleistungen unter reduzierter Anodenbeladung

Loading began with the standard loading of $2.25 \text{ mg cm}^2 \text{ IrO}_2$ (AAe) and was reduced to 0.6 and $0.3 \text{ mg cm}^2 \text{ IrO}_2$ (AAe). The polarization curves of the three loadings are shown in Fig. 73.

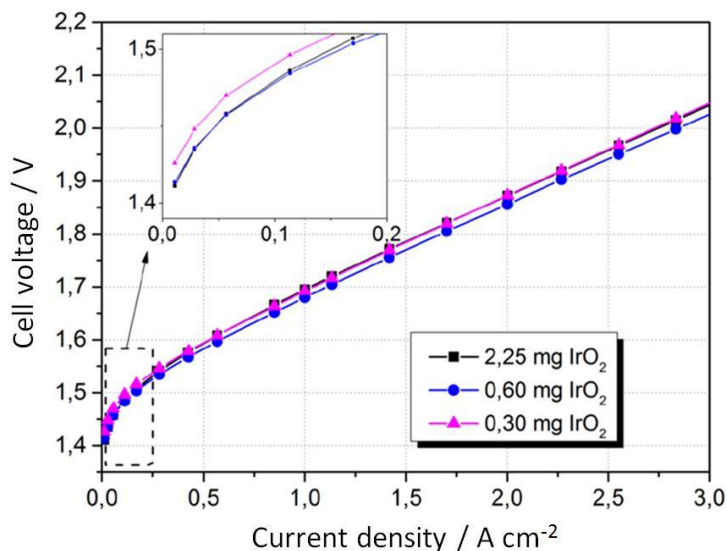


Fig. 73: Polarization curves of cells with anode loadings of 2.25 – 0.6 – 0.3 $\text{mg cm}^2 \text{ IrO}_2$ (AAe)

A comparison of the polarization curves of the three different loadings in Fig. 73 shows that all three loadings have a comparable polarization curve after a run-in time of 74 h. At 2 A cm^2 , the CCMs with anode loadings of 2.25 mg cm^2 and 0.3 mg cm^2 both had a voltage of 1.872 V and the CCM with an anode loading of 0.6 mg cm^2 had a cell voltage of 1.856 V . The lowest current density $U_{j_{0.01}}$ increases with decreasing loading by a total of 13 mV to 1.426 V . The polarization curves show that it is possible to reduce the loading of the anode by 87% to 0.3 mg cm^2 without impacting on cell performance. This in turn reduces the amount of iridium required for the installation of 28 GW of PEM electrolysis capacity from 39 tonnes to 4.6 tonnes . This corresponds to only slightly more than twice the annual amount currently mined. For the same performance, the amount of iridium saved is therefore almost twice the amount saved when the new catalyst is used. This was tested with an iridium loading of 0.62 mg cm^2 ; however, from 0.67 A cm^2 , it exhibited much higher cell voltages. The literature also indicated that the iridium loading of the anode only has a small impact on the polarization curve of the CCMs²⁸.

²⁸ Hui Xu: High-Performance, Long-Lifetime Catalysts for Proton Exchange Membrane Electrolysis, Annual Merit Review Proceedings, Newton, MA (2014)

4.4.2 Long-term stability under reduced loading of the anode

The cell voltage curve for anode loading of 0.3 mg cm^{-2} is shown in Fig. 74 and is also divided into two areas (0) and (I). In area (I), the cell voltage increases at a rate of $39 \text{ } \mu\text{V h}$. The anode potential increases in the same time frame at a rate of $40 \text{ } \mu\text{V h}$ and the cathode potential rises by $1 \text{ } \mu\text{Vh}$. The increase in cell voltage in this area can therefore be fully attributed to the anode. Cell voltage U_{j2} shown in the polarization curve increases in area (I) by 34 mV . This value agrees with the cell voltage increase of 36 mV in long-term testing. However, U_{j2} is lower by an average of 15 mV than the cell voltage in the long-term test.

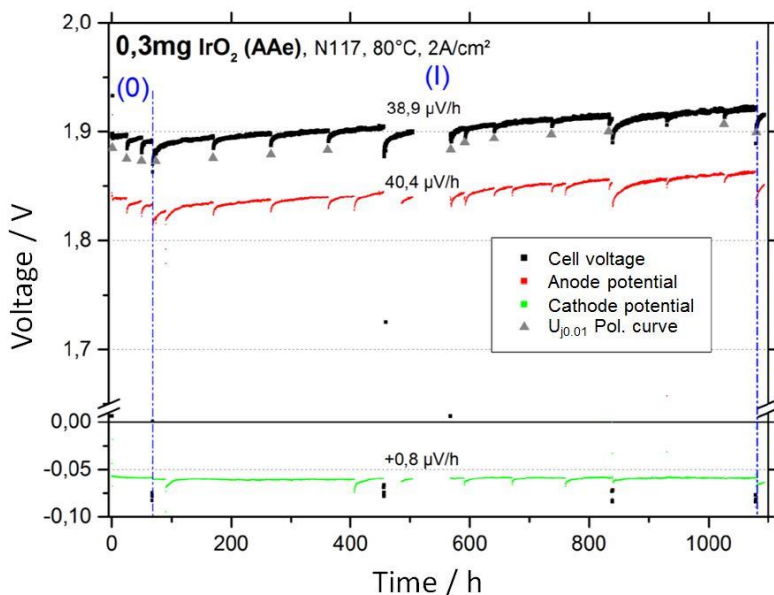


Fig. 74: Reduced anode loading with $0.3 \text{ mg cm}^{-2} \text{ IrO}_2 \text{ (AAe)}$. Cell voltage and single potentials over time

Reducing the loading of the anode from 2.25 to 0.3 mg cm^{-2} has no influence on the cell voltage of 1.872 V at 2 A cm^{-2} . This corresponds to an iridium reduction of 87% . CCMs with reduced anode loading, however, exhibit higher degradation rates. Whereas during standard loading, operation led to degradation rates of 0 to $6 \text{ } \mu\text{Vh}$, degradation increased at 0.6 mg cm^{-2} to $14 \text{ } \mu\text{Vh}$ and at 0.3 mg cm^{-2} to $39 \text{ } \mu\text{Vh}$. The main reason for degradation here is the decreasing exchange current density. This has cathodic and anodic parts. The cathodic part is due to a reduced platinum surface, which decreases by 13% to 22% . Changes in the ohmic resistance play a minor role in the degradation of these cells.

4.5 Solid oxide fuel cell system with integrated shielding-gas production

Among the challenges that SOFC systems present is the relatively high operating temperature of more than 600 °C. In particular, the high temperatures in combination with the use of nickel as a fuel catalyst within the fuel cell and the pre-reformer pose extreme challenges to the operator during preheating, cooling, and in emergency situations (e.g. disruptions in the grid connection or the system). In contrast to system operation, there is no reducing fuel gas atmosphere in these cases. There is therefore the risk of an oxidizing atmosphere on the fuel side of the system, e.g. through uptake of atmospheric oxygen. In this case, the nickel catalyst reacts with oxygen to form nickel oxide at temperatures above 300 °C.

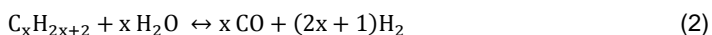


This reoxidation reduces the activity of the nickel catalyst. Furthermore, the oxygen uptake increases the volume of the nickel structure, leading to mechanical stresses which can cause cracks in the electrolyte and, in the worst case, result in failures in the fuel-cell system. The three operating conditions described above thus require the use of a shielding gas, which usually consists of roughly 96 vol% of an inert gas (e.g. argon or nitrogen) and 4 vol% hydrogen. In all three scenarios, the shielding gas flows through the fuel side of the system, preventing the formation of an oxygen-rich atmosphere.

Since there is usually no shielding-gas infrastructure, the inert gas must be supplied from pressure gas cylinders. The required amount of shielding gas and thus the required storage volumes are significant. Typical heating rates of SOFC systems are in the range of 0.5–10 K/min. Assuming a shielding-gas stream of 1 NI/min for each cell, a 5 kW system with 36 cells would require 2,430–48,600 NI inert gas for the preheating process alone. Due to the high thermal mass of an SOFC system, the cooling-down period can be longer than the preheating time, considerably increasing the amount of inert gas required. In addition to the large storage space, the empty gas cylinders must be replaced or refilled before the next preheating or cooling-down process can be initiated. The demanding logistic requirements and the cost-intensive production of the inert gas represent another challenge.

A solution was therefore developed and realized, in which the shielding gas is generated within the system. This shielding-gas generator permits on-demand production of a reducing atmosphere using the existing infrastructure (i.e. water, natural gas, and electricity). The shielding gas is produced as needed directly in the system, with the advantage of making storage unnecessary, thus reducing the total system size. In addition, empty gas cylinders no longer need to be replaced, reducing the logistic effort and the operating costs of the system.

The shielding-gas generator consists of an evaporator and a steam reformer (Fig. 75). It comprises an electrical heater, natural-gas and water connections, and a gas outlet. In order to operate the shielding-gas generator, the evaporator has to be preheated to at least 100 °C and the reformer to a minimum of 400 °C. This is effected by two electrical heating elements located inside the evaporator and the reformer. As soon as the target temperatures have been reached, water is pumped into the evaporator, where it is evaporated; it then flows towards the reformer inlet. Simultaneously, natural gas is added to the steam flow. A fuel–steam mixture is then chemically converted in the reformer via endothermic steam reforming (Eq. 2):



and the competing water-gas shift reaction (Eq. 3):



The resulting gas mixture at the shielding-gas generator outlet, consisting of methane, steam, carbon dioxide, carbon monoxide, and hydrogen, forms the synthetic inert gas. The greater the amount of hydrogen and carbon monoxide, the better is the reducing effect of the gas stream and thus the reoxidation protection of the nickel in the system. High reformer temperatures (above 400 °C) and high steam concentrations shift the chemical balance of the steam reforming reaction (Eq. 2) towards the product side, increasing the hydrogen production and thus the protection against reoxidation.

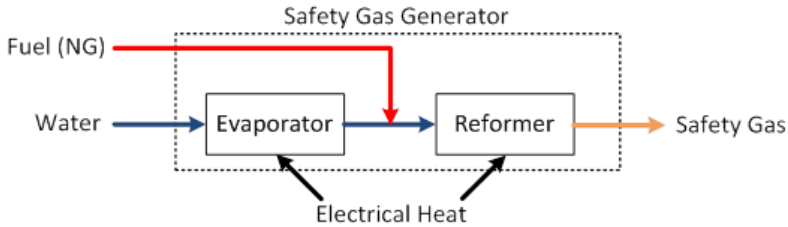


Fig. 75: Simplified schematic of the newly developed shielding-gas generator

In general, an SOFC system comprises a stack, an off-gas burner, a pre-reformer, an air preheater, and an evaporator. Natural gas (NG) would be the usual choice for a fuel since it is widely available. The higher hydrocarbons in the fuel present a challenge since they decompose at temperatures above 150 °C and facilitate the formation of carbon in the system. This clogs the gas pipes, increases pressure losses, and can lead to leaks. The stream of natural gas is therefore mixed with steam at the pre-reformer inlet (position 3 in Fig. 76). This steam inhibits the formation of carbon when the mixing ratio S/C is above 1.6:

$$\frac{S}{C} = \frac{\dot{n}_{\text{H}_2\text{O}}}{\dot{n}_{\text{NG}}} \quad (4)$$

S/C is the ratio of steam to carbon, where \dot{n} describes the molar flow of each component.

The hydrogen-rich fuel-gas mixture flows back into the stack at position 4 in Fig. 76. The stack converts hydrogen and carbon monoxide into steam and carbon dioxide and generates electrical energy in the process. Since the stack only utilizes up to 85 % of the fuel, the remaining fuel is then burned in the off-gas burner (position 5 in Fig. 76). The generated heat (position 6 in Fig. 76) can then be used to heat the air stream in the air preheater in order to support the evaporation process and the endothermic steam reforming reaction in the pre-reformer.

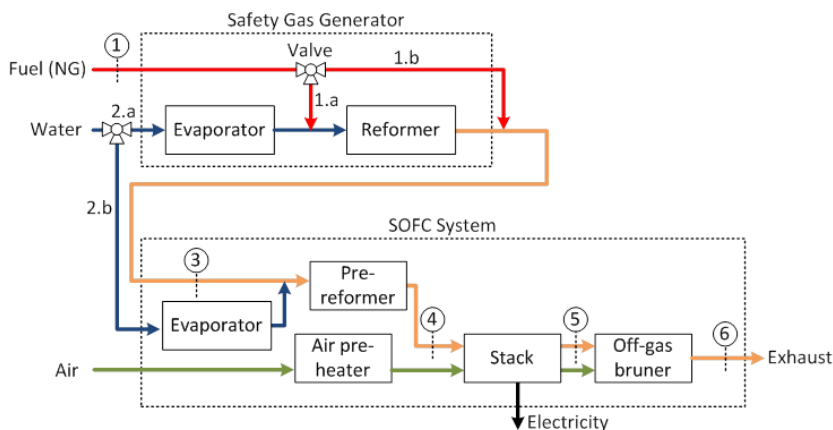


Fig. 76: Schematic of an SOFC system in combination with a shielding-gas generator

In order to connect a typical SOFC system to the shielding-gas generator, an additional feed-in must be installed between the fuel inlet and shielding-gas generator. The preheating strategy begins with the heating of the SOFC system by heating the pre-reformer and the stack to 300 °C. This can be effected either via an ignition burner or via electrical heating elements. During this preheating sequence, the fuel side of the SOFC system is not perfused. Simultaneously, the shielding-gas generator is also preheated (the evaporator section to more than 100 °C and the reformer section of the shielding-gas generator to above 400 °C). Shielding gas must under no circumstances be produced before stack and pre-reformer have reached a temperature of at least 180 °C. Below this temperature, feeding the shielding gas in would induce a reaction between the nickel catalyst and carbon monoxide, forming nickel tetracarbonyl:



At temperatures above 180 °C, the chemical equilibrium of this reaction (Eq. 5) tips towards the educt side, inhibiting the formation of nickel tetracarbonyl. In order to save natural gas and thus costs, shielding gas production is only started once the stack has reached a temperature of above 300 °C since the reoxidation potential of nickel inside the stack and the pre-reformer is not reached below temperatures of above 300 °C. Just before shielding-gas production begins, the fuel side of the SOFC system is flushed with steam from the shielding-gas generator and thus inertialized (position 2.a in Fig. 76). For the shielding-gas production process described in the following, natural gas is fed into the shielding-gas generator via connection 1.a and water via connection 2.a. The shielding gas produced then flows through the entire fuel side of the SOFC system. Subsequently, the SOFC system is brought to an operating temperature of 700 °C. As soon as the operating temperature is reached, the shielding-gas generator is switched off and the natural gas flows directly into the system via connection 1.b. At the same time, water is fed into the evaporator (position 2.b in Fig. 76) in order to inhibit the formation of carbon in the pre-reformer. Afterwards, electricity can start to be generated in the stack.

The functionality of the shielding-gas generator developed here was investigated by means of an experiment. For this purpose, a shielding-gas generator was manufactured for a 5 kW

system based on a stack with 36 cells. Its reformer component was designed for operation at a temperature range of 400–700 °C. The dimensions of the shielding-gas generator are 0.15 x 0.2 x 0.4 m.

The CAD geometry of the shielding-gas generator prototype is shown in Fig. 77. The evaporator is realized as a double-pipe heat exchanger. The interior pipe contains a heating cartridge with electrical power of 400 W. The exterior and interior pipes are separated by a gap of 1 mm through which the water flows and is evaporated by the heat input from the heating cartridge. The reformer consists of a catalyst bed manufactured by Johnson Matthey. The catalyst consists of elements from the platinum group deposited onto a metal-oxide substrate. Another heating cartridge with electrical power of 400 W is located in the reformer, where it provides energy to the endothermic steam reforming reaction.

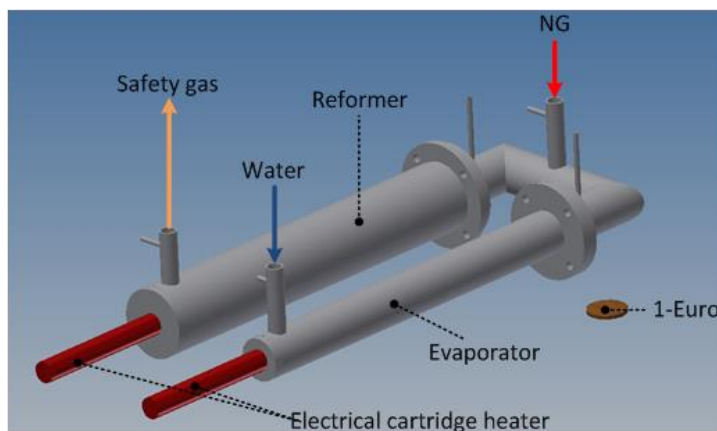


Fig. 77: CAD image of the shielding-gas generator prototype

Fig. 78 a shows as an example a cycle of the heating and cooling process of a 4-cell stack in combination with the shielding-gas generator. During the transition from phase 1 to 2, the cell voltage increases very rapidly due to the inflowing synthetic shielding gas. Additional heating of the stack further increases the stack voltage until it has reached the Nernst potential. At this point, Fig. 78 a shows fluctuating voltage. This is due to the fluctuating water evaporation process of the shielding-gas generator. Phase 3 is initiated by switching from shielding-gas to hydrogen supply. Within this phase, a characteristic curve was measured in order to characterize stack properties. Phase 4 comprises cooling the stack down to 300 °C using shielding gas. At the transition from phase 4 to 5, the shielding-gas supply is shut down, leading to a sudden drop in stack voltage.

Fig. 78 b shows the individual cell voltages and the stack temperature at a current density of 500 mA/cm² during each of the 11 cycles executed. Cycles 1–3 were conducted as reference cycles during which the conventional preheating process was used. This includes the supplying of conventional shielding gas (96 vol% argon and 4 vol% hydrogen) during the preheating process from room temperature to operating temperature and during the cooling phase. These three reference cycles show that a thermal cycle (preheating and cooling) does not negatively influence the cell voltages.

During cycles 4 and 5, the stack was heated to 300 °C without supplying any shielding gas. Above this temperature, the conventional shielding-gas supply was switched on, with the same process being applied during the cooling phase. These two cycles show that not supplying shielding gas before 300 °C is reached does not have a negative influence on cell performance and thus does not lead to any nickel reoxidation. The cell voltages were not impacted by this modification.

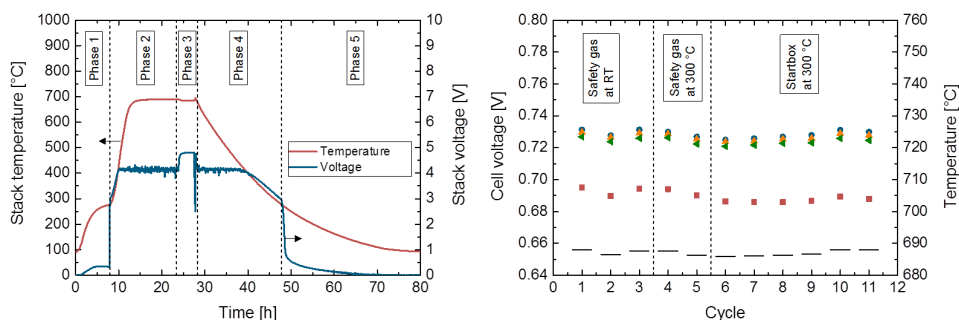


Fig. 78: Example of a test cycle: a) stack temperature and stack voltage as a function of the testing time (left); b) cell voltages and stack temperature at 500 mA/cm² and 4.5 NI/min hydrogen as a function of the cycles (right)

During cycles 6–11, the shielding-gas generator was used for the heating and cooling phases. As Fig. 78 b shows, the cell voltages did not deteriorate during these six cycles, demonstrating that the shielding-gas generator developed here can replace conventional shielding-gas supply techniques.

4.6 PRECORS: Spin-off for corrosion-resistant coating technologies

The core product of the spin-off project PRECORS is a carbon-based material consisting of a layered structure with functional groups. The layers are stacked on top of each other, forming a compact and robust laminated structure. The use of this material focuses primarily on applications in fuel cells. The carbon layers produced are highly electrically conductive and chemically stable to withstand aggressive media. These properties are exploited as corrosion protection in the application: the metallic components are coated in order to protect them from corrosion damage and simultaneously to preserve electrical conductivity. Metallic materials in contact with corrosive environments such as acidic or saline solutions are taken into consideration for this application.

This novel coating system was developed as part of Vitali Weißbecker's doctorate at the Institute of Energy and Climate Research (IEK-3), in Prof. Lehnert's group, with the aim of protecting metallic bipolar plates in polymer electrolyte fuel cells from degradation effects and simultaneously increase their durability and power density. The PRECORS start-up was founded in March 2017 in order to further develop and commercialize the technology. The spin-out was initially supported financially by Jülich's External Funding and Technology Transfer (TT funding for Vitali Weißbecker for 6 months in 2015 and for two scientific employees for 6 months each in 2016/17) and subsequently by funding attracted from the BMWi programme EXIST (€ 1.2 million). In addition, the science-based PRECORS spin-off has been honoured by various external experts as well as with the 2016 f-cell award and achieving first place in the 2015 AC² business plan competition.

Bipolar plates, an example of which is shown in Fig. 79, are an important component of the repeating units of a fuel cell stack. Their main functions comprise establishing electrical contacting with neighboring cells, ensuring uniform transport and distribution of the gases, and removing the water produced.

Compared to graphite-based composite materials²⁹, which are currently used as bipolar plates, metallic bipolar plates have the following advantages:

- Improved performance through higher electrical and thermal conductivity
- Vibration stability thanks to high flexibility
- Increased durability since no electrolyte losses occur through uptake into the material microstructure
- Cost-effective series production through stamping or hydroforming³⁰
- Reduced weight and volume thanks to thinner bipolar plates

²⁹ State of the art: graphite microstructure with added polymers for increased mechanical stabilization

³⁰ Hydroforming: shaping metallic materials using water pressure

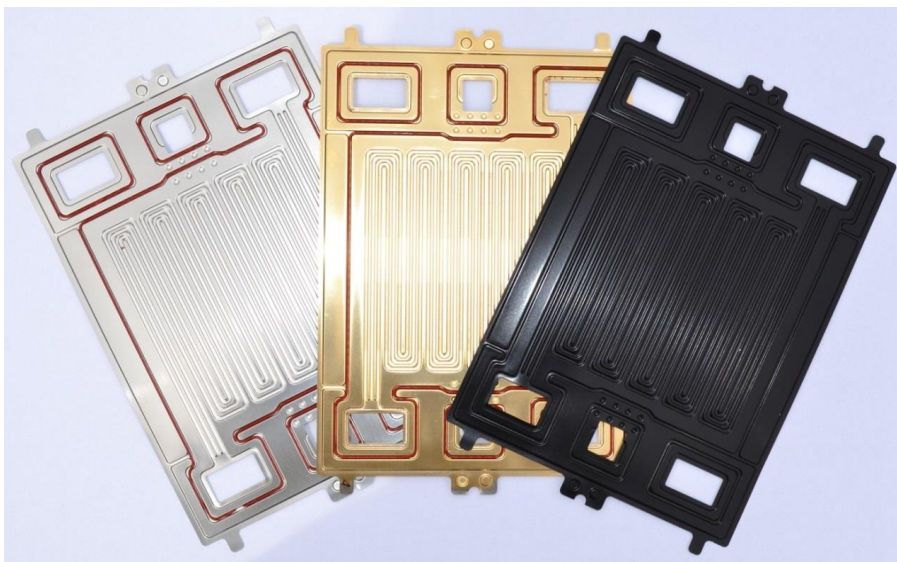


Fig. 79: Coated metallic bipolar plates (base material 1.4301) with various layer thicknesses; uncoated plates produced as part of the MIFULAS project

Table 7 compares a typical chromium–nickel stainless steel (base material 1.4301) with a graphite-composite material as an example. In spite of low material densities, graphite-based bipolar plates have a component thickness of 1.5–3 mm, depending on the manufacturer and the manufacturing process³¹, due to production techniques. Metallic bipolar plates, in contrast, can be cost-efficiently manufactured as thin foils 0.1 mm thick. Ultimately, this aspect has the advantageous effect of reducing the weight by 70 %³².

Material	Density [g/cm ³]	Plate thickness [mm]	Specific plate weight [g/cm ²]	Power weight at 0,5 W/cm ² [kg/kW]
Graphite composite	~1,9	1,5	0,29	1,14
Stainless steel 1.4301	7,9	0,1	0,08	0,32

Table 7: A comparison of the material required for bipolar plates per kW electrical power reveals a considerable weight reduction when using metallic materials in contrast to graphite-based materials

³¹ Injection molding and milling techniques

³² The calculation is guided by the minimum material thickness of 1.5 mm of graphite-composite materials and an average cell power of 0.5 W/cm²

Such improvements to the fuel cell stack make fuel cell technology more attractive for the market, particularly for automotive applications, where weight and volume are decisive factors. In order to use metallic bipolar plates, however, a cost-efficient coating technique suitable for series production is required in addition to long-term stability. The coating developed here, which is deposited via a spraying technique, fulfills all requirements in comparison with vapor deposition processes in the literature; these exhibit considerably higher costs and poor scalability.

The reduced weight and volume of metallic bipolar plates lead to a considerably higher specific power (gravimetric and volumetric). Furthermore, the production costs (hydroforming, stamping) of metallic bipolar plates are lower than those of graphitic bipolar plates, which are produced via the capital-intensive injection molding or hot-press processes.

The coating technologies for metallic bipolar plates currently competing involve physical vapor deposition (PVD) at high temperatures above 300 °C in an ultrahigh vacuum. These coatings are thin layers based on gold, doped diamond, or chromium or titanium nitrides. Coating technologies based on vapor deposition incur high investment and material costs. Since they cannot be integrated into any existing production line and due to the processing times, the scalability of the technology is limited.

The coating technique developed by PRECORS is a high-quality, scalable, and economically viable replacement technology for the coating of metallic bipolar plates. The coated metallic bipolar plates thus achieve optimal electrical conductivity as well as low contact resistance. The power level is comparable to that of metallic bipolar plates gold-coated via PVD methods, which provide the highest electrical conductivity at present. Long-term tests (currently > 4000 operating hours) have revealed high corrosion resistance and thus high long-term stability, see Fig. 80 below. The comparison of typical current–voltage characteristic curves shows that they have a low aging rate of < 5 $\mu\text{V/h}$ (attributed, for example, to the membrane electrode assembly) as well as operating behavior similar to that of bipolar plates coated via PVD. Uncoated bipolar plates, in contrast, display a significant decrease in cell performance. Compared with other coatings, the PRECORS coating displays hydrophilic wetting behavior, permitting improved water removal from the fuel cell. This also has a positive effect on cell performance.

In addition to the gain in quality described, the coating technology offers an enormous potential for cost savings resulting from the use of cheap and environmentally friendly production materials as well as low investment costs. Costs can thus be reduced by approximately 50 % compared to PVD-coated bipolar plates.

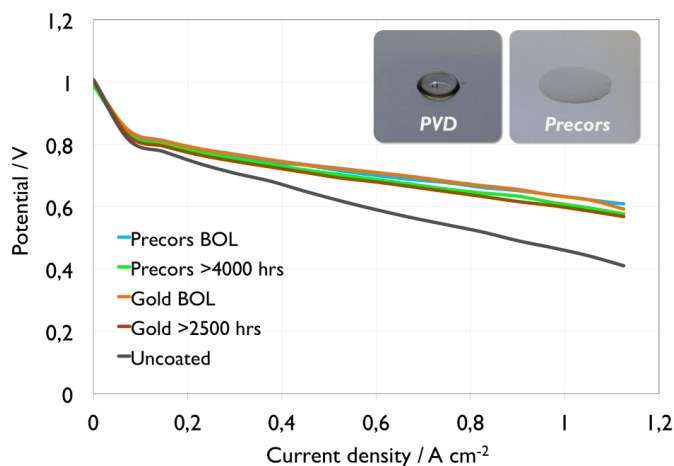


Fig. 80: Characteristic current–voltage curves of fuel cells with PRECORS bipolar plates and gold-plated bipolar plates (state of the art) at the beginning of their life cycle (BOL) and after more than 4000 hours and 2500 hours exhibiting comparably low cell aging ($< 5 \mu\text{V/h}$); in contrast, uncoated bipolar plates have much lower characteristic curves

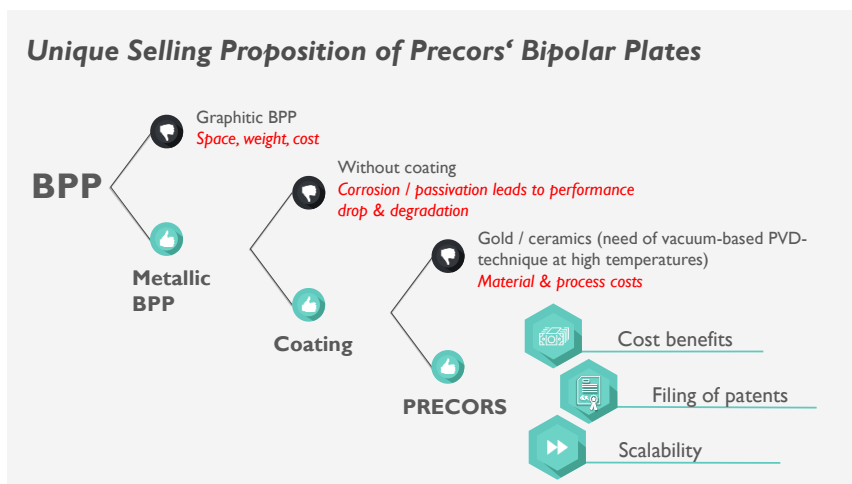


Fig. 81: Comparison of graphitic and metallic bipolar plate designs and advantages of the carbon-based coating technology developed at IEK-3 compared to the current state of the art

The coating concept suitable for series production comprises a scalable spraying process. In contrast to the currently available coating technologies based on a PVD coating concept, the technology developed by the project team can be integrated into existing production lines of bipolar plates. Fig. 81 summarizes the advantages potential clients would have and the unique selling point of the spin-off project.

The spin-off team has developed and expanded a sector-specific network comprising primarily contacts with experts, industry insiders, and industrial and cooperation partners. In internal tests and field trials, the coating technology was successfully tested and validated by car, fuel cell, and bipolar plate manufacturers. The further development of the network through regular visits to trade fairs and the targeted contacting of further potential clients is an important part of current activities within the scope of the EXIST research transfer. The team also arranges regular coaching courses with a business angel, who offers his expertise and extensive automotive knowledge, representing important support for various issues and feedback rounds. In addition, there is close contact with technology support centers (Jülich's Technology Transfer, AGIT, RWTH Aachen University) and other start-ups.





5

Outlook

Outlook for New R&D Projects

- Solid oxide cells for reversible plant operation
- The multiscale modeling of fuel cells
- Photolysis – photoelectric hydrogen production
- Supply systems for alternative fuels
- New topics in energy systems analysis and integration

5.1 Solid oxide cells for reversible plant operation

A new way of temporally uncoupling the processes of electricity generation and consumption is a reversible solid-oxide cell (rSOC) unit. It utilizes surplus electricity from renewable energy sources in order to conduct electrolysis. The resulting product gas is temporarily stored and – using solid-oxide fuel cells – converted back into electrical energy as soon as additional electricity is needed. Solid-oxide cells exhibit low activation overpotentials, thus permitting high efficiencies during electricity generation and gas production. Jülich's rSOC unit is operated at atmospheric pressure and utilizes gaseous hydrogen, steam, and air. The general setup of an rSOC unit is shown in Fig. 82.

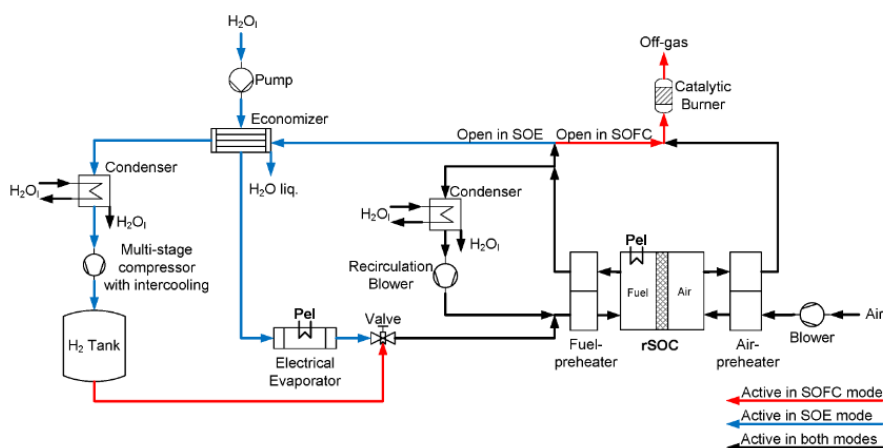


Fig. 82: rSOC unit concept: the electrolysis process (SOE operation) is represented by a dashed blue line and the reverse (SOFC operation) mode by a solid red line; the air side is represented by a solid blue line for both modes of operation

During electrolysis (SOE operation), the electrical evaporator produces the steam in the media-supply region. A fact to be taken into account is that oxidizing conditions (e.g. pure steam) degrade the nickel electrode at the fuel-inlet side. For this reason, the steam produced is either mixed with 10 vol% hydrogen from the H₂ tank before it is fed into the stack, or the hydrogen is added to the steam via the off-gas recirculation system. The hydrogen released from the stack is separated from the unconverted steam via a liquid–gas phase separation process in a condenser. The subsequent multistage compression with intercooling compresses the hydrogen to storage pressure. In order to discharge the oxygen produced from the unit, a minimum air stream is transported on the air side.

In fuel-cell operation (SOFC) mode, the hydrogen stored in the tank is fed into the stack. The off-gas contains unconverted hydrogen, which is oxidized in the catalytic burner for safety reasons. In order to regulate the stack temperature, the air side must be cooled via an increased air stream. Critical thermomechanical stresses inside the solid-oxide cell stack are prevented by preheating the gases fed into the stack. In order to keep the waste-heat losses to a minimum and to realize a compact structure, the high-temperature components (stack, heating plates, and air and fuel preheater) are designed in an integrated modular manner. The gas outlet temperatures from the integrated module are below 300 °C.

In order to also keep thermomechanical stresses to a minimum during switching processes, the average stack temperature is kept constant in both modes of operation. During electrolysis operation, the stack is operated below the thermoneutral voltage, with the stack being maintained at the specified temperature by the heating plates. In fuel-cell mode, the temperature is adjusted by controlling the amount of air.

The design data of the rSOC unit are listed in Table 8. The rSOC unit has a power output of 5 kW at the design point of the fuel-cell mode of operation. In the electrolysis mode of operation, the unit produces approximately 3.3 Nm³/h hydrogen.

	SOE	SOFC	Einheit
T_{stack}	750	750	°C
P_{stack}	1	1	bar
j_{max}	0,6	0,5	A/cm ²
H_{2min}	10	-	vol. %
P_{tank}	100	-	bar
H_{air blower}	30	30	%
H_{recirculation blower}	20	20	%
H_{inverter}	94	94	%
Parastic consumption	50	50	W
T_{condenser recirculation}	75	35	°C
T_{from condenser}	40	40	°C

Table 8: Design data of the unit

In order to achieve high efficiency in fuel-cell operation, the hydrogen withdrawn from the tank must be optimally exploited. Fuel-side recirculation was therefore introduced, which feeds the gas released by the fuel electrode back to the inlet (Fig. 82). Since large proportions of steam decrease cell voltages in SOFC mode, the steam proportion in the recirculated gas stream is reduced in a condenser. The steam produced in the stack is separated to a large extent by cooling it down to 35 °C. This recirculation concept now permits the system fuel utilization to be increased almost as desired, at constant stack fuel utilization. In this way, an operating point can be achieved that permits high system fuel utilization levels of > 95 % in fuel-cell mode. During electrolysis operation, the recirculation system can provide the proportion of hydrogen necessary to protect the fuel electrode.

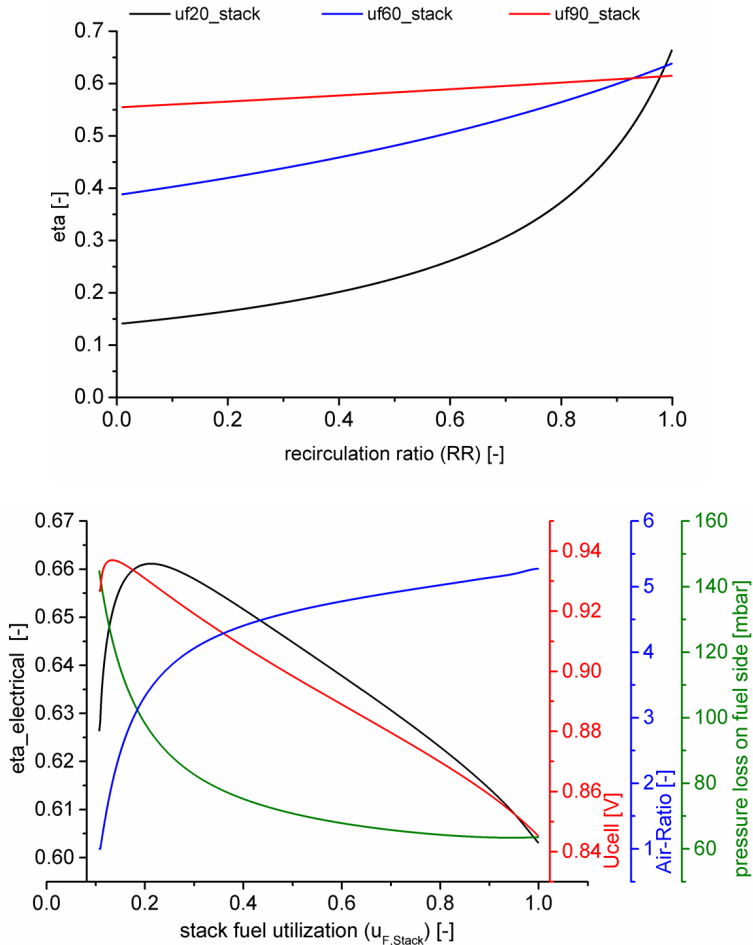


Fig. 83: rSOC unit concept: a) electrical unit efficiency as a function of the recirculation rate for various stack fuel utilization rates (top); b) electrical unit efficiency, pressure drop in the anode recirculation loop, cell voltage, and surplus air as a function of the stack fuel utilization rate at a recirculation rate of 99 % (bottom)

Fig. 83 a shows SOFC efficiencies for stack fuel utilization levels of between 20% and 90%. If the unconverted hydrogen is fed back via the recirculation system, the system fuel utilization rises with increasing recirculation rate and at constant stack fuel utilization. At recirculation rates of $> 90\%$, the characteristic curves intersect. Low stack fuel utilization levels generate a large proportion of hydrogen on the fuel side. In addition to the higher cell voltage, the increased amount of fuel acts as additional cooling. This can lower the amount of air needed to cool the stack during fuel-cell operation, reducing the air-side compressor power and improving the efficiency.

Fig. 83 b shows the results for a recirculation rate of 99 %, leading to system fuel utilization of almost 100 % at any stack fuel utilization. The maximum efficiency of approximately

66.2 % is achieved at a stack fuel utilization of roughly 20 %. Due to the large amount of recirculated hydrogen on the fuel side, the pressure drop increases with decreasing fuel utilization. The cell voltage also rises since the average proportion of hydrogen in the stack is increased. At stack utilization levels of < 20 %, the cell voltage decreases due to the sharply reduced amount of air in this section. The amount of air is reduced due to the cooling effect on the fuel side. If permanent and complete off-gas recirculation is the target of fuel-cell operation, the afterburner is superfluous.

In analogy to the hydrogen in fuel-cell mode, the steam in the stack cannot be utilized completely during electrolysis operation. The energy invested for the evaporation of the unconverted steam is released from the system in the form of waste heat at the condenser, which is located within the recirculation loop. There, the gas stream is cooled down to 75 °C in order to reduce the thermal demands imposed on the blower. The influence of recirculation with and without cooling to 75 °C was investigated in more detail. In both cases, hydrogen was recirculated in addition to the steam. The hydrogen cannot simply be separated as is the case in fuel-cell operation by means of condensation. The amount of recirculated hydrogen increases with a rising recirculation rate. At a steam utilization of 90 % in the stack, 10 vol% steam is present at the outlet, which could potentially be recirculated. At a steam utilization rate of 40 %, the proportion of steam at the outlet is 60 %, which could be recirculated. The recirculation makes the withdrawal of hydrogen from the pressure storage tank unnecessary, reducing the compressor power for tank storage. This leads to a slight initial rise in all efficiencies with increasing recirculation until the required 10 vol% H₂ can be provided. Based on these investigations, the unit thus achieved a maximum efficiency of 75 % at a steam utilization rate of 90 % in the stack and a recirculation rate of 11 %.

Using the following definitions of the efficiency in fuel-cell operation and electrolysis operation

$$\eta_{el,SOFC} = \frac{P_{AC,net}}{\dot{m}_{H_2} \cdot LHV} \quad \eta_{H_2,SOE} = \frac{\dot{m}_{H_2} \cdot LHV}{P_{AC,stack} + P_{AC,BoP}}$$

results in the following values:

	j [A/cm ²]	T [°C]	η _{LHV} [%]	η _{HHV} [%]
SOFC	0,5	750	66	55,8
SOEC	0,6	750	73,5	86,9

Relative to the heating value of the hydrogen consumed and produced and taking into consideration the compression to 70 bar of the hydrogen produced, the overall efficiency of the reversible system is thus

$$\eta_{tot} = \eta_{el,SOFC} \cdot \eta_{H_2} = 0,66 \cdot 0,735 = 0,485$$

this corresponds to 48,5%.

5.2 The multiscale modeling of fuel cells

Computational fluid dynamics in porous structures of fuel cells

In real technical systems, a very complex system is concealed behind the simple principle of fuel cells – a system that provides the basis for various research fields. Optimal management of media flows going in and coming out is fundamental for efficient functioning. In polymer electrolyte fuel cells (PEFCs), the gas diffusion layer (GDL) contributes decisively to the uniform distribution of the gases at the electrodes. In simulations, this layer is sometimes not resolved separately but included in the models as a parameter – which is often determined experimentally. The work done on simulating mass transport phenomena in the porous components of fuel cells picks up from this point and provides an understanding, obtained through fluid-dynamics methods, of the micrometer-sized structure of the gas diffusion layer and its operating principle in the fuel cell.

The flow simulation is based on the lattice Boltzmann algorithm. Since its code can be parallelized effectively, it permits flow simulations to be carried out for a macroscopically relevant area. The microscopic structure of the gas diffusion layer is resolved down to the fiber structure and taken into consideration for the analysis. The algorithm's optimal input parameters can be determined from experimental and analytical reference values for various geometries. This applies in particular to its use with regard to gas diffusion layers.

The underlying geometric structures come from two sources: At Helmholtz-Zentrum Berlin, the microstructure of GDLs was determined in the BESSY synchrotron and made available to IEK-3 for transport simulations. In addition, the Institute of Stochastics at Ulm University developed stochastic models of the microstructure of GDLs from different suppliers. These led to artificial structures that are stochastically equivalent to the real structure. These structures were also made available for transport simulations.

Gases are distributed across the active area of a fuel cell via suitable flow fields. The microstructure of the GDL influences the flow in the channels of the flow distributor. Fig. 84 shows the schematic structure of a simulation domain. The schematic shows the medium flowing from the front through the GDL, whose microstructure is given by a series of binary images – in this case a fiber-based paper material.

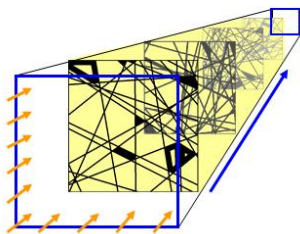


Fig. 84: Schematic structure of the simulation area

The channel-rib structure of the flow distributor causes an imbalance in the gas supply to the electrode: an above-average supply below the channel and a below-average supply below the rib. The GDL enables the area below the rib to be utilized by making a cross-flow through the porous structure possible, which distributes the gas fairly homogeneously to the electrode. During the operation of PEFCs, liquid water forms at the cathode side, which has to be transported into the channels through the GDL. The transport of the water in the GDL is

simulated using the lattice Boltzmann method. The fibres of the GDL are partially covered with PTFE, which leads to hydrophobic behavior towards liquid water in these areas, while they otherwise tend to be hydrophilic. The model parameters for calculating the cohesion and adhesion forces ultimately determine the contact angle between the liquid–gas interface of the water and the surface of the solid material. A contact angle of 0° , for example, represents hydrophilic behavior and a contact angle of 120° hydrophobic behavior. Fig. 85 shows the different behaviors of liquid water in hydrophobic (left) and hydrophilic (right) situations. A small section (approx. $0.1 \times 0.1 \text{ mm}^2$) of a fiber-based fleece material is shown.

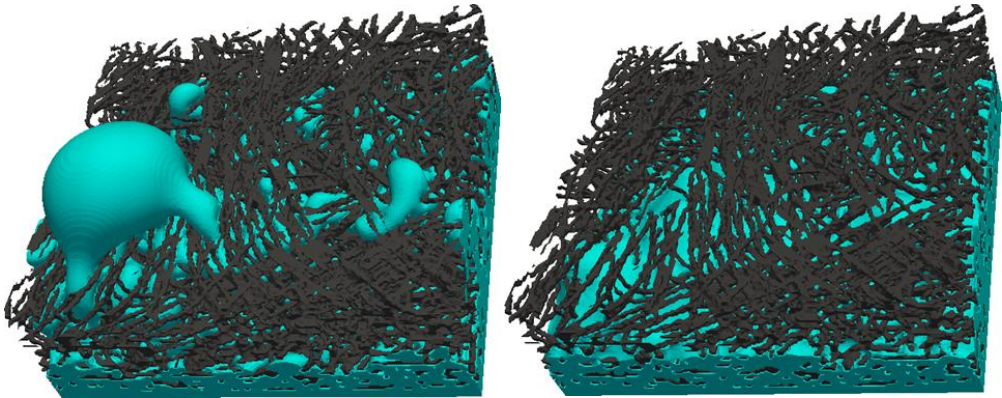


Fig. 85: Transport of liquid water through a section of the GDL at different contact angles (left: 120° , right: 0°)

Lattice Boltzmann simulations permit an extensive analysis of one- and two-phase mass transport processes in different gas diffusion layers. Effective parameters to describe transport phenomena – which are often only available by means of experiments otherwise – can be generated from the flow simulations.

The transport simulations were performed using hardware (JUROPA and JURECA) at the Jülich Supercomputing Centre (JSC).

5.3 Photolysis – photoelectric hydrogen production

More than 7 % of Germany's net electricity demand is already covered by photovoltaics. On sunny days, this value can reach as much as 50 % around midday (source: ISE). In contrast to other renewable energies, however, photovoltaic cells cannot provide electrical energy at night or in bad weather; a consistent supply of energy can thus only be achieved by means of suitable storage technology.

One option for storing energy is by splitting water electrochemically, i.e. by means of electrolysis. Electrolysis can be directly connected with photovoltaics systems in various configurations, forming a module that directly produces hydrogen. This solar hydrogen is a versatile fuel that stores the energy from sunlight in chemical form. Hydrogen produced in this way can be used as a fuel for heaters, for example, or transformed back into electrical energy via a fuel cell.

The aim of the PECSYS project (technology demonstration of large-scale photo-electrochemical system for solar hydrogen production) is developing a demonstration system with a surface area of up to 10 m² for the direct production of hydrogen via photovoltaics. The solar energy is transformed into chemical energy and stored as hydrogen fuel. It is envisioned that the production costs for hydrogen should in future fall below € 5 per kg hydrogen; they are around € 8 per kg today. In order to conclude the project, the partners from Germany, Sweden, and Italy are planning the construction of several modules with a total surface area of 10 m² so that stability and yield can be demonstrated on a large scale. The project, entitled "Fuel Cells and Hydrogen 2 Joint Undertaking" (number 735218), is part of the EU Framework Programme Horizon 2020 and will receive € 2.5 million in funding over four years.

According to a socio-economic evaluation, the investment costs for the new technology, including complete gas analysis (hydrogen and oxygen production, purification, online analysis, storage, etc.), should permit costs to fall well below € 5 per kg hydrogen as soon as the production method has been scaled. The components used for the system should be free of toxic or scarce materials such as III/V semiconductors or platinum. Under certain circumstances, however, it may be reasonable to use small amounts of platinum as a catalyst material for electrolysis. The photoabsorbers will be made of silicon, CIGS, or perovskite.

One of the systems is to be established at Forschungszentrum Jülich in Germany (global irradiance: ~ 1250 kWh/m²/year). A H₂ production rate of > 15 g/h must be achieved and at least 10 kg hydrogen produced over an operating period of 6 months. The efficiency of solar energy and hydrogen will be evaluated by means of simultaneous measurement of the global and diffuse irradiance on the 10 m² surface and should be above 5 % at full capacity. The system efficiency for transforming solar energy into hydrogen is intended to degrade by less than 10 % over more than 6 months of operation under aggressive conditions.

5.3.1 Electrolysis

This project focuses on two types of low-temperature electrolyzers based on well-established electrolytes: alkaline electrolysis and PEM electrolysis (see Fig. 86)

Alkaline electrolysis is a well-established technology. The major advantage is the use of cheap nickel-based catalyst materials, which are very stable in the alkaline regime and

display acceptable cell overpotentials for both cathode and anode electrodes. The cell must be supplied with a water–potassium-hydroxide mixture, and within each cell water flows from the anode to the cathode. When several electrolysis modules are combined in a test field, the electrolyte must be recirculated, as can also be seen in the following figure. Due to safety concerns, the circulation of an alkaline solution is a challenge, which may present a disadvantage in the implementation of such an alkaline-based system.

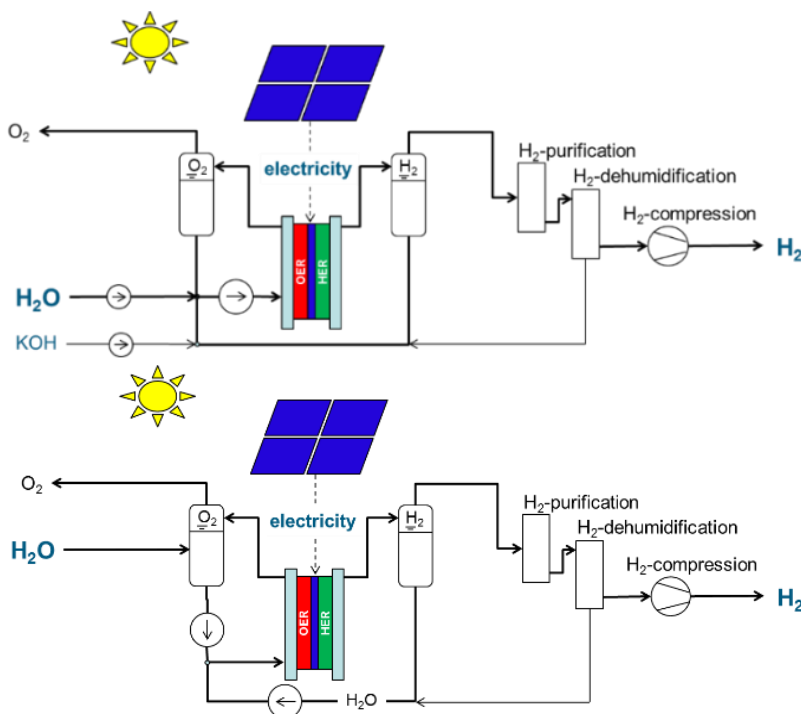


Fig. 86: Schematic of alkaline (above) and PEM (below) electrolysis systems

PEM water electrolysis has some advantages with respect to its simplicity and safe operation compared to an alkaline regime. Thanks to smaller cell resistances, it furthermore provides a much wider power range, which can be attributed to the thin (< 200 μm) membrane electrolyte. Additionally, it is also possible to integrate the required gas separator, which separates hydrogen from water, in the same cassette as the electrolysis process. This means that only a feed-in hose for water and an additional hose to collect the hydrogen will be necessary. The disadvantage of using pure water is the possibility of the system freezing at temperatures below 0 °C.

The project therefore aims to clarify how to operate the system at temperatures below 0 °C, and also to further reduce the noble metal loading to cut investment costs.

5.4 Supply systems for alternative fuels

According to present projections, the global demand for liquid fuels will grow considerably in the coming decades up to 2050. Alternatives to fossil fuels include liquid synthetic fuels produced from biomass (BTL) or in PTF processes using carbon dioxide and hydrogen, hydrogen and methane from PTG processes, and methane from biomass fermentation (bio CH₄).

5.4.1 Fuel requirements

Limiting the increase in the average temperature to 2 K is the basis of policy decisions to drastically reduce CO₂ emissions. CO₂ must be reduced in all sectors: power production, transportation, industrial processes, manufacturing, households, and small consumers. To do so, established boundaries will have to be overcome between stationary power generation and transportation as well as other sectors. The German Mobility and Fuels Strategy (MKS) considers an integrated approach to be necessary for the generation of renewable power and its utilization in decarbonizing public transportation. It also proposes expanding the fuel basis for trucks to include natural gas as an energy carrier and for aviation to include biofuels, particularly biokerosene, as well as a transition in maritime shipping towards diesel and LNG. The targets for reducing energy consumption in the transportation sector are 10 % by 2020 and 40 % by 2050 in relation to 2005 levels.

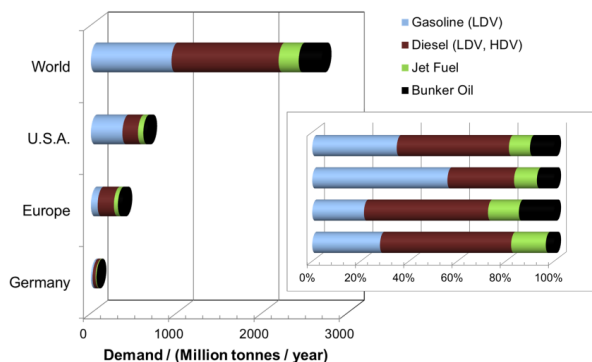


Fig. 87: Demand in millions of tonnes per annum for gasoline, diesel, kerosene and bunker oil in Germany, Europe, the USA and globally over the years 2014–2015^{33,34,35}

Fuel demand in the transportation sector is shown in Fig. 87 in millions of tonnes per annum (Mt/a) for the four categories gasoline, diesel, kerosene, and bunker oil. The data originate from various studies from the years 2014–2015^{33,34,35}. As shown in Fig. 87, Germany's geographic location means that ocean-going ships account for only a small proportion of fuel

³³ Hua, T., Ahluwalia, R., Eudy, L., Singer, G., Jermer, B., Asselin-Miller, N., et al.: Status of hydrogen fuel cell electric buses worldwide, *Journal of Power Sources*, 269 (2014), 975-993

³⁴ Administration, U. S. E. I. (2015, 2.6.2015), *International Energy Statistics*, verfügbar: <http://www.eia.gov/cfapps/ipdbproject/iedindex3.cfm?tid=5&pid=63&aid=2&cid=r3.&syid=2009&eyid=2013&unit=TBD>

³⁵ FuelsEurope, (2014, 2.6.2015), *Statistical report fuels Europe*, verfügbar: <https://www.fuelsEurope.eu/dataroom>

demand. Germany's gasoline and diesel shares are comparable to global levels. In the USA, the gasoline share dominates. The low kerosene share is initially conspicuous. However, the mean per capita consumption is 5.1 GJ/a/inhabitant in Germany and 8.5 GJ/a/inhabitant in the USA.

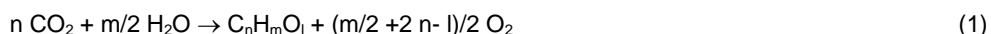
Current figures do not yet allow conclusions to be drawn on future trends. The German petroleum industry association ("Mineralölwirtschaftsverbands e.V., MWV) published projections for the period up to 2025 for gasoline, diesel and kerosene, which predict a reduction in the consumption of gasoline and diesel in light-duty vehicles (LDVs) and an increase in the consumption of diesel and gasoline in trucks³⁶. The baseline year for the projections was 2009. Accordingly, gasoline consumption in Germany will drop sharply from 19.7 Mt/a to 11.7 Mt/a. Diesel for cars will follow the trend, with a reduction from 12.1 Mt/a to 10.8 Mt/a. Consumption of truck diesel, in contrast, will rise from 18.3 Mt/a to 19.7 Mt/a and kerosene from 8.7 Mt/a to 10.9 Mt/a. Over this period, the number of registered vehicles will remain almost constant up to 2040, according to a Shell study³⁷. This study also predicts lower consumption due to efficiency improvements in engines.

These projections indicate the need for a smart, market-oriented strategy. This should be developed for German and Europe first and then transferred step by step to other countries worldwide. The high global growth rates and the resulting projected twofold increase in demand mean that the present potential to cover 25–40 % of demand is low. To achieve high shares of alternative fuels, all options for fuel production must be taken into account. The availability of raw materials, efficiency, and fuel production costs all play an important role here. These considerations provide a starting point for assessing what global raw material potential can be used to produce what quantities of fuel.

5.4.2 Potential synthesis routes for fuels

For a future supply of liquid fuels, a range of options must be tested. These can be subdivided into process chains using biomass and those using CO₂ incorporating hydrogen.

Fig. 88 shows the different routes. Carbon dioxide and water are used in photolytic processes in plants to synthesize various hydrocarbons C_nH_mO_l while oxygen is released.



A range of options are available to produce fuel from this biomass. Suitable types of biomass will be outlined in the sections that follow. In principle, vegetable oil can be used directly in internal combustion engines without having to be converted. Transesterification with the addition of methanol is more widespread as is the hydrogenation of vegetable oils in an industrial process (gray arrows in Fig. 88). The latter is gaining ground in the biodiesel market^{38,39}.

³⁶ Mineralölwirtschaftsverband: MWV-Prognose 2025 für die Bundesrepublik Deutschland, (2011), Mineralölwirtschaftsverband e. V., Berlin

³⁷ Adolf, J.: SHELL Pkw-Szenarien bis 2040, präsentiert bei: Mobilität im Wandel, (2014), Düsseldorf

³⁸ FNR, (2012, 16.4.2014), Biokraftstoffe, verfügbar: <http://biokraftstoffe.fnr.de/kraftstoffe/>

³⁹ UFOP, (2014, 16.4.2014), Rohstoffbasis der Biodieselanteile in Dieselmotoren, verfügbar: http://www.ufop.de/files/9413/9176/4863/UFOP_Analyse_Biodiesel_Rohstoffstoffbasis

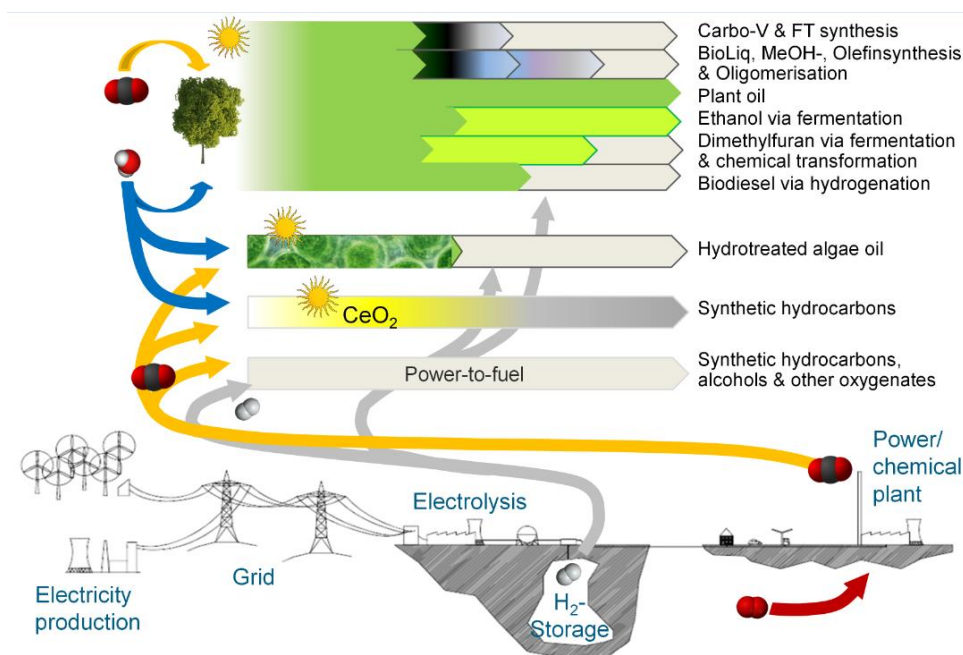
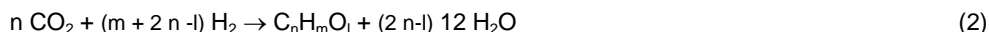


Fig. 88: Different synthesis routes for fuels from biomass and carbon dioxide

Ethanol as a biofuel component in gasoline is produced biochemically (light-green arrow in Fig. 88 by fermenting sugar or starch using yeast bacteria. Biochemical and chemical processes are combined for the synthesis of dimethylfuran as an alternative to gasoline⁴⁰. Algae oils have a very high area-specific production rate^{41,42}. Algae are supplied with nutrients, water, and carbon dioxide in closed reactors or in open breeding tanks to produce fuel. Industrial flue gases, e.g. from power plants, can be treated and used as a carbon dioxide source. Thermosolar processes imitate this process using CeO_2 and TiO_2 catalysts^{43,44}.

Another route involves the use of CO_2 emissions to synthesize fuels with the incorporation of hydrogen. This hydrogen is produced by electrolysis using surplus power.



A disadvantage here is that oxygen is released in the form of water, in contrast to the photocatalytic process which releases molecular oxygen. Some of the hydrogen is therefore

⁴⁰ Roman-Leshkov, Y., Barrett, C. J., Liu, Z. Y., Dumesic, J. A.: Production of dimethylfuran for liquid fuels from biomass-derived carbohydrates, *Nature*, 447 (2007), 982-985

⁴¹ Chisti, Y., Yan, J.: Energy from algae: Current status and future trends, *Algal biofuels – A status report*, *Applied Energy*, 88 (2011), 3277–3279

⁴² Weyer, K. M., Bush, D. R., Darzins, A., Willson, B. D.: Theoretical maximum algal oil production, *BioEnergy Research*, 3 (2009), 204-213

⁴³ Endres, C., Falter, C., Roth, A., Riegel, F., Sizmann, A.: Renewable aviation fuels - assesment of three selected fuel production pathways, in *Deutscher Luft- und Raumfahrtkongress 2012*, Berlin, DocumentID: 281191

⁴⁴ Somnath C. Roy, Varghese, O. K., Paulose, M., Grimes, C. A.: Toward solar fuels: photocatalytic conversion of carbon dioxide to hydrocarbons, *ACS Nano*, 4 (2010), 1259-1278

re-combusted directly in the synthesis process. A good example is the synthesis of methanol. Of the hydrogen produced, one third is used to absorb oxygen.



What quantities of alternative fuels are actually available? Assessments can only be made within a certain range. The essential question is what limiting factors are involved in producing these alternative fuels. Table 9 lists these factors, the relevant process chains and competing uses. Considering the competing uses of raw materials appears to be the key to the strong deviations to be expected between fuel potentials and possible future market shares. However, it is impossible to predict precisely how the conversion technologies and future pricing will develop in the competing markets. Monte Carlo simulations are therefore performed to estimate the ranges.

	Source	Competing use	Process chains
H ₂	Via electrolysis, using electricity from wind energy	Electricity generation	PTF, HVO
CO ₂	Industry Biomass gasification	Chemistry Biogas	PTF, solar fuel HVO from algae
Area	Agriculture Abandoned fields Cultivated forest Natural landscape Barren land	Food Furniture, heat Cooking, heat	Vegetable oil, ethanol from corn FT from KUP FT from waste wood Vegetable oil, halophytes, miscanthus
H ₂ O	Fresh water Waste water Sea water	Food Desalination	Vegetable/algal oils, solar fuel, ethanol from corn, FT from SRC Algal oil Algal oil, halophytes, miscanthus
Solar energy	Sunlight		Solar fuel, vegetable / algal oils
Waste wood	Cultivated forest	Heat	FT
Waste straw	Food production	Animal feed, Recycling	FT, Bioliq
Animal/fish fat	Food production	Animal feed, cosmetics	HVO

Table 9: Limiting factors in the production chains of alternative fuels. FT: Fischer–Tropsch; HVO: hydrotreated vegetable oil; SRC: short rotation coppice (cultivated wood); Bioliq: straw gasification

What conclusions can be drawn from Table 9?

- Hydrogen from renewable energy chains is generally required for all PTF processes and for the hydrogenation of vegetable oils.
- Carbon dioxide from industrial flue gases or from biomass gasification limits the production volume of solar fuels, algae oils, and PTF.

- The area available for the cultivation of energy crops is limited due to competing usage for food production. As a result, only land no longer used to produce food crops or land with a soil quality that is unsuitable for food crops can be used.
- Water is an important resource. All process chains requiring water in the production process – energy crop cultivation, solar fuel and algae cultivation – must not hinder the cultivation of food crops. Depending on the strain, algae can be cultivated in waste water or in saltwater. Some halophytes can be cultivated with seawater; miscanthus as an energy grass is highly tolerant and also grows in soils irrigated with brackish water.
- Residues from forestry and agriculture, as well as from meat and fish production are very limited due to the available quantities and competing usage.

5.4.3 PTF Fuels

Whether a fuel produced via power-to-fuel processes will prevail on the market depends on two fundamental conditions: on the one hand, it must harmonize with current fuels and their infrastructure. On the other hand, its production must be technologically and economically viable. No significant changes to infrastructure and existing vehicles should be necessary in order to use the fuel. Furthermore, suitable non-fossil and non-biological fuels should be available for the various areas of application in the transport sector. As is the case for the currently fossil-dominated market, a diversification of the fuel range is necessary.

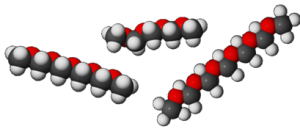
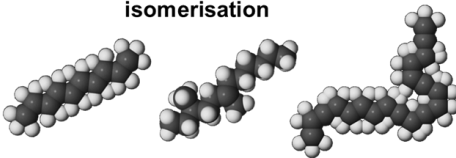
OME ₃₋₅	Diesel from Fischer-Tropsch and isomerisation
	
<ul style="list-style-type: none"> + Improved emissions + High cetane number + Strongly reduced particle numbers compared to fossil diesel - Viscosity in regard to DIN EN 590 too high 	<ul style="list-style-type: none"> + Higher heating value as OME₃₋₅ + High cetane number + Strongly reduced particle numbers compared to fossil diesel - Byproducts (usable) - Viscosity in regard to DIN EN 590 too low
Results from Aspen simulations:	
$\eta_{PTL} < 35.3 \%$ (Energy demand only partly included)	$\eta_{PTL} = 54 \%$ (further optimization potential)
$\eta_{LHV} = 70.4 \%$	$\eta_{LHV} = 62.6 \%$
<ul style="list-style-type: none"> ➤ High selectivity for OME₃₋₅ ➤ No undesired by-products ➤ Synthesis via four intermediates ⇒ fünf Anlagen inklusive Trenntechnik 	<ul style="list-style-type: none"> ➤ Prozess optimization for maximum diesel share ➤ Byproducts: (gas), naphtha, waxes ➤ Subsequent hydrocracker, autothermal gas reformer, rectification column, μ-reactor

Fig. 89: Comparison of the two power-to-fuel pathways, OME synthesis and Fischer-Tropsch

At IEK-3, a comparative overview of various alternative fuels and their production is being developed, including Fischer-Tropsch hydrocarbons and polyoxymethylene dimethyl ethers (OMEs). Both these products can be blended with conventional diesel. Market introduction is

therefore considered conceivable. In spite of having the same application, the processes and products differ considerably. Fig. 89 summarizes the insights from AspenPlus simulations for both types of fuel.

On a molecular level, Fischer–Tropsch hydrocarbons are very similar to fossil diesel. This does not apply to ethers such as OME. Although OME has a lower heating value, it does have outstanding potential for improving exhaust-gas values. Industrial-scale Fischer–Tropsch processes have been state of the art for decades. This does not apply to OME processes since the demand for these products is low. There are various fundamental options in plant design for both processes. Plant design and process parameters have an influence on educt and energy demand as well as product quality, joint products, and by-products. The challenges of product processing are different for Fischer–Tropsch and OME3–5 synthesis. Thus, the difficulty with hydrocarbons is in the wide product distribution. The difficulties of OME3–5 synthesis are in the liquid–liquid separation due to diverse miscibility gaps and azeotropes. The techno-economic analysis of the production processes plays an important role in the implementation strategy for a climate-neutral transport sector, as does an analysis of the product specification. Initial estimates reveal an advantage concerning the efficiency of the entire well-to-tank chain of FT synthesis. Future analyses will refine these indications.

5.5 New topics in energy systems analysis and integration

New topics in energy systems analysis and integration can be subdivided into three research areas: mobility, stationary energy systems, and sector coupling and infrastructures. These three research areas also reveal the current priority topics in Process and Systems Analysis (VSA) and will be described in more detail in the following.

5.5.1 Mobility

The compulsory greenhouse gas (GHG) reduction targets of the Federal Government of at least 80 % by 2050 require drastic emission cuts in all sectors of the economy. For road transport, IEK-3 has shown the high GHG reduction potential that results from using renewably generated electricity to produce hydrogen and its use in fuel cell vehicles (FCVs). This now presents the challenge of developing an introduction strategy for hydrogen which will provide prospects for the cost-optimized development of a hydrogen supply chain based on models to be developed and data from base years. For this purpose, the techno-economic and ecological properties of various supply pathways will be identified so that they can be prioritized in the course of the temporal development of market introduction as a function of spatially and temporally resolved demand development.

Another focus of this consideration is the issue of the types of drives required in the future. For this reason, primarily FCVs and battery-electric vehicles (BEVs) will be extensively analyzed with regard to their strengths and weaknesses in the future mobility environment. In addition to environmental characteristics of such vehicles that will be unchanged from those of present cars, these will include performance parameters such as power, range, the time needed to fill the tank, and costs, as well as requirements for suitable filling and charging infrastructures. In addition to FCVs and BEVs, advanced cars with combustion engines and hybrid drives will also be considered. In addition to a cost and demand model, conformity of the GHG emissions of the entire vehicle fleet with the GHG targets will be integrated into the consideration. The aim is to make the drive mix of the future describable using models.

Finally, potential impacts of autonomous driving on the existing vehicle fleet and annual mileage will be analyzed. Trends in mobility research in particular will be incorporated in the analysis. Private ownership of cars is already being discussed intensively and questioned today. In combination with autonomous driving, vehicle utilization could in future be considerably improved and therefore the number of vehicles reduced. Since the described changes could have a substantial impact on the way vehicles are used in future, the insights gained will also be incorporated into the consideration of the market introduction strategy and the transport model.

5.5.2 Stationary energy systems

Climate-gas emissions caused by buildings make up approximately 13.2 % of all national emissions. In order to achieve the ambitious climate-gas reduction targets set by the Federal Government, emissions must also be reduced significantly in this end-consumer sector. By encouraging the development of renewable energy sources, electricity will be the dominant form of energy in a future energy supply, fulfilling various supply tasks. This will lead to a closer interlinkage between supply tasks; they can no longer be regarded as separate from each other, resulting in closer coupling between sectors. Against this backdrop, low-emission

supply concepts will in future be analyzed on various system levels. Under the premise of cost efficiency, supply concepts and technology systems for heat and electricity supply systems will be developed on the building level. For this purpose, an existing mathematical optimization model for supply systems to buildings will be expanded; in addition to individual supply methods, it will also incorporate thermal insulation in the optimization calculation. The consideration of storage methods for electricity and heat as well as the necessary temporal resolution represent a particular challenge.

In addition to individual buildings, comparable analyses will in future also be conducted for urban neighborhood supply systems in cities. In cooperation with an industrial partner, real city neighborhoods will be selected to serve as examples in deriving supply concepts, which will include both heat and electricity supply as well as the mobility sector. For this purpose, suitable GIS-based model approaches will be developed, which will permit a comparison between different supply concepts with regard to efficiency and costs and which will reveal the infrastructure demand.

5.5.3 Sector coupling and infrastructures

Replacing fossil energy carriers to a large extent is tantamount to a decarbonization of the energy supply. Electricity generation based on renewable energy will in future play the central role. It will include primarily fluctuating sources such as wind and photovoltaic plants. Due to the temporal discrepancy between production and consumption as well as grid bottlenecks, there will be a “negative residual energy”, which can be used for power-to-X applications such as power-to-heat or power-to-gas. A well-founded estimate of this negative residual energy requires high spatial and temporal resolution of consumption, production, and the simulation of the electricity grid. For this purpose, a dispatch and a power-grid model are currently being developed, which will permit a well-founded estimate of negative residual energies, which will in turn form the basis for further hydrogen-based supply tasks.

Furthermore, VSA's systems-analysis model portfolio comprises a multitude of models which can be used to conduct detailed analyses of selected areas (e.g. buildings, transport, electricity sector) of the energy supply. These activities have so far been based on the approach of interlinking various partial models to form an overall model. This approach has various advantages and disadvantages, see chapter 3.6.2.1. For this reason, it is planned to continue developing a highly aggregated overall model with which national climate-gas reduction strategies can be generated and analyzed, and which results in a national overview.

Germany has at its disposal a historically evolved infrastructure for the natural-gas supply. A hydrogen-based energy supply system requires a transport and distribution structure. Within the scope of new topics, we will investigate the question whether and to what extent the existing natural-gas supply infrastructure could also be used as a hydrogen supply system. In this context, the basic feasibility and any modification requirements will be analyzed with regard to efficiency and costs.



Data

Facts and Figures

- The Institute of Electrochemical Process Engineering (IEK-3)
- Overview of department expertise
- Publications, technology transfer, and resources
- Committee work
- Contributions to trade fairs and exhibitions
- How to reach us
- List of abbreviations

6.1 The Institute of Electrochemical Process Engineering IEK-3

For IEK-3, the 2015–2016 period under review was characterized by the fact that the institute's research and development priorities – fuel cells and electrolysis – are now an integral part of the newly formed program on storage and cross-linked infrastructure (SCI) of the Helmholtz Association (HGF), in addition to other priorities such as batteries, synthetic hydrocarbons, heat storage, as well as superconductivity, grids, and system integration. Together with two further HGF programs for renewable energy sources and energy efficiency, materials, and resources, the new SCI program's objective is to work out solutions for the energy supply that are economically, ecologically, and socially viable. The SCI program conducts R&D into adequate energy storage systems to compensate the volatile provision of energy, efficient infrastructures to overcome the challenges of energy transmission and distribution, and cross-sector interlinkage to increase the flexibility, efficiency, and economic viability of the energy systems.

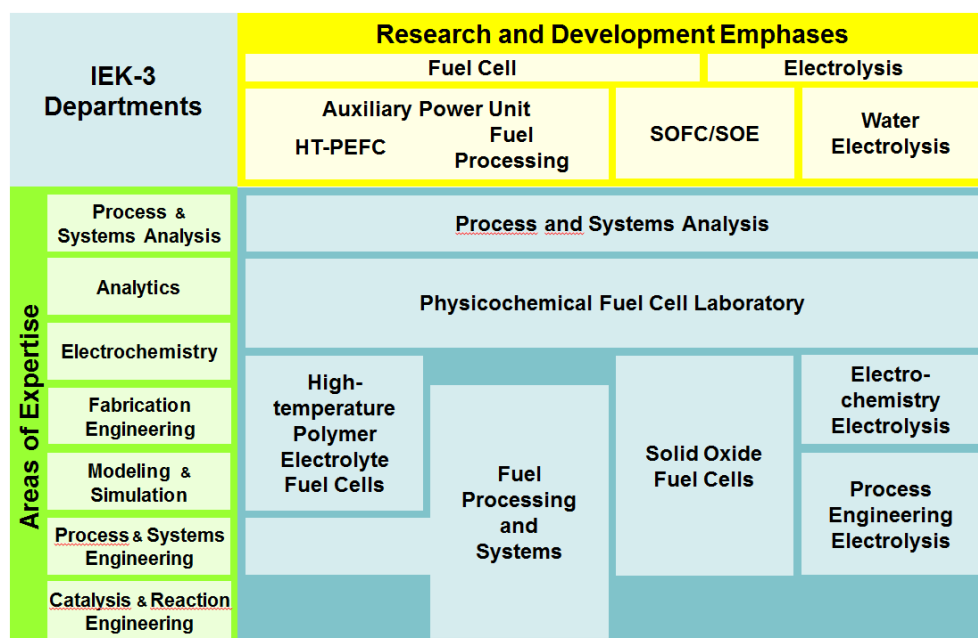


Fig. 90: Departments, areas of expertise, and R&D priorities

With the launch of the updated HGF programs, the Energy System 2050 initiative was set up in the research field of Energy in order to work out by 2019 concrete and exploitable systems technology findings and technological solutions which politics and industry can utilize. Within the scope of this collaborative systems analysis project, IEK-3 is responsible for energy and raw materials pathways using hydrogen as a research topic. In cooperation with the HGF centers GFZ, HZB, DLR, and UFZ, scientists from IEK-3 investigate the role of hydrogen in the reduction of greenhouse gases, work out concepts for the development of an integrated electricity and hydrogen supply infrastructure, evaluate options for the energetic and chemical self-sufficiency of industry and households, and analyze the chances of global infrastructures for the provision of renewable energies and hydrogen. These new activities have resulted in a considerable increase in personnel in process and systems analysis, so that the working group was upgraded to a department with a new head as of 2016. In late

2016, another collaborative project was approved by an international panel of experts: the project will be funded from the HGF Initiative and Networking Fund (IVF) and involves the HGF centers concerned with energy systems analysis. The underlying pioneering topic of energy systems integration will help prepare the corresponding program for the next program funding period. With a total of three work packages, IEK-3 is involved in work package 1, “multimodal energy system 2050”.

Another large-scale project with IEK-3 involvement is the BMBF-funded Kopernikus project entitled “Power-to-X (P2X)”, which was also launched in 2016. Coordinated by DECHEMA, Forschungszentrum Jülich, and RWTH Aachen University, a total of 62 working groups from the fields of academia, industry, and socio-economics will work on a more flexible usage of renewable resources. Two departments of IEK-3 are involved and will provide contributions on high-temperature co-electrolysis and liquid hydrogen carriers.



Institute of Energy and Climate Research
IEK-3: Electrochemical Process Engineering
Forschungszentrum Jülich GmbH
52425 Jülich

Head of Institute
Prof. Dr.-Ing. Detlef Stolten
Tel.: 02461-61-3076
Email: d.stolten@fz-juelich.de

Through a refocusing of research priorities in order to meet the needs of the latest developments, the number of IEK-3 R&D topics was reduced to three. High-temperature polymer electrolyte fuel cells (HT-PEFCs) and fuel-gas production from liquid energy carriers to be used for supplying hydrogen to fuel cells together form the research topic on systems for auxiliary power supply systems. Ceramic high-temperature fuel and electrolysis cells (SOFC/SOE) as well as low-temperature electrolysis are further topics at IEK-3, shown in Fig. 90 with the corresponding competence fields. Focusing more closely on concrete areas of application enables IEK-3 to work on all aspects of each of these R&D topics from the basic phenomena up to process engineering for entire systems with teams of supercritical size and in research facilities of up to pilot-plant scale. Synergies between the scientific disciplines will be exploited. The analysis and study results of technology-based process and energy systems analysis serve as a strategic orientation for the technology-based departments of IEK-3 responsible for analyzing, conceiving, designing, evaluating, and comparing future-oriented processes and energy systems. The approach used here accounts for technical, economic, and ecological aspects, and permits quantitative

conclusions to be drawn on the performance efficiency and sustainability of an energy system. Application-oriented R&D activities are additionally accompanied by basic research aiming to clarify structure-activity relationships using selected advanced analysis methods. These activities are pooled in the physicochemical fuel cell laboratory, which works together with the technology-oriented departments within the institute.

Jülich has the largest institutional research team (approx. 150 employees) working on fuel cells and electrolysis in Europe. Of these 150 employees, around half work in the SOFC/SOE field, and approx. one-fifth of these are involved in IEK-3 activities. Three other institutes also work in the SOFC/SOE field. IEK-1 is responsible for manufacturing materials, IEK-2 tests the materials and conducts steel research, and IEK-9 focuses on the electrochemical principles. The Central Institute of Engineering and Technology (ZEA-1) is concerned with stack construction. Of the some 101 IEK-3 employees (not including visiting scientists, student assistants, or trainees), 86 work on technological developments for low-temperature fuel cells and electrolyzers as well as energy systems analysis. A coordinator is responsible for the fields of work at IEK-3, and is also available to answer generic questions.



Deputy head and scientific coordinator

Dr.-Ing. Bernd Emonts

Tel.: 02461-61-3525

Email: b.emonts@fz-juelich.de

6.2 Overview of department expertise

High-Temperature Polymer Electrolyte Fuel Cells

Fuel Processing Systems

Fields of work, range of services

Work on the HT-PEFC extends from the electrode to the stack and is conducted in cooperation with internal and external partners. New electrode structures and preparation methods are developed. MEAs are manufactured and electrochemically characterized.

Structure–activity relationships of MEA components are also investigated. Metallic and graphitic bipolar plates are developed and tested in cells and stacks. Comprehensive modeling and simulation activities from the component level up to the stack level support their development. In the field of LT-PEFCs, two-phase flow phenomena are investigated experimentally and theoretically.

H₂ produced from commercially available fuels expedites the early introduction of fuel cell technology. Work here concentrates on reforming in the power classes of 3 kW_{el} and 50 kW_{el} of middle distillates (kerosene, diesel and heating oil) and diesel-like biofuels. In developing mobile on-board power supply systems, in-house HT-PEFC 5 kW_{el}–10 kW_{el} stacks are preferred. In addition, PEFC and SOFC systems with diesel reforming are evaluated in cooperation with project partners and within the framework of systems analyses.

Facilities, processes, methods

Equipment

- Test stands for the electrochemical characterization of MEAs
- Test stands for electrochemical studies on stacks up to 5 kW_{el}
- Equipment for the fabrication of gas diffusion electrodes

Models

- Simulation models to describe mass, charge and heat transport processes in cells and stacks
- Lattice–Boltzmann simulation tools
- CFD Simulation tools (OpenFOAM aTools)

Equipment

- Test stands for the examination of reactors and whole systems
- Test stands for the screening and examination of catalyst activity and selectivity
- Analytical devices for the determination of reaction gas concentrations (GC, GC/MS, NDIR, FTIR)
- Apparatus for fractional distillation of fuels

Models

- CFD simulation programs for reactor and system design

Contact



Prof. Dr. Werner Lehnert

Tel.: 02461-61-3915

Email: w.lehnert@fz-juelich.de



Prof. Dr.-Ing. Ralf Peters

Tel. 0261-61-4260

Email: ra.peters@fz-juelich.de

Solid-Oxide Fuel Cells

Electrochemical Electrolysis

Fields of work, range of services

A key area of scientific and technical expertise is the development and optimization of stacks and systems for high-temperature fuel cells as well as high-temperature electrolysis. Stacks, systems, and system components are devised, designed, constructed, assembled, and tested. To optimize concept evaluation, the experimental studies are accompanied by the development of thermomechanical and process-engineering models. Priorities here are the electrochemical characterization of stacks and the development, testing, and evaluation of new system concepts, control technology concepts and components in cooperation with industry.

Advanced PEM electrolyzers facilitate the economic production of H_2 from excess renewable electricity. With support from project partners in research and industry, development work concentrates on membrane electrode assemblies (MEAs) in which the platinum group metals required for catalytic reactions are either reduced or completely replaced while retaining comparable performance. New types of membranes aim to lend planned large-scale systems sufficient stability. Further topics include the identification of cost-effective materials and the development of replicable fabrication techniques for MEA development and production.

Facilities, processes, methods

Test stands

- Characterization: high-temperature heat exchangers up to $850\text{ }^{\circ}\text{C}$ @ $200\text{ m}^3\text{ air/h}$
- Characterization: reformers and afterburners for stacks up to 5 kW
- Characterization: 20 kW system
- Electrochemical characterization: 100 W–10 kW stacks in fuel cell and electrolysis operation

Models

- CFD/FEM models to determine flow and voltage distribution in stacks and system components
- Simulation models for the design of fuel cell systems

Equipment

- Test stands for the characterization of electrocatalysts (rotating disk electrode)
- Test stands for the characterization of membranes (gas permeation measurements, fluorine release rate)
- Test stands for the electrochemical characterization of CCMs
- Test stand for electrochemical studies up to 30 kW_{el}
- Coating facility (roll-to-roll) for continuous electrode fabrication

Contact



Prof. Ludger Blum

Tel.: 02461-61-6709

Email: l.blum@fz-juelich.de



Dr. Marcello Carmo

Tel. 0261-61-5590

Email: m.carmo@fz-juelich.de

Fields of work, range of services

Using ideas for new concepts, electrolysis stacks and systems are developed and modeled. The aim is to improve efficiency, power density, and lifetime while simultaneously reducing the amount of material needed. Work is validated in component tests and by characterizing entire stacks and systems. In cooperation with project partners, coatings, stack components, stacks, and systems are optimized and characterized. Combined with automated fabrication on an industrially relevant scale, this work builds a bridge between science and technology.

As the technical development of new pioneering energy systems progresses, scientific work is becoming increasingly important for understanding basic phenomena. The department therefore focuses on fully elucidating material and structural properties as well physicochemical and electrochemical processes. Imaging, physical, and spatially resolved analysis techniques are used to determine chemical and structural changes, mechanical and thermodynamic suitability, and fluid dynamic and electrochemical performance.

Facilities, processes, methods**Equipment**

- Test stands for electrochemical studies of electrolyzers up to 100 kW_{el} and fuel cells (DMFCs)
- Visualization tests
- Corrosion test stands for the evaluation of coatings
- Analysis of ion-exchange materials with media containing specific impurities
- Laser coating for local modification of surfaces
- Robot facility for the reproducible fabrication of stacks

Models

- Description of mass, charge and heat transport

Equipment and methods

- Imaging analysis techniques: high-resolution scanning electron microscope (H-SEM) with EDX analysis, optical microscopes, confocal laser scanning microscope
- Spatially resolved analysis techniques: segmented cell technology (SCT), magnetic imaging, and mass spectroscopy (SRMS)
- Physicochemical analysis techniques: thermogravimetric analysis (TG, TGA), differential scanning calorimetry (DSC), contact angle measurement (KF analysis), impedance spectroscopy/CV, RDE, climate cabinet, tensile testing machine with climate chamber, BET and standard porosimeter, particle size measuring unit

Contact**Dr.-Ing. Martin Müller**

Tel.: 02461-61-1859

Email: mar.mueller@fz-juelich.de**PD Dr. Carsten Korte**

Tel.: 02461-61-9035

Email: c.korte@fz-juelich.de

Process and Systems Analysis

Fields of work, range of services

Selection, development, and implementation of future energy systems demand approaches analyzing and evaluating the sustainability and economic viability of entire systems. Techno-economic comparisons of competing technologies for energy conversion and storage are the foundation for this. The broad experimental basis and extensive modeling at IEK-3 make it possible to design energy systems, describe them in models, and compare them with competing technologies under realistic conditions as well as to identify development potential and shortcomings. Studies for industry are also conducted while protecting sensitive information, and policy recommendations are derived on a neutral basis.

Facilities, processes, methods

Methods

- Energy systems modeling using modeling environments such as METIS (models for energy transformation and integration systems), a Python- and database-based environment developed at IEK-3
- Potential analyses of renewable energies in the overall European system, for example
- Dynamic simulations (Python, Matlab/Simulink)
- Well-to-wheel analyses (spreadsheets)
- Technology-based benchmarking
- Economic evaluations (SWOT, WACC, CAPM, Monte Carlo simulations)
- Process analysis and optimization (Fluent, AspenPlus)

Contact



Dr.-Ing. Martin Robinius

Tel.: 02461-61-3077

Email: m.robinius@fz-juelich.de

6.3 Publications, technology transfer, and resources

The results of scientific and technical work carried out at IEK-3 are published in relevant journals and presented to interested specialist audiences at national and international conferences. In 2015, scientists from IEK-3 published four articles in journals with great influence, i.e. a high impact factor (see Table 10).

Journal	Impact factor	2015	2016
Energy & Environmental Science	25,427	1	0
Progress in Energy & Combustion Science	16,784	1	0
American Chemical Society	13,038	1	0
Nanoscale	7,760	1	0
Power Sources	6,333	2	12
Chemistry – A European Journal	5,771	1	0
Applied Energy	5,746	1	2
Chemical Engineering Journal	5,310	0	2
Electrochimica Acta	4,803	2	2
Energy Conversion and Management	4,801	0	1
Electrochemistry Communications	4,569	1	0
Energy	4,292	0	2
Dalton Transactions	4,177	0	1
Physical Chemistry	4,173	2	0
Greenhouse Gas Control	4,064	1	1
Colloid and Interface Science	3,782	1	0
Computer Physics Communications	3,635	1	0
Hydrogen Energy	3,205	12	6
Electrochemical Society	3,014	10	7
Magnetic Resonance	2,889	0	1
Electroanalytical Chemistry	2,822	1	0
Materials	2,728	0	1
Energy Technology	2,557	0	1
Energy Research	2,529	0	1
Solid State Ionics	2,380	1	0
Applied Electrochemistry	2,223	1	0
Energies	2,077	0	1
Fuel Cells	1,769	2	3
Computing in Science and Engineering	1,361	0	1
Review of Scientific Instruments	1,336	1	0
Chemie-Ingenieur-Technik	0,798	2	0
Advanced ElectronicMaterials	keine Angabe	1	0

Table 10: Publication performance of IEK-3 in peer-reviewed journals

In addition, other journals were addressed whose thematic orientation corresponds to the work priorities of IEK-3 to a major extent. This led to a maximum number of publications in the three favored journals of between 6 and 12 articles per year and journal. The total number of articles published in peer-reviewed journals amounted to 47 in 2015 and 45 in 2016 (see Table 11).

with IEK-3 involvement in 2015 included the 228th ECS Meeting in Phoenix, USA, with 5 talks, and the ECS Conference on Electrochemical Energy Conversion & Storage in Glasgow, UK, with 4 talks. In 2016, IEK-3 contributed 7 talks each to the 21st WHEC in Zaragoza, Spain, to the 12th European SOFC & SOE Forum in Lucerne, Switzerland, and to the 13th Symposium for Fuel Cell and Battery Modeling and Experimental Validation in Lausanne, Switzerland. IEK-3 also made 5 contributions to the 230th ECS Meeting in Honolulu, USA. Various departments at IEK-3 also contributed papers and presentations to numerous other specialist conferences both in Germany and abroad.

During the period under review (2015–2016), 13 doctoral theses were completed on SOFCs (3), HT-PEFCs (2), BGS (3), PEM-EL (3), and BAT (2), as were 4 undergraduate dissertations evaluating pioneering energy systems (see Table 11). Furthermore, Professor Stolten assessed 4 successful doctoral projects of external doctoral researchers in 2015.

Year		2015	2016
Publications	Peer-reviewed journals ¹⁾	47	45
	Books and journals	19	10
	Article in a book	15	17
	Doctoral theses ²⁾	9	8
Technology Transfer	Ongoing projects with third-party funding	36	30
	HGF initiatives & funds	3	3
	Patent applications	7	6
	Patents granted	3	8
Resources³⁾	Personnel (PoF ⁴⁾ / third-party funding)	112 (92/20)	115 (98/17)
Explanatory notes	¹⁾ according to ISI citation index ²⁾ internal doctoral researchers ³⁾ data in PY/a ⁴⁾ PoF: Program-oriented funding		

Table 11: IEK-3 core data for 2015 and 2016

In order to guarantee substantial knowledge and technology transfer, IEK-3 is involved in numerous national and international R&D projects (2015: 36; 2016: 30), funded by the European Commission (EC; 2015: 5; 2016: 4), the Federal Ministry for Economic Affairs and Energy (BMWi; 2015: 8; 2016: 7), the Federal Ministry of Education and Research (BMBF; 2015: 5; 2016: 3), various ministries of the federal states of North Rhine-Westphalia and Bavaria (2015: 5; 2016: 3), as well as the German Research Foundation (DFG; 2015: 5; 2016: 5), or financed by industry (2015: 6; 2016: 7) (see Table 11). Some of these projects were headed and coordinated by IEK-3.

During the reporting period, two large-scale R&D projects and one project application were supported by additional funding from the Helmholtz Association. IEK-3 received funding for HGF expansion investments in order to develop a MW electrolysis plant as Jülich's building block towards future power-to-gas processes of the cross-centre Energy Lab 2.0. The application phase for the preparation of an HGF initiative on urban research was not recommended for funding from the Initiative and Networking Fund (IVF) of the HGF president by the panel of experts set up especially for this purpose. As part of the initiative of the research field of Energy, supported by 8 HGF centers, IEK-3 attracted further HGF funding from the IVF for the techno-economic evaluation of a pioneering Energy System 2050, concerning topics such as energy and raw material pathways involving hydrogen. Furthermore, IEK-3 received additional funding for device investments from the Jülich technology transfer fund in order to bolster promising innovations with commercialization prospects. Further building blocks for organized technology transfer include numerous patent applications (2015: 7, 2016: 6) and patents granted (2015: 3, 2016: 8) in this period (see Table 11).

During the period under review, the number of employees at IEK-3 fluctuated between 112 (2015) and 115 (2016). They were financed through the Helmholtz Association's (HGF) program-oriented funding (POF) as well as by third-party funds (see Table 11). In contrast to previous years, in addition to part-time employees, a significant portion of IEK-3 personnel were employed for less than one year during this period, so that the effective personnel capacity amounted to 96 PY/a in 2015 and 94 PY/a in 2016.

6.4 Committee work

IEK-3's national and international reputation in the field of fuel cells and hydrogen technology is reflected in the fact that IEK-3 scientists are members of and collaborate with national and international committees. The impact of numerous scientists from IEK-3 in leading roles for the Technology Collaboration Programme on Advanced Fuel Cells of the International Energy Agency (IEA) provides IEK-3 with great international visibility. On the national level, Prof. Stolten is a member of the Executive Board and Advisory Council of the VDI Society for Process Engineering and Chemical Engineering, Chair of the ProcessNet Subject Division Energy Process Engineering, and member of the advisory council. An overview of committee work performed by IEK-3 employees is set out in detail below.

Technology Collaboration Programme on Advanced Fuel Cells/Advanced Fuel Cells Implementing Agreement der International Energy Agency

since 2000, Prof. D. Stolten

Head of the German Delegation on the Executive Committee

since 2002, Prof. D. Stolten

Vice-Chairman of the Executive Committee

since 2009, Dr. R.C.Samsun

Member of the Executive Committee

since 2011, Prof. D. Stolten

Chairman of the Executive Committee

since 2011, Prof. D. Stolten

Operating Agent for Annex 36 „Systems Analysis“

since 2011, Dr. R.C. Samsun

Member of Annex 36 „Systems Analysis“

since 2013, Prof. L. Blum

Member of Annex 32 „Solid Oxide Fuel Cells“

since 2014, Prof. S. Beale

Operating Agent for Annex 37 „Modeling of Fuel Cell Systems“

since 2014, J. Mergel

Operating Agent for Annex 30 „Electrolysis“

since 2014, Prof. D. Stolten, Prof. L. Blum, Dr. M. Carmo, Dr. W. Lücke, Dr. M. Müller

Member of Annex 30 „Electrolysis“

since 2014, Prof. W. Lehnert

Member of Annex 31 „Polymer Electrolyte Fuel Cells“

since 2014, Dr. T. Grube

Member of Annex 34 „Fuel Cells for Transportation“

since 2014, Dr. M. Müller

Member of Annex 35 „Fuel Cells for Portable Applications“

since 2014, Prof. L. Blum, Dr. D. Fritz, D. Froning, Prof. A. Kulikovskiy, Prof. W. Lehnert, Dr. U. Reimer

Member of Annex 37 „Modeling of Fuel Cell Systems“

Institute of Mechanical Engineering (IMEchE), UK

since 1980, Prof. S. Beale

Member

American Society of Mechanical Engineers (ASME), USA

since 1981, Prof. S. Beale

Member

Professional Engineers Ontario, Kanada

since 1985, Prof. S. Beale

Member

Working Group of Electrochemical Research Facilities (AGEF)

since 1990, Dr. K. Wippermann

Member

since 2000, Prof. D. Stolten

Member

since 2010, J. Mergel

Member of the Board of Directors

German Chemical Society (GDCh)

since 1990, Dr. K. Wippermann

Member of GDCh and of the GDCh Special Interest Group for Applied Electrochemistry

since 1999, Prof. W. Lehnert

Member

German Physics Society (DPG)

since 1993, Prof. W. Lehnert

Member

since 2010, Dr. U. Reimer

Member of the Energy Working Group

German Bunsen Society for Physical Chemistry (DBG)

since 1993, PD Dr. C. Korte

Member

Institute of Electrical and Electronics Engineers (IEEE), USA

since 1996, Prof. S. Beale

Member

International Society of Electrochemistry (ISE), Switzerland

since 1998, Prof. W. Lehnert

Member

since 2005, Prof. A. Kulikovsky

Member

Electrochemical Society (ECS), USA

since 1999, Prof. W. Lehnert

Member

since 2005, Prof. A. Kulikovsky

Member

Association of German Engineers (VDI)

since 1999, Prof. W. Lehnert

Member

since 2013, Dr. T. Grube

Member

German Informatics Society

since 2002, D. Froning

Member

German Informatics Society – special interest group on numerical simulation

since 2015, D. Froning

Member

ProcessNet Subject Division Energy Process Engineering

since 2003, Prof. D. Stolten

Member

since 2006, Prof. D. Stolten

Vice-Chairman

since 2008, Prof. D. Stolten

Chairman

since 2012, Prof. R. Peters

Member of the Advisory Board

German Hydrogen and Fuel Cell Association (DWV)

since 2004, Prof. W. Lehnert

Member

since 2011, Prof. D. Stolten

Representative of Forschungszentrum Jülich GmbH as a full member

Fuel Cell Qualification Initiative

since 2005, Dr. B. Emonts

Member of the Executive Committee

BREZEL Expert Committee of the Association of German Engineers

since 2005, Prof. L. Blum

Member of the Expert Committee

WILEY-VCH “Fuel Cells” Journal

since 2006, Prof. D. Stolten

Member of the Advisory Board

National Organization for Hydrogen and Fuel Cell Technology (NOW)

2008–2013, 2015–2016, Prof. D. Stolten

Member of the Advisory Board and HGF/BMBF representative for the field

N.ERGHY in EU FCH Undertaking

since 2008, Prof. D. Stolten

Representative of Forschungszentrum Jülich GmbH as a full member

2008–2012, Prof. R. Peters

Member of the Working Group for AA Transport and Refuelling Infrastructure

since 2013, Prof. R. Peters

Member of the Working Group Transport Pillar

ProcessNet Section SuPER

since 2008, Prof. D. Stolten

Member of the Steering Committee

ASME K-10 Heat Transfer Technical Committee (heat transfer equipment)

since 2008, Prof. Dr. S. Beale

Member

Computational Thermal Sciences Journal, begellhouse

since 2008, Prof. Dr. S. Beale

Member of the Editorial Board

Renewable Energy Research Association (FVEE)

since 2009, Dr. B. Emonts

Representative of Forschungszentrum Jülich GmbH for Fuel Cells

h2-netzwerk-ruhr

since 2009, Dr. B. Emonts

Member of the Advisory Board

since 2012, Dr. B. Emonts

Vice-Chair of the Advisory Board

since 2015, Dr. B. Emonts

Chair of the Advisory Board

ASME K-20 Heat Transfer Technical Committee (computational heat transfer)

since 2010, Prof. S. Beale

Member

ASME Research Committee on Energy-Water Nexus

since 2010, Prof. S. Beale

Member

ASME Research Committee on Sustainable Products and Processes

since 2010, Prof. S. Beale

Member

Thermopedia Journal, begellhouse

since 2010, Prof. S. Beale

Member of the Editorial Board

Max Planck Institute for Dynamics of Complex Technical Systems Magdeburg

since 2011, Prof. D. Stolten

Member of the Scientific Advisory Board

Society for Chemical Engineering and Biotechnology e.V. (DECHEMA)

since 2011, Prof. D. Stolten

Member

VDI Society for Process Engineering and Chemical Engineering (VDI-GVC)

since 2011, Prof. D. Stolten

Member of the Executive Board and Advisory Council

VDI-Vieweg publishing house – VDI-Fachbuch, Berlin

since 2011, Prof. R. Peters

Member of the Advisory Board

Fuel Cells and Hydrogen Network NRW

since 2012, Dr. B. Emonts and Dr. T. Grube

Chairmen of the Hydrogen Platform and the Working Group for H₂ Systems

Wuppertal Institut für Klima, Umwelt, Energie

seit 2012, Prof. D. Stolten

Mitglied des Aufsichtsrats

International Association of Hydrogen Energy (IAHE)

seit 2012, Prof. D. Stolten

Vizepräsident des Vorstands

seit 2012, Dr. B. Emonts

Mitglied

Applied Energy Journal, Elsevier
seit 2012, Prof. D. Stolten
Mitglied des Redaktionsausschusses

seit 2015 – 2016, Prof. D. Stolten
Fachredakteur

Institute of Electrochemistry and Energy Systems of the Bulgarian Academy of Sciences
since 2012, Prof. W. Lehnert
Member of the Advisory Board

Clean Power Net
since 2012, Dr. M. Müller
Member

Hydrogen Power Storage & Solutions East Germany (HYPOS)
2013–2015, Prof. D. Stolten
Member of the Board

VDMA Fuel Cells Group PG HT-BZ (SOFC)
since 2013, Prof. L. Blum
Member

Journal of Hydrogen Energy, Elsevier
since 2014, Prof. D. Stolten
Member of the Editorial Board

Journal of Energy Storage, Elsevier
since 2014, Prof. D. Stolten
Member of the editorial board and the editorial committee

TRENDS2015 – Transition to Renewable Energy Devices, Aachen
2015, Prof. D. Stolten
Chairman of the Conference and the Organizing Committee

2015, Prof. R. Peters
Vice-Chairman of the Conference and the Organizing Committee

Project House TESA – Technology-Based Energy System Analysis
since 2015, Prof. D. Stolten
Spokesman of the Steering Committee

since 2015, Dr. B. Emonts
Office manager

Profile Area Energy, Chemical & Process Engineering (ECPE) of RWTH Aachen University
since 2015, Prof. D. Stolten
Member

JARA-Energy – Processes Pillar
since 2015, Prof. D. Stolten
Head of department (together with Prof. Leitner, RWTH Aachen University)

Guideline committee VDI 4657 on the planning and integration of energy storage systems
since 2015, Dr. P. Stenzel
Member

**Scientific Advisory Committee for the 12th European SOFC & SOE Forum,
Switzerland**

2016, Prof. D. Stolten

Member

German National Academy of Science and Engineering (acatech)

since 2016, Dr. M. Robinius

Member of the working group on pathway dependences and decision strategies

**BMW research network on entire systems analysis: working group on model
coupling and overall system**

since 2016, Dr. P. Markewitz

Group spokesman

Advances Journal of the Royal Society of Chemistry

since 2016 – Dr. J. Pasel

Co-editor

German Association for Electrical, Electronic and Information Technologies (VDE)

since 2016, Dr. M. Robinius

Member

**Hydrogen Implementing Agreement International Energy Agency – Task 38 Power to
Hydrogen to X**

since 2016, Dr. M. Robinius

Member

6.5 Contributions to trade fairs and exhibitions

IEK-3 showcases its innovativeness and R&D results at trade fairs and exhibitions which provide an excellent environment for establishing contact with interested visitors and exchanging information with partners and experts with similar specializations. During the year under review 2015, IEK-3 took part in five trade fairs and exhibitions in Hannover, Frankfurt am Main, Glasgow, Hamburg, and Stuttgart. Details of these fairs and exhibitions are listed below:

2015

Hannover Messe 2015

13–17 April 2015, Hannover

Fuel cell and electrolysis research

ACHEMA

15–19 June 2015, Frankfurt am Main

Research contributions to a sustainable provision of energy

ECS SOFC XIV

26–31 July 2015, Glasgow, Scotland, UK

SOFC research and technological development

H2 expo

23–26 September 2015, Hamburg

Auxiliary power units using fuel cells for use with diesel or kerosene

f-cell

12–14 October 2012, Stuttgart

Battery-supported fuel cell systems and electrolyzers for energy storage

The annual highlight is the joint stand on hydrogen and fuel cells at the technology trade fair in Hannover (see Fig. 91). In 2015, IEK-3 presented the latest technological developments in the field of fuel cell and electrolysis research. A reactor manufactured industrially and an HT-PEFC stack with metallic interconnector plates demonstrated the state of the art of autothermal reforming and electrochemical conversion of reformates into electricity. In addition, a system for uninterruptable power supply (USV) served as an example of the versatility of DMFCs as a battery replacement. Structure and function of a SOFC stack for transforming natural gas or hydrogen was visually demonstrated using a cell stack that was cut open and various cell components. The first approaches to large-scale hydrogen generation using PEM electrolysis were shown to the public via the demonstration of a cell with about 1.5 m² active area and a production sample from IEK-3's roll-to-roll electrode manufacture. A highlight at Jülich's stand was a visit by State Secretary Rachel (see Fig. 91, center). As part of the "Technical Forum", Dr. Martin Robinius gave a talk entitled "Assessment of excess power for different scenarios of wind power extension in Germany", describing his latest analysis results for the expansion of German wind energy usage. During the "Public Forum", which took place in parallel, Dr. Robinius answered questions by the moderator, on preparing the electricity market for integrating large quantities of renewable power.



Fig. 91: Hannover Messe 2015 – Jülich’s stand and team with State Secretary Rachel (center)

An overview of the events in which IEK-3 participated in 2016 and the topics concerned is given below.

2016

10th IRES 2016

15–17 March 2016, Düsseldorf

Energy and raw material pathways involving hydrogen

Hannover Messe 2016

25–29 April 2016, Hannover

Fuel cell and electrolysis research

ADB Annual Meeting

2–5 May 2016, Frankfurt am Main

Technology-based energy systems analysis

21st World Hydrogen Energy Conference 2016

13–16 June 2016, Zaragoza, Spain

Research for the efficient production and use of hydrogen

12th European SOFC & SOE Forum

5–8 July 2016, Lucerne, Switzerland

Research into energy converters using ceramic electrolytes

When wind supplies our gas: PtG as a long-term storage system

16 September 2016, Düsseldorf

Sustainable and flexible energy pathways involving hydrogen

World of Energy Solutions 2016

10–12 October 2016, Stuttgart

Battery-supported fuel cell systems and electrolyzers for commercial energy storage

“Engineering the Energy Future” was the topic which IEK-3, together with IEK-1 and ZEA-1 presented at Hannover Messe 2016. The exhibits ranged from cell components, cells, and stacks to PEM electrolysis, from SOFCs and HT-PEFCs to reactors for fuel-gas production (see Fig. 92, left). Dr. Weißbecker presented his spin-off project to the public in the forums running parallel to the trade fair, with a talk entitled “Unraveling the challenges of metallic bipolar plates for PEM fuel cells”. Dr. Marcelo Carmo used the Public Forum to talk about his topic, “Towards the establishment of cost efficient water electrolyzers”, concerning the latest research results with respect to the more economical use of noble metals in the electrode catalysts of PEM electrolyzers (see Fig. 92, right).



Fig. 92: Hannover Messe 2016 – Jülich trade fair stand and the team (left), interview with Dr. Carmo (right)

6.6 How to reach us

6.6.1 By car

Coming from Cologne on the A4 motorway (Cologne–Aachen) leave the motorway at the Düren exit, then turn right towards Jülich (B56). After about 10 km, turn off to the right onto the L253, and follow the signs for “Forschungszentrum”.

Coming from Aachen on the A44 motorway (Aachen–Düsseldorf) take the “Jülich-West” exit. At the first roundabout turn left towards Jülich, and at the second roundabout turn right towards Düren (B56). After about 5 km, turn left onto the L253 and follow the signs for “Forschungszentrum”.

Coming from Düsseldorf Airport, take the A52 motorway (towards Düsseldorf/Mönchengladbach) followed by the A57 (towards Cologne (Köln)) to Neuss-West. Then take the A46 (towards Jüchen/Grevenbroich), before turning onto the A44 (towards Aachen). Continue as described in “Coming from Düsseldorf”.

Coming from Düsseldorf on the A44 motorway (Düsseldorf–Aachen) you have two choices:

1. (Shorter route but more traffic) turn right at the Jülich-Ost exit onto the B55n, which you should follow for approx. 500 m before turning right towards Jülich. After 200 m, before the radio masts, turn left and continue until you reach the “Merscher Höhe” roundabout. Turn left here, drive past the Solar Campus belonging to Aachen University of Applied Sciences and continue straight along Brunnenstrasse. Cross the Römerstrasse junction, continue straight ahead onto Wiesenstrasse, and then after the roundabout and the caravan dealers, turn left towards “Forschungszentrum” (signposted).

2. (Longer but quicker route) drive until you reach the “Jülich-West” exit. At the first roundabout turn left towards Jülich, and at the second roundabout turn right towards Düren (B56). After about 5 km, turn left onto the L253 and follow the signs for “Forschungszentrum”.



Fig. 93: Euregio Rheinland map

Navigation systems: In your navigation system, enter “Wilhelm-Johnen-Strasse” as the destination. From here, it is only a few hundred meters to the main entrance – simply follow

the signs. Forschungszentrum Jülich itself is not part of the network of public roads and is therefore not recognized by navigation systems.

6.6.2 By plane

Cologne Bonn Airport: From the railway station at the airport, either take the S13 to Cologne main train station (Köln Hauptbahnhof) and then continue with the regional express to Düren, or go to Köln-Ehrenfeld by regional express and then take the S12 to Düren. Continue from Düren as described under “By train”.

By train from Düsseldorf Airport: From the railway station at the airport, travel to Cologne main train station (Köln Hauptbahnhof) and then continue on to Düren. Some trains go directly to Düren whereas other connections involve a change at Cologne main train station. Continue from Düren as described under “By train”.

6.6.3 By train

Take the train from Aachen or Cologne to Düren’s main train station (Hauptbahnhof). Then take the local train to Jülich (“Rurtalbahn”) and get out at the “Forschungszentrum” stop. From here, you need to keep right and walk towards the main road before turning right towards Forschungszentrum Jülich. The main entrance to Forschungszentrum Jülich is about 20 minutes by foot.



Fig. 94: Forschungszentrum Jülich campus map

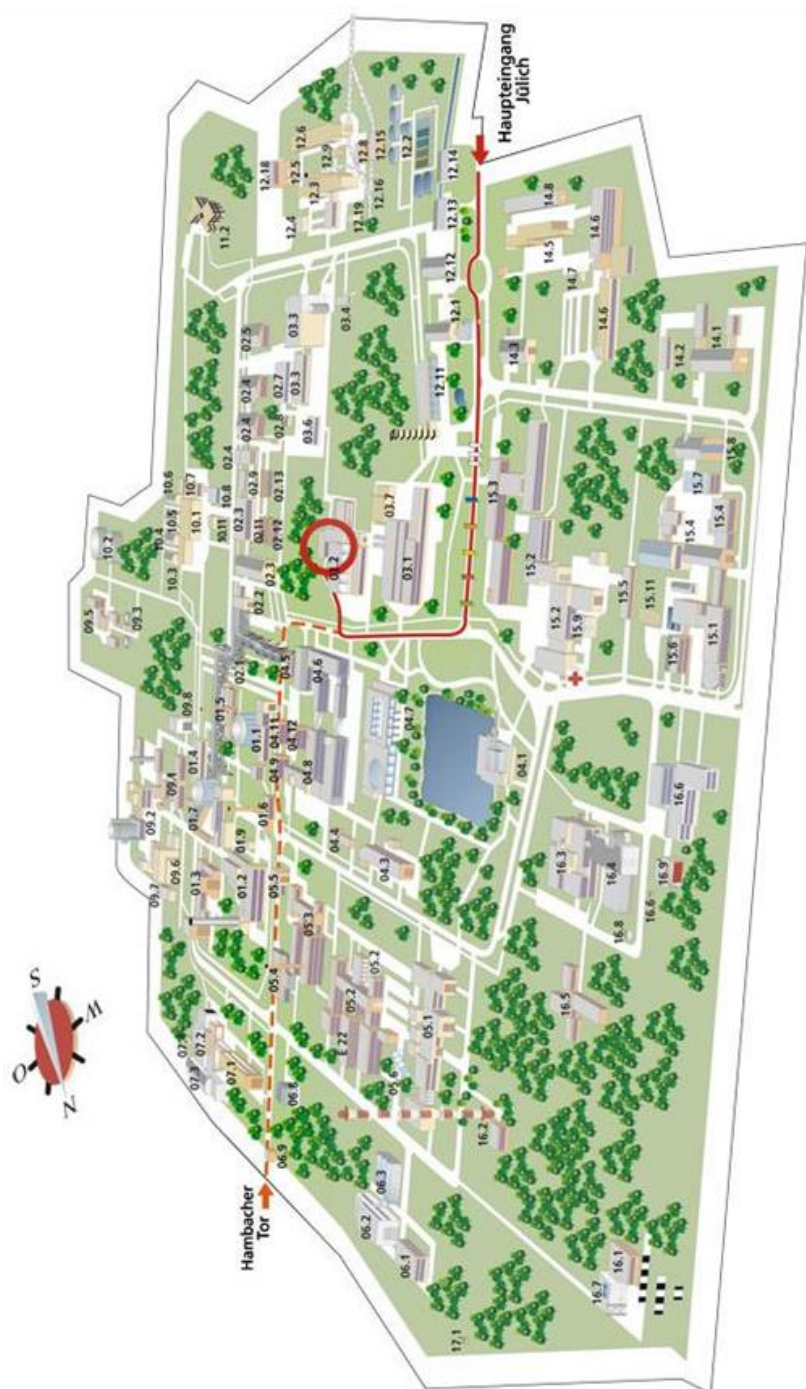


Fig. 95: Location of Institute of Energy and Climate Research, IEK-3: Electrochemical Process Engineering, Helmholtz Ring H8, building

6.7 List of abbreviations

acatech	German National Academy of Science and Engineering
ACHEMA	DECHEMA-organized world forum for chemical engineering
ADB	Asian Development Bank
ADELHEID	NRW project – from the laboratory into the air
AGEF	Working Group of Electrochemical Research Facilities
AGIT	Aachener Gesellschaft für Innovation und Technologietransfer mbH (Aachen society for innovation and technology transfer)
APS	atmospheric plasma spraying
ASC	anode-supported cell
ASME	American Society of Mechanical Engineers
ATR	autothermal reforming
BAT	battery
BESSY	Berlin Electron Storage Ring for Synchrotron Radiation
BET	analytical technique for the determination of surface area (Brunauer- Emmett-Teller)
BEV	battery-electric vehicle
Bio-CH ₄	biologically produced methane
BMBF	Federal Ministry of Education and Research
BMWi	Federal Ministry for Economic Affairs and Energy
BOL	beginning of life
BOS	authorities and organizations with security and safety tasks, aka emergency services
BREZEL	fuel cells expert committee of the Association of German Engineers (VDI)
BtL	biomass-to-liquid
CAB	catalytic burner
CAD	computer-aided design
CAN	Center for Applied Nanotechnology
CAPM	capital asset pricing model
CCM	catalyst-coated membrane
CCS	carbon capture and storage
CCU	carbon capture and utilization
CFD	computational fluid dynamics
CIGS	copper indium gallium selenide
CPE	constant phase element
CS design	cassette design
CV	cyclic voltammetry
CVD	chemical vapor deposition
DBG	German Bunsen Society for Physical Chemistry
DC	direct current
DFG	German Research Foundation
DLR	German Aerospace Center
DMC	dimethyl carbonate
DME	dimethyl ether
DMFC	direct methanol fuel cell
DPG	German Physics Society
DRT	distribution of relaxation times
DSC	differential scanning calorimeter
DWV	German Hydrogen and Fuel Cell Association
EBSD	electron backscatter diffraction

EC	ethylene carbonate
ECPE	Profile Area Energy, Chemical & Process Engineering of RWTH Aachen University
ECS	Electrochemical Society
EDX	energy-dispersive X-ray spectroscopy
EEL	electrochemistry electrolysis group
EIS	electrochemical impedance spectroscopy
EOL	end of life
EU	European Union
EXIST	BMWi funding program for start-ups in science
FCGEN	EU project on fuel-cell-based power generation
FCV	fuel cell electric vehicle
FLEXSIM	NRW project for a flexible simulation package for multiphase flows in fuel cells
FT	Fischer–Tropsch
FTIR	Fourier-transform infrared spectroscopy
FVEE	Renewable Energy Research Association
FZJ	Forschungszentrum Jülich GmbH
GC/MS	Gas chromatography–mass spectrometry
GDC	gadolinium-doped cerium oxide
GDCh	German Chemical Society
GDL	gaseous diffusion plant
GFZ	German Research Centre for Geosciences
GIZ	German society for international cooperation
HDH	hydrocracking distillation hydrotreating (treatment process for titanium powder)
HEV	hybrid electric vehicle
HGF	Helmholtz Association of German Research Centres
HM-RDE	hanging meniscus rotating disk electrode
H-SEM	high-resolution scanning electron microscope
HT-PEFC	high-temperature polymer electrolyte fuel cell
HV-	high voltage
HYPOS	BMBF project Hydrogen Power Storage & Solutions East Germany
HZB	Helmholtz-Zentrum Berlin
IAHE	International Association for Hydrogen Energy
IEA	International Energy Agency
IEEE	Institute of Electrical and Electronics Engineers
IEK-1	Institute of Energy and Climate Research – Materials Synthesis and Processing
IEK-2	Institute of Energy and Climate Research – Microstructure and Properties of Materials
IEK-3	Institute of Energy and Climate Research – Electrochemical Process Engineering
IEK-9	Institute of Energy and Climate Research – Fundamental Electrochemistry
IMechE	Institution of Mechanical Engineers
IQ-BZ	Fuel Cell Qualification Initiative
IRES	International Renewable Energy Storage Conference
ISE	International Society of Electrochemistry
IVF	HGF Initiative and Networking Fund
JARA	Jülich Aachen Research Alliance

JCNS	Jülich Centre for Neutron Science
JESS	Joint European Summer School
JSC	Jülich Supercomputing Centre
JuLab	Jülich schools laboratory
JULABOS	Jülich software for lattice Boltzmann simulations
JURECA	Jülich Research on Exascale Cluster Architectures
JUROPA	Jülich Research on Petaflop Architectures
KF	determination of water content using Karl Fischer titration
LiBs	lithium-ion batteries
LLZO	lithium lanthanum zirconate
LNG	liquefied natural gas
LOHC	liquid organic hydrogen carrier
LSCF	lanthanum strontium cobaltite ferrite
MBE	molecular beam epitaxy
MCF	manganese-cobalt-iron protective layer
MEA	membrane electrolyte assembly
METIS	models for energy transformation and integration systems
MIFULAS	BMBF project on microstructured functional layers deposited by laser build-up welding
MILP	mixed-integer linear optimization program
MKS	Mobility and Fuels Strategy
MnOx	manganese oxide protective coating
MWV	German petroleum industry association
NCA	anode made of lithium nickel cobalt aluminum oxide
NDIR	nondispersive infrared adsorption analyzer
NG	natural gas
NMC	anode made of lithium nickel manganese cobalt oxide
NMHCs	non-methane hydrocarbons
NOW	National Organization for Hydrogen and Fuel Cell Technology
NRW	North Rhine-Westphalia
NT-PEFC	low-temperature polymer electrolyte fuel cell
OME	oxymethylene ether
OpenFOAM	Open Source Field Operation and Manipulation (a free simulation software package for continuum-mechanics problems)
ORR	oxygen reduction reaction
P2X	Power-to-X
PBI	polybenzimidazole
PECSYS	EU project for the technology demonstration of large-scale photo-electrochemical system for solar hydrogen production
PEFC	polymer electrolyte fuel cell
PEM	polymer electrolyte membrane
PILs	proton-conducting ionic liquids
PLD	pulsed laser deposition
PoF	HGF program-oriented funding
PRECORS	innovative IEK-3 spin-off company for preventive corrosion systems
PtF	power-to-fuel
PTFE	polytetrafluoroethylene
PtG	power-to-gas
PV	photovoltaics
PVD	physical vapor deposition

RDE	rotating disk electrode
SEM/EDX	scanning electron microscope combined with energy-dispersive X-ray spectroscopy
RoBiPo	BMW i project for the development of robust bipolar plates for HT-PEFCs
rSOC	reversible solid oxide cell
RW	abbreviation for the IEK-3 DMFC stack
RWTH	RWTH Aachen University
SAED	selected area electron diffraction
SCT	segmented cell technology
SEI	solid electrolyte interface
SEM	scanning electron microscope
SG	shielding gas
SGG	shielding-gas generator
SLEI	solid–liquid electrolyte interphase
SOE	solid oxide electrolysis
SOEC	solid oxide electrolysis cell
SOFC	solid oxide fuel cell
SRMS	spatially resolved mass spectrometry
SS	summer semester
SuPER	sustainable production, energy, and resources
SVI	storage and cross-linked infrastructure
SWOT	method of evaluating strengths, weaknesses, opportunities, and threats
SWPC	Siemens Westinghouse Power Corporation
SWS	summer/winter semester
TEM	transmission electron microscope
TESYS	Project House Technology-Based Energy System Analysis
TG	thermogravimetric analysis
TGA	thermogravimetric analyzer
GHG	greenhouse gas
TPD	temperature-programmed desorption
TPO	temperature-programmed oxidation
TPR	temperature-programmed reduction
TRENDS	conference concerning the transition to renewable energy devices and systems
USV	uninterruptable Power Supply
VDI	Association of German Engineers
VDI-GVC	Association of German Engineers – Society for Process Engineering and Chemical Engineering
VSA	process and systems analysis group
WACC	method of evaluating companies based on weighted average cost of capital
WBZU	Fuel Cell Education and Training Centre, Ulm
WGS	water-gas shift reaction
WILEY-VCH	WILEY publishing house chemistry
WPS	wet powder spraying
WS	winter semester
XRD	X-ray diffraction
YSZ	yttrium-stabilized zirconia
ZEA-1	Central Institute of Engineering, Electronics and Analytics – Engineering and Technology

Band / Volume 372

**Analysis and Simulation of Macroscopic Defects in Cu(In,Ga)Se₂
Photovoltaic Thin Film Modules**

B. Misić (2017), iv, 147 pp

ISBN: 978-3-95806-228-3

Band / Volume 373

**Chemical and physical properties of sodium
ionic conductors for solid-state batteries**

M. Guin (2017), ix, 126 pp

ISBN: 978-3-95806-229-0

Band / Volume 374

**Prediction of Oxidation Induced Life Time for
FCC Materials at High Temperature Operation**

R. Duan (2017), vi, 180 pp

ISBN: 978-3-95806-230-6

Band / Volume 375

**Microstructure Evolution of Laves Phase Strengthened
Ferritic Steels for High Temperature Applications**

J. K. Lopez Barrilao (2017), XVI, 134 pp

ISBN: 978-3-95806-231-3

Band / Volume 376

**Drying front formation in topmost soil layers as evaporative restraint
Non-invasive monitoring by magnetic resonance and numerical simulation**

S. Merz (2017), xxii, 108 pp

ISBN: 978-3-95806-234-4

Band / Volume 377

**Low Temperature Thin-Film Silicon Solar Cells
on Flexible Plastic Substrates**

K. Wilken (2017), 194 pp

ISBN: 978-3-95806-235-1

Band / Volume 378

**Dissolution Behaviour of Innovative Inert Matrix Fuels
for Recycling of Minor Actinides**

E. L. Mühr-Ebert (2017), xii, 164 pp

ISBN: 978-3-95806-238-2

Band / Volume 379

**Charakterisierung und Modifizierung von Kupferoxid- und Kupfersulfid-
Nanopartikeln für Dünnschichtsolarzellen**

J. Flohre (2017), 141, iii pp

ISBN: 978-3-95806-241-2

Band / Volume 380

**Einzelfaserkomposite aus Pulvermetallurgischem
Wolfram-faserverstärktem Wolfram**

B. Jasper (2017), v, 92, XVIII pp

ISBN: 978-3-95806-248-1

Band / Volume 381

**Untersuchungen zur Deckschichtbildung auf $\text{LiNi}_{0,5}\text{Mn}_{1,5}\text{O}_4$ -
Hochvoltkathoden**

Die Kathoden/Elektrolyt-Grenzfläche in Hochvolt-Lithium-Ionen-Batterien

K. Wedlich (2017), xvi, 157, xvii-xxvi pp

ISBN: 978-3-95806-249-8

Band / Volume 382

**Charakterisierung gradierter Eisen/Wolfram-Schichten
für die erste Wand von Fusionsreaktoren**

S. Heuer (2017), x, 234 pp

ISBN: 978-3-95806-252-8

Band / Volume 383

High resolution imaging and modeling of aquifer structure

N. Güting (2017), viii, 107 pp

ISBN: 978-3-95806-253-5

Band / Volume 384

IEK-3 Report 2017

Sektorkopplung –

Forschung für ein integriertes Energiesystem

(2017), 182 pp

ISBN: 978-3-95806-256-6

Band / Volume 385

**Bestimmung der Wolframerosion mittels optischer Spektroskopie
unter ITER-relevanten Plasmabedingungen**

M. Laengner (2017), vi, 184, XI pp

ISBN: 978-3-95806-257-3

Band / Volume 386

IEK-3 Report 2017

Sector Coupling –

Research for an Integrated Energy System

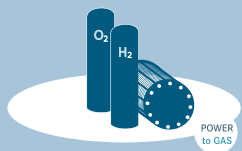
(2017), 175 pp

ISBN: 978-3-95806-258-0

Weitere **Schriften des Verlags im Forschungszentrum Jülich** unter

<http://www.zb1.fz-juelich.de/verlagextern1/index.asp>

IEK-3 is one of the thirteen subinstitutes that currently constitute the Institute of Energy and Climate Research. Research work at IEK-3 focuses on technical solutions for a sustainable energy supply chain. Priority is given to electrochemistry and process engineering for fuel cells with and without reforming as well as for water electrolysis. These conversion technologies are investigated by an interdisciplinary team of scientists – from the underlying scientific principles to application in technical systems. IEK-3 has laboratories for imaging, physicochemical, and electrochemical investigations. In addition, universal test setups enable extensive operational testing and characterization of diverse converters with dimensions ranging from a square centimeter to square meters. In anticipation of technology transfer, IEK-3 has established a technical facility to concurrently fabricate functional layer systems, such as electrodes, gas diffusion layers and membrane-electrode assemblies, in a reproducible manner on an industrial scale. The facility also enables the precise assembly of multicomponent stacks. Process and systems analyses make it possible to identify and evaluate promising future R&D topics, to compare in-house technological developments with conventional technologies, to design energy pathways and energy supply networks, and to derive recommendations and provide guidance for interested sectors of society. In addition to its R&D services, IEK-3 cooperates closely with universities and other educational establishments, providing an extensive range of further education and training opportunities.



In a process called POWER-to-GAS, hydrogen is produced from electricity, which is in turn generated from fluctuating wind and photovoltaic power plants. Water electrolysis is used to transform electrical energy into chemical energy in the form of H₂ on an industrial scale. The energetically valuable gas is suitable for large-volume storage in salt caverns, can be transported over long distances via pipelines, and can be used directly as a fuel in the transport sector or as a chemical raw material in industry.



The BIO-to-LIQUID energy pathway makes use of biogenic raw materials to produce liquid fuels and chemicals without competing with crops. Synthesis based on H₂ and a carbon source is possible through various transformation processes. For this purpose, residual wood from logging is transformed into synthesis gas through gasification. In addition, CO₂ separated in biogas facilities in combination with electrolysis H₂ can be used for synthesis. Liquids produced in this way can complement or even substitute conventional fuels while simultaneously increasing the efficiency of vehicles and reducing pollutant emissions.



In a process termed POWER-to-HEAT, heating or cooling energy produced from electricity is another flexibilization option for an energy supply dominated by renewables. Renewable power is used in heat pumps and heating rods in order to provide heat or it is used in air conditioning units for cooling. Direct use in households is just as feasible as feeding heating/cooling energy into a grid for a user grid located further away.